

AD-A112 009

MECHANICAL TECHNOLOGY INC LATHAM N Y

F/G 13/9

INTERACTIVE GRAPHIC SIMULATION OF ROLLING ELEMENT BEARINGS. PHA--ETC(U)

NOV 81 P K GUPTA

F33615-80-C-5152

UNCLASSIFIED

MTI-81TR66

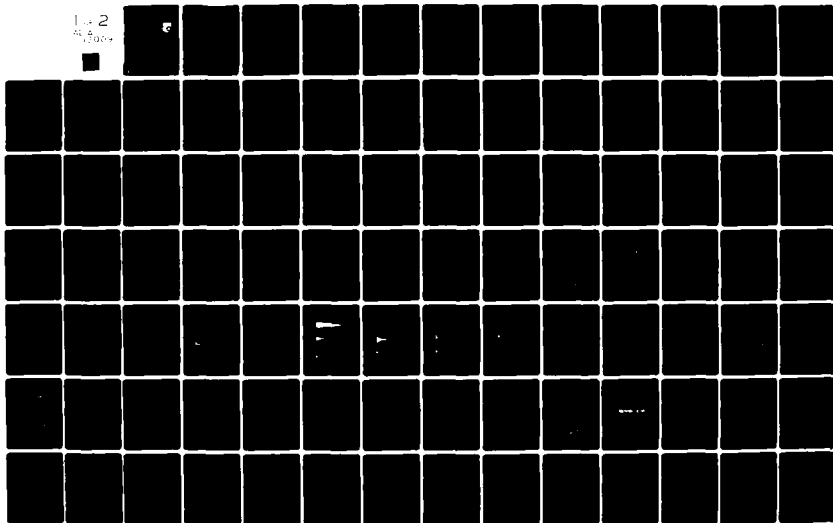
AFWAL-TR-81-4148

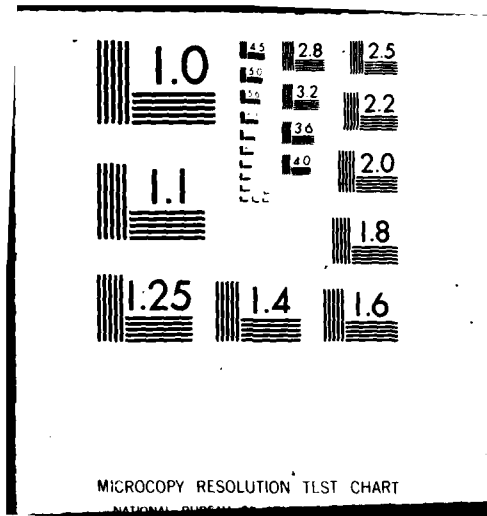
NL

1 of 2

415

1000+





12

AFWAL-TR-81-4148

INTERACTIVE GRAPHIC SIMULATION OF ROLLING ELEMENT BEARINGS  
Phase I: Low Frequency Phenomenon and RAPIDREB Development

Mechanical Technology Incorporated  
968 Albany-Shaker Road  
Latham, New York 12110



November 1981

FINAL REPORT FOR PERIOD AUGUST 1980 - SEPTEMBER 1981

APPROVED FOR PUBLIC RELEASE; DISTRIBUTION UNLIMITED

MATERIALS LABORATORY  
AIR FORCE WRIGHT AERONAUTICAL LABORATORIES  
AIR FORCE SYSTEMS COMMAND  
WRIGHT-PATTERSON AIR FORCE BASE, OHIO 45433

DTIC  
MAR 15 1982  
H

82 00 10 019

ADA112009

# NOTICE

When Government drawings, specifications, or other data are used for any purpose other than in connection with a definitely related Government procurement operation, the United States Government thereby incurs no responsibility nor any obligation whatsoever; and the fact that the Government may have formulated, furnished, or in any way supplied the said drawings, specifications, or other data, is not to be regarded by implication or otherwise as in any manner licensing the holder or any other person or corporation, or conveying any rights or permission to manufacture use, or sell any patented invention that may in any way be related thereto.

This report has been reviewed by the Office of Public Affairs (ASD/PA) and is releasable to the National Technical Information Service (NTIS). At NTIS, it will be available to the general public, including foreign nations.

This technical report has been reviewed and is approved for publication.

Howard E. Bandow

HOWARD E. BANDOW  
Project Engineer

B. D. McConnell

B. D. McCONNELL, Chief  
Fluids, Lubricants and Elastomers Branch

FOR THE COMMANDER

F. D. Cherry

F. D. CHERRY, Chief  
Nonmetallic Materials Division

"If your address has changed, if you wish to be removed from our mailing list, or if the addressee is no longer employed by your organization please notify AFWAL/MLBT, W-PAFB, OH 45433 to help us maintain a current mailing list".

Copies of this report should not be returned unless return is required by security considerations, contractual obligations, or notice on a specific document.

UNCLASSIFIED

SECURITY CLASSIFICATION OF THIS PAGE (When Data Entered)

REPORT DOCUMENTATION PAGE		READ INSTRUCTIONS BEFORE COMPLETING FORM
1. REPORT NUMBER AFWAL-TR-81-4148	2. GOVT ACCESSION NO. AD-A112009	3. RECIPIENT'S CATALOG NUMBER
4. TITLE (and Subtitle) INTERACTIVE GRAPHIC SIMULATION OF ROLLING ELEMENT BEARINGS Phase I: Low Frequency Phenomenon and RAPIDREB Development	5. TYPE OF REPORT & PERIOD COVERED Final August 1, 1980 - September 30, 1981	6. PERFORMING ORG. REPORT NUMBER MTI 81TR66
7. AUTHOR(s) Dr. Pradeep K. Gupta	8. CONTRACT OR GRANT NUMBER(s) F33615-80-C-5152	
9. PERFORMING ORGANIZATION NAME AND ADDRESS Mechanical Technology Incorporated 968 Albany-Shaker Road Latham, New York 12110	10. PROGRAM ELEMENT, PROJECT, TASK AREA & WORK UNIT NUMBERS 24210208	
11. CONTROLLING OFFICE NAME AND ADDRESS Materials Laboratory (AFWAL/MBT) Air Force Wright Aeronautical Laboratories (AFSC) Wright-Patterson Air Force Base, Ohio 45433	12. REPORT DATE November 1981	13. NUMBER OF PAGES 138
14. MONITORING AGENCY NAME & ADDRESS (if different from Controlling Office)	15. SECURITY CLASS. (of this report) Unclassified	15a. DECLASSIFICATION/DOWNGRADING SCHEDULE
16. DISTRIBUTION STATEMENT (of this Report) <div style="border: 1px solid black; padding: 5px; transform: rotate(-2deg); display: inline-block;"> <b>DISTRIBUTION STATEMENT A</b>            Approved for public release;            Distribution Unlimited         </div>		
17. DISTRIBUTION STATEMENT (of the abstract entered in Block 20, if different from Report)		
18. SUPPLEMENTARY NOTES		
19. KEY WORDS (Continue on reverse side if necessary and identify by block number) Ball Bearings Cage Instability DMA Bearings High Speed Engine Bearings		
20. ABSTRACT (Continue on reverse side if necessary and identify by block number) A selective suppression of the very high frequency content of the generalized motion simulated by the original DREB computer program has led to a considerable increase in the maximum permissible time step size and hence performance simulations over relatively large time domains (several shaft revolutions) have been economically possible with the updated version RAPIDREB. Capabilities of RAPIDREB are demonstrated for both light load, low speed DMA (Despun Mechanical Assembly) ball bearings and the heavy load, high speed (cont'd)		

DD FORM 1 JAN 73 1473

EDITION OF 1 NOV 65 IS OBSOLETE

UNCLASSIFIED

SECURITY CLASSIFICATION OF THIS PAGE (When Data Entered)

SECURITY CLASSIFICATION OF THIS PAGE(When Data Entered)

engine type ball bearings. From the simulations obtained over a shaft revolution it is shown that the race guided cage in the DMA bearings is generally stable while the ball guided cage produces relatively noisy and to some extent unstable cage motion. The high speed engine bearing performance is simulated over more than seven shaft revolutions. The steady whirl and continued contact of the cage with the guiding race is simulated under a combined thrust and radial load applied on the bearing. Thus conditions of excessive cage wear and eventual failure are simulated.

Accession For	
NTIS GRA&I	<input checked="checked" type="checkbox"/>
DTIC TAB	<input type="checkbox"/>
Unannounced	<input type="checkbox"/>
Justification	
By	
Distribution/	
Availability Codes	
Dist	Avail and/or Special
A	



UNCLASSIFIED

SECURITY CLASSIFICATION OF THIS PAGE(When Data Entered)

# TABLE OF CONTENTS

<u>SECTION</u>		<u>PAGE</u>
1.0	INTRODUCTION. . . . .	1
2.0	GENERAL TIME SCALES . . . . .	3
	2.1 Ball/Race Interaction. . . . .	3
	2.2 Ball/Cage and Race/Cage Interactions . . . . .	5
	2.3 Low Frequency Components . . . . .	5
3.0	DREB MODIFICATIONS AND RAPIDREB DEVELOPMENTS. . . . .	11
	3.1 Suppression of High Frequency Content. . . . .	11
	3.1.1 Ball Motion Constraints . . . . .	11
	3.1.2. Damping Considerations. . . . .	12
	3.2 Integrating Algorithms . . . . .	14
	3.2.1 Adams Type Predictor-Corrector in Divided Differences . . . . .	15
	3.2.1.1 Predictor Formula. . . . .	15
	3.2.1.2 Corrector Formula. . . . .	17
	3.2.1.3 Computation of Coefficients. . . . .	18
	3.2.1.4 Step Changing Criterion. . . . .	19
	3.2.1.5 Change or Order. . . . .	20
	3.2.1.6 Computational Considerations . . . . .	20
	3.2.2 Explicit Runge-Kutta Type Algorithms . . . . .	21
	3.3 Modifications for Ball/Cage Guidance in DMA Bearings . . . . .	28
	3.4 Recommendations for Using the RAPIDREB Version of DREB. . . . .	30
4.0	PERFORMANCE SIMULATION OF DMA BEARINGS. . . . .	33
	4.1 Bearing Geometry . . . . .	33
	4.2 Operating Conditions . . . . .	33
	4.3 Ball/Race Traction Models. . . . .	35
	4.4 Performance Simulations of 100 mm DMA Bearings . . . . .	38

<u>Section</u>		<u>Page</u>
	4.5 Performance Simulations of the 150 mm DMA Bearings . . . . .	49
5.0	ENGINE BEARING PERFORMANCE SIMULATION . . . . .	71
	5.1 Bearing Geometry . . . . .	71
	5.2 Lubricant Traction Models. . . . .	71
	5.3 Operating Conditions . . . . .	71
	5.4 Performance Simulations. . . . .	73
6.0	CONCLUSIONS . . . . .	84
	REFERENCES. . . . .	88
	APPENDIX A - Input Data Description for the Computer Programs DREB and DREBP, Version: RAPIDREB	90
	APPENDIX B - Typical Computer Output for the 100 mm and 150 mm DMA Bearings . . . . .	110
	APPENDIX C - Typical Computer Output for the 100 mm Engine Bearing. . . . .	123



# LIST OF ILLUSTRATIONS

<u>NUMBER</u>		<u>PAGE</u>
2-1	Characteristic Ball Mass Center Vibration Pattern in an Angular Contact Ball Bearing . . . . .	4
2-2	Variations of Computed Elastic Contact Frequency, $\omega_e$ and Bearing Kinetic Frequency, $\omega_k$ as a Function of Ball-Race Contact Load . . . . .	6
2-3	Typical Ball/Cage Contact Vibration. . . . .	7
2-4	Typical Ball/Cage Collisions in an Angular Contact Ball Bearing with Combined Axial and Radial Load. .	8
3-1	Simple Spring and Damper Model for Any Contact Interface . . . . .	13
3-2	Exaggerated Pocket Geometry for a Ball Riding Cage . .	29
4-1	Geometrical Data for the 100 mm DMA Ball Bearing with Inner Race Guided Cage . . . . .	34
4-2	Geometry of the 150 mm DMA Ball Bearing with Ball Guided Cage . . . . .	36
4-3	Geometry of the Ball Guided Cage . . . . .	37
4-4	Ball/Race Traction Characteristics for the DMA Bearings . . . . .	39
4-5	Ball Cage Interaction for the 100 mm DMA Ball Bearing .	40
4-6	Dimensionless Cage Angular Accelerations for the 100 mm DMA Bearing with Gravity Acting Along the Bearing Axis. Scale = $1.319 \times 10^7$ RPM/S. . . . .	41
4-7	Cage Whirl and Skid Parameters for the 100 mm DMA Bearings. . . . .	42
4-8	Bearing Torque Variations for the 100 mm DMA Bearing with Gravity Acting Along the Bearing Axis. . . . .	44
4-9	Dimensionless Ball Angular Velocity for the 100 mm Bearing. Scale = $1.22 \times 10^4$ RPM. . . . .	45
4-10	Ball/Race Spin-to-Roll Ratio for the 100 mm DMA Bearing . . . . .	46
4-11	Ball/Cage Force Variations for the 100 mm Bearing with Gravity Acting Normal to the Bearing Axis. . .	47

# LIST OF ILLUSTRATIONS (cont'd)

<u>Number</u>		<u>Page</u>
4-12	Normal Contact Force at the Cage/Race Interface When Gravity Acts Normal to the Bearing Axis in the Case of the 100 mm DMA Bearing . . . . .	48
4-13	Dimensionless Angular Accelerations of the 100 mm Bearing Cage When Gravity Acts Normal to the Bearing Axis. . . . .	50
4-14	Dimensionless Ball Angular Velocity for the 100 mm Bearing with Gravity Acting Normal to the Bearing Axis. . . . .	51
4-15	Cage Whirl and Skid Parameters for the 100 mm Bearing with Gravity Acting Normal to Bearing Axis. . . . .	52
4-16	Variation in Bearing Torque in Case of the 100 mm Bearing with Gravity Acting Normal to the Bearing Axis. . . . .	53
4-17	Dimensionless Ball Angular Velocity Variation for the 100 mm DMA Bearing with Gravity Oriented Normal to the Bearing Axis. . . . .	54
4-18	Ball/Race Spin Variation for the 100 mm Bearing with Gravity Acting Normal to Bearing Axis. . . . .	55
4-19	Ball Orbital Acceleration Resulting from the Ball/Cage Collision due to Eccentric Cage in the 100 mm Bearing with Gravity Normal to Bearing Axis. . . . .	56
4-20	Ball/Cage Interaction in the 150 mm Bearing with Ball Guided Cage Operating Horizontal with Gravity Acting Along the Bearing Axis . . . . .	57
4-21	Dimensionless Cage Mass Center Accelerations Result- ing From the Noisy Ball/Cage Interaction, for the 150 mm Bearing. Scale = $1.198 \times 10^4 \text{ M/S}^2$ , $1.03 \times 10^7 \text{ RPM/S}$ . . . . .	59
4-22	Cage Whirl and Skid Parameter for the 150 mm DMA Bearing. . . . .	60
4-23	Bearing Torque Variation for the 150 mm Bearing with Gravity Acting Along the Bearing Axis . . . . .	61
4-24	Dimensionless Angular Velocities of the Ball in the 150 mm DMA Bearing. Scale = $9.918 \times 10^4 \text{ RPM}$ . . . . .	62

# LIST OF ILLUSTRATIONS (cont'd)

<u>Number</u>		<u>Page</u>
4-25	Ball/Race Spin for the 150 mm DMA Bearing. . . . .	63
4-26	Ball/Cage Interaction at the Cylindrical Pocket Surface for the 150 mm Bearing with Gravity Acting Normal to the Bearing Axis . . . . .	64
4-27	Ball/Cage Interaction at the Conical Guidance Surface for the 150 mm Bearing with Gravity Acting Normal to Bearing Axis . . . . .	65
4-28	Dimensionless Angular Velocity of the Ball for the 150 mm Bearing with Ball Guided Cage. Scale = $9.918 \times 10^3$ RPM . . . . .	66
4-29	Ball Orbital Accelerations Resulting From the Excessive Ball/Cage Interaction for the 150 mm DMA Bearing . . . . .	67
4-30	Dimensionless Angular Velocity of the Ball Guided Cage in the 150 mm Bearing with Large Ball/Cage Interaction. Scale $\sim 9.918 \times 10^3$ RPM . . . . .	68
4-31	Dimensionless Cage Mass Center Accelerations Resulting from the Excessive Ball/Cage Interaction in the 150 mm Bearing with Gravity Acting Normal to the Bearing Axis. Scale = $1.199 \times 10^4$ M/sec <sup>2</sup> , $1.030 \times$ $10^7$ RPM/sec. . . . .	69
4-32	Cage Whirl and Skid Parameters for the 150 mm Bearing with Ball Guided Cage and with Gravity Acting Normal to the Bearing Axis . . . . .	70
5-1	Geometrical Description of the 100 mm Engine Bearing with Inner Race Guided Cage . . . . .	72
5-2	Variations in Ball/Race Load, Contact Angle and Spin-to-Roll for the 100 mm Engine Bearing. . . . .	74
5-3	Dimensionless Ball Angular Velocity Variation for the 100 mm Engine Bearing. Scale = $7.84 \times 10^4$ RPM .	75
5-4	Ball/Cage Interaction for the 100 mm Engine Bearing . .	76
5-5	Repeated Cage/Race Collisions in the 100 mm Engine Bearing. . . . .	77
5-6	Steady Orbit of the Cage Mass Center for the 100 mm Engine Bearing. Scale = 0.009525 M. . . . .	79

# LIST OF ILLUSTRATIONS (concluded)

<u>Number</u>		<u>Page</u>
5-7	Dimensionless Velocity of Cage Mass Center for the 100 mm Engine Bearing. Scales = 78.17 M/Sec, 7.84 x 10 <sup>4</sup> RPM . . . . .	80
5-8	Dimensionless Angular Velocity of a Ball in the 100 mm Engine Bearing. Scale - 7.84 x 10 <sup>4</sup> RPM . .	81
5-9	Cage Whirl and Skid Parameters for the 100 mm Engine Bearing . . . . .	82
5-10	Bearing Torque and Power Loss Variations in the 100 mm Engine Bearing . . . . .	83

## 1.0 INTRODUCTION

With the availability of advanced computer codes, such as the Dynamics of Rolling Element Bearings (DREB) computer program [1-5], the interest in real time performance simulation of rolling bearings has been growing rather rapidly over the past few years. The most generalized dynamic model underlining DREB has been employed for the purpose of both design and performance diagnosis in advanced rolling bearing systems. However, in spite of the rapidly advancing computer technology, the computational effort required in using DREB has proven to be a practical limitation. This is related directly to the nature of the model in the sense that the maximum step size for the numerical integration of a system of differential equations of motion is determined by the highest frequency present in the system, which is often several orders of magnitude higher than the shaft rotational speed. Thus in order to simulate effects of the order of shaft speed, integration over a very large time domain is required and since the maximum step size is limited by the high frequencies, the computing costs, specially for very low speed applications, have proven to be prohibitive. The primary objective of the present investigation is to examine the various time scales in the general behavior of a ball bearing and accordingly modify DREB to suppress the very high frequencies and thereby develop a "rapid version" of DREB, which has been called RAPIDREB.

For a typical ball bearing the high frequency present in the system is defined by the ball/race Hertzian contact. If the ball is free to translate, vibratory motion corresponding to this natural frequency has been observed. Also, as will be discussed in the next section, a relatively high frequency is also associated with the kinematics of ball motion. In order to suppress these high frequencies the ball mass center may be constrained in a suitable manner. Once this is done the step size can be made relatively large and also predictor-corrector type algorithms can be employed to considerably reduce the computing costs. However, if a cage is present in the bearing, the discontinuities associated with the ball/cage and race/cage collisions can produce stability problems for the predictor-corrector schemes and therefore such algorithms can only be effectively used in the

case of a cageless bearing, and considerable care will be required in using such algorithms when there are repeated ball/cage or race/cage collisions. In general it will be necessary to re-start the predictor-corrector process at the time of the start and end of such collisions if the collision time is large. For short collisions an explicit formula can be used during the entire collision. The ultimate integrating scheme may therefore be of a hybrid nature employing both explicit and implicit algorithm. Thus, the incorporation of both types of formulae has been one of the objectives of the present work.

The next section of this report reviews the various time scales associated with generalized motion of the rolling elements in a ball bearing. Section 3 contains the essential modifications to the existing program DREB in order to develop the RAPIDREB version. Some dynamic simulations for both the very low speed DMA\* bearings and high speed engine bearings are then presented as typical test cases demonstrating the capabilities of RAPIDREB. Descriptions of program inputs are presented in Appendix A, and typical outputs of the program are shown in Appendices B and C.

---

\* Despun Mechanical Assembly

## 2.0 GENERAL TIME SCALES

The characteristic frequencies in the general dynamic performance of ball bearings normally cover a wide spectrum. Frequencies associated with the elastic contact phenomenon are on the high end while the shaft speed is on the low end of the spectrum. Fortunately for most operating environments the high frequencies are several orders of magnitude greater than the frequencies of the order of shaft revolution speed and therefore it is relatively easy to constrain the motion to eliminate all the high frequencies in order to look at the low frequency phenomenon in depth. To understand the physical mechanism behind each frequency the basic model for each interaction and the fundamental kinematics of ball motion must be reviewed.

### 2.1 Ball/Race Interaction

The normal contact loads at the ball/race interaction are computed by the Hertzian elastic contact theory. For small changes in load the non-linear Hertzian load-deflection relation can be suitably linearized.

Now if the ball is free to translate arbitrarily a vibration frequency corresponding to this spring will be observed. This has been discussed in depth by Gupta et al [6]. To review the phenomenon briefly Figure 2-1 shows typical axial and radial components of ball mass center as it travels in its orbit. The high frequency component corresponds to the elastic contact phenomenon. For most ball bearings this frequency can be in the range of 1 to 50 kHz. A large bearing will normally have a lower elastic contact frequency due to heavier balls.

Figure 2-1 also shows a distinct low frequency whose axial and radial components are  $180^\circ$  out of phase. This frequency has been termed as a kinematic frequency [6] since it is a strong function of race curvatures and it is proportional to square root of ball/race contact load. Again the actual frequency for a given bearing depends on the geometry of bearing and the applied conditions but the general range is from about 500 Hz to 10 kHz.

It is interesting to review the load dependence of both the above frequencies. The kinematic frequency, by definition, has a square root variation as dis-

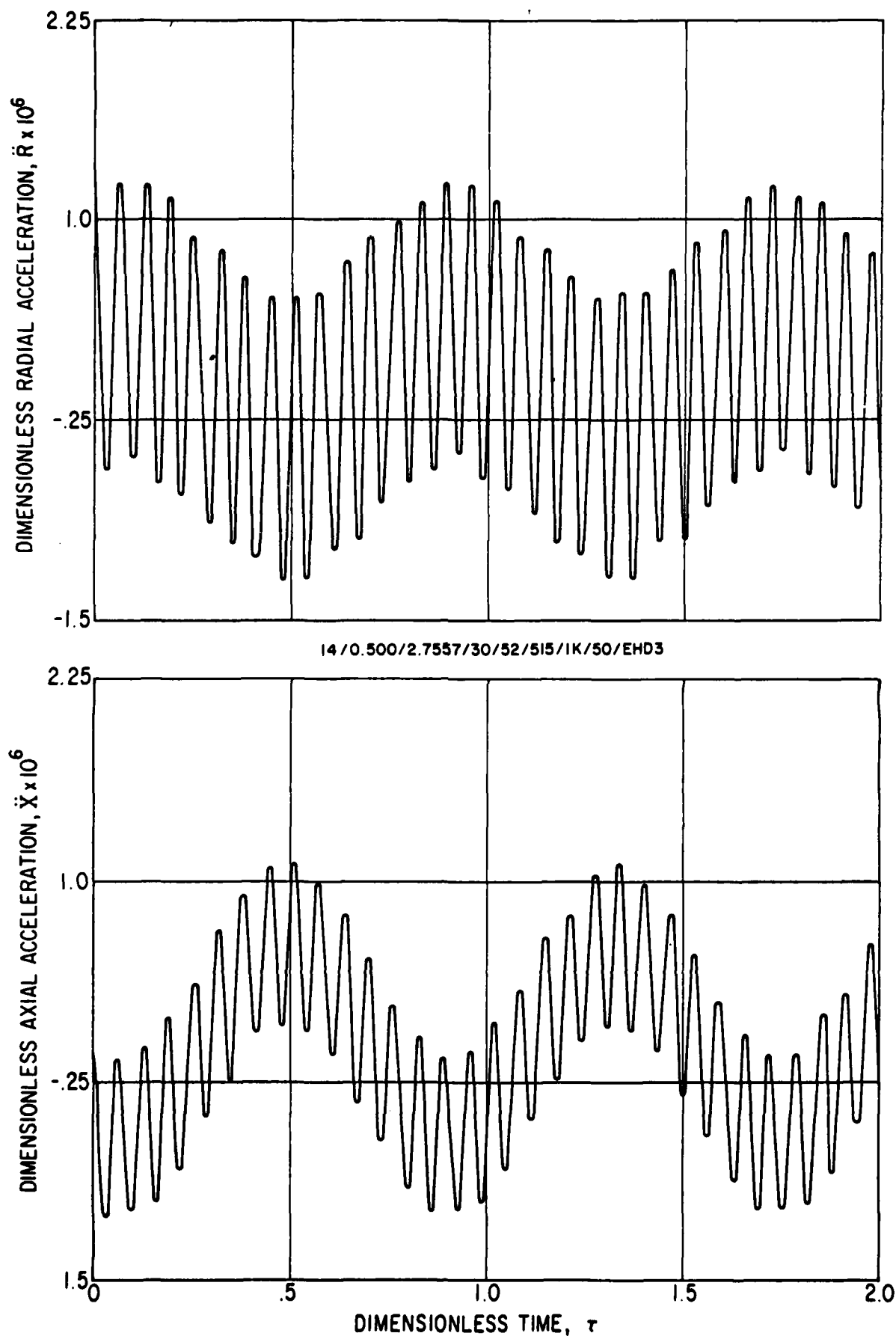


Fig. 2-1 Characteristic Ball Mass Center Vibration Pattern  
in an Angular Contact Ball Bearing



cussed above and the load dependence of the elastic contact frequency can be easily shown as 1/6 power of load:

$$\text{Hertz contact load } Q = K \delta^{3/2}$$

$$\text{Stiffness } k = \frac{\partial Q}{\partial \delta} = \frac{3}{2} K \delta^{1/2} = \frac{3}{2} K \left(\frac{Q}{K}\right)^{2/6}$$

$$\text{Natural frequency} = \sqrt{\frac{k}{m}} \sim Q^{1/6}$$

Figure 2-2 shows such a dependence for a ball bearing with 12.7 mm diameter balls and 70 mm pitch diameter. It is seen that as the contact load increases the two characteristic frequencies come close together. Thus either at high applied loads or at high speeds, the distinction between the two frequencies may not be as clearly seen in the ball acceleration plots as it is seen in Figure 2-1.

## 2.2 Ball/Cage and Race/Cage Interactions

The dynamics of ball/cage interaction can be quite complicated depending on the operating conditions and the ball pocket clearances. For a simple thrust loaded condition with gravity acting along the bearing axis, the cage weight will be supported uniformly by all the balls and therefore ball/cage contact will be established in each pocket. For such a condition the elastic contact spring modeling the normal contact will produce a vibratory motion if the cage is allowed to translate axially relative to the balls. Such a phenomenon is demonstrated in Figure 2-3. Again the frequencies will be generally high compared to the shaft rotational speed.

In most instances the ball/cage contacts may be of impulsive nature and the total time of contact may be very small. A typical example is presented in Figure 2-4. Such impulsive contacts will produce definite discontinuities in the motions of both the balls and the cage and considerable care will be required in integrating the equations of motion.

## 2.3 Low Frequency Components

This class of motion basically contains frequencies of the order of race angular velocities. The components of interest generally include ball

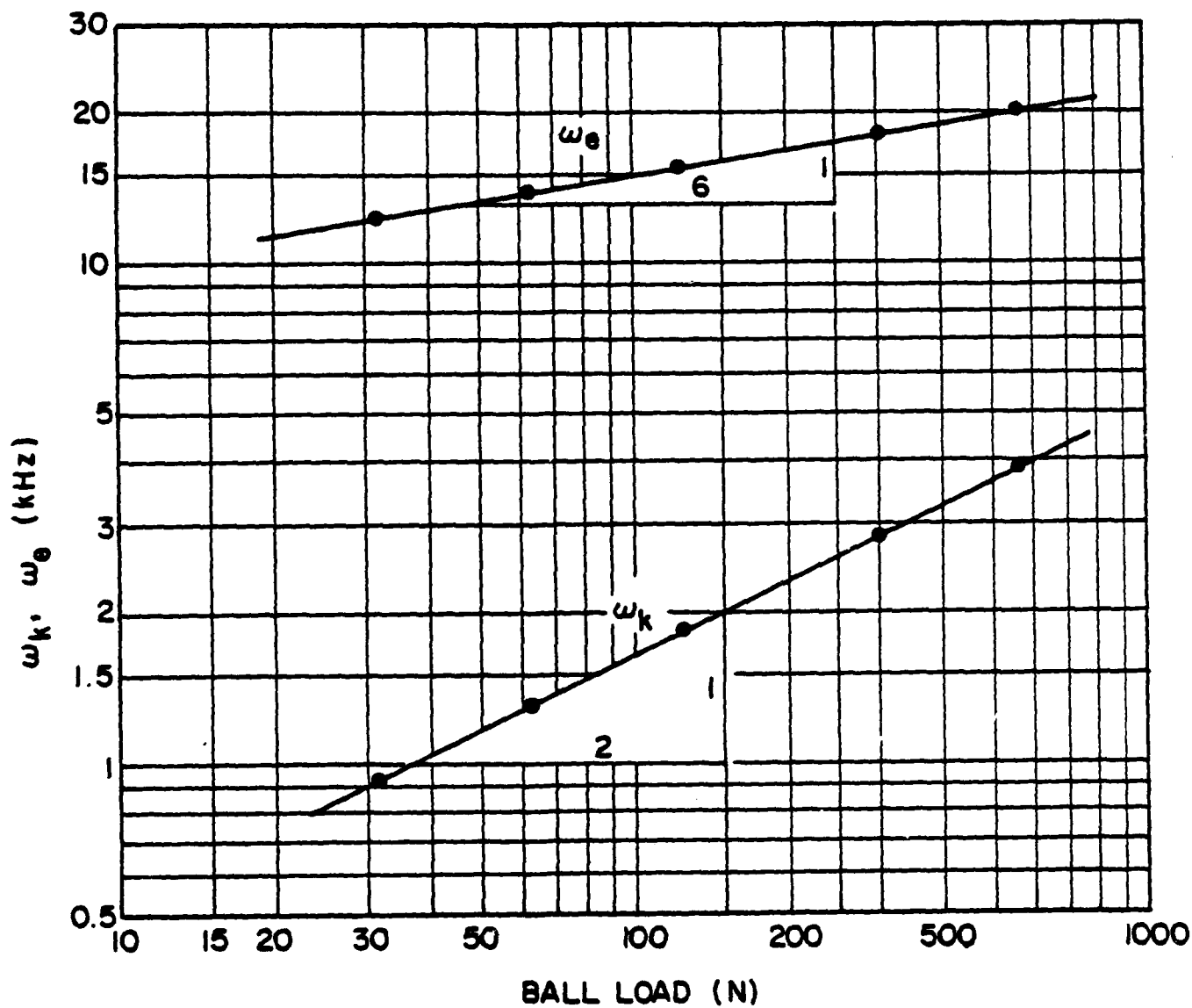
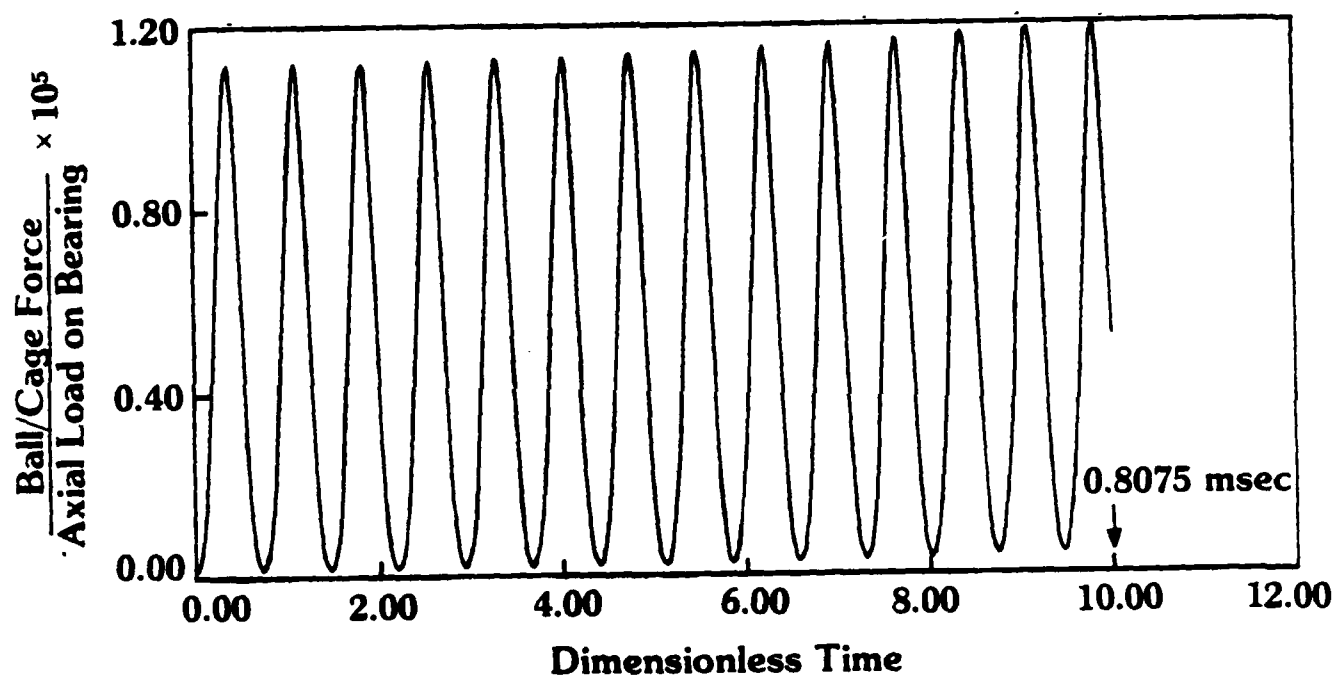


Fig. 2-2 Variations of computed elastic contact frequency,  $\omega_e$  and bearing kinetic frequency,  $\omega_k$  as a function of ball-race contact load



802875-1

Fig. 2-3 Typical Ball/Cage Contact Vibration

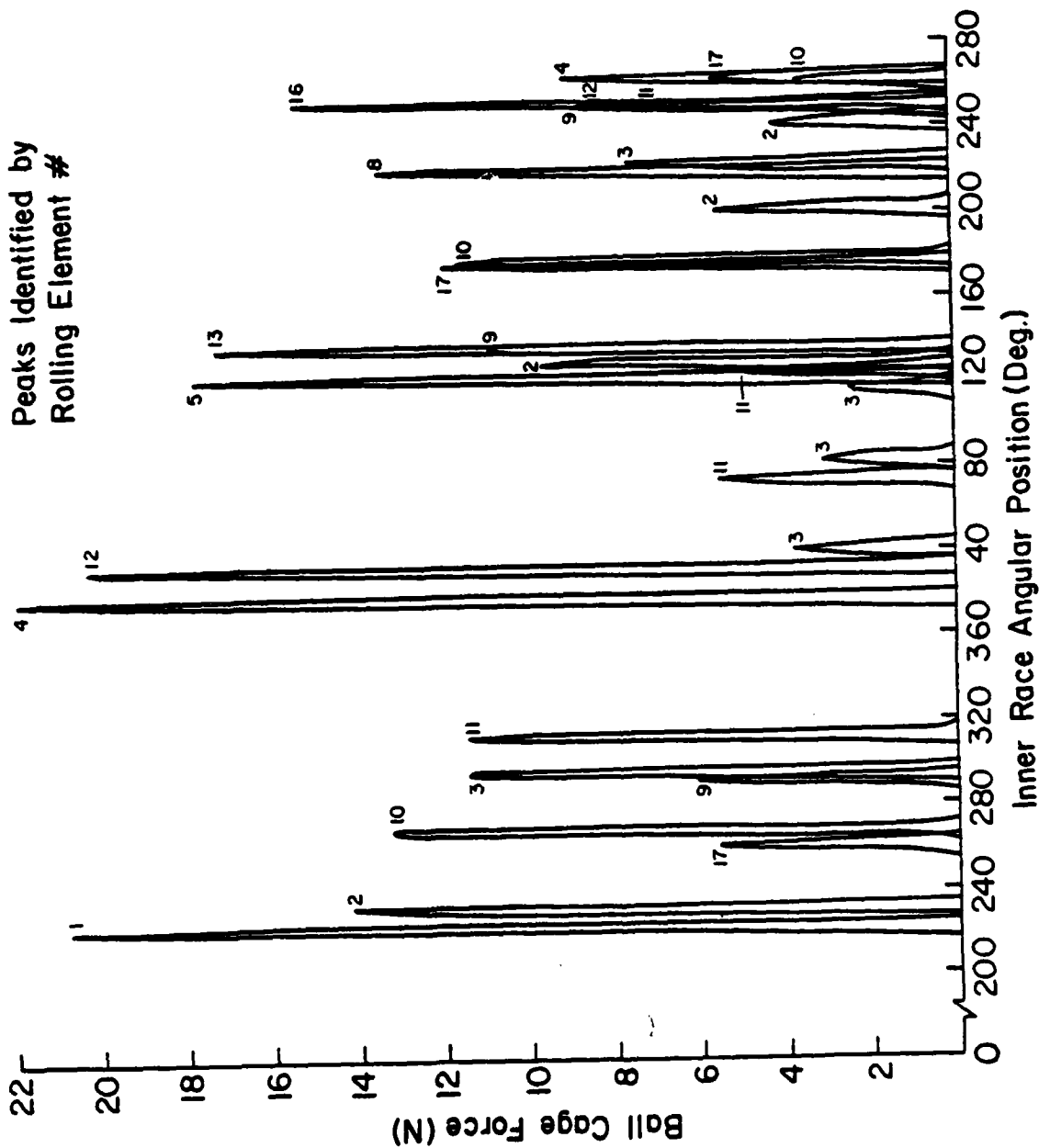


Fig. 2-4 Typical Ball/Cage Collisions in an Angular Contact Ball Bearing with Combined Axial and Radial Load

angular velocity, ball orbital velocity, ball pass frequency (rate at which a given point on the race is passed by the balls) etc. All of these frequencies may not be constant depending on the operating conditions. In fact, the variation in ball angular velocity may sometimes be quite large. This can be easily illustrated if the equations of ball angular motion are written in a coordinate frame rotating with a velocity  $\dot{\theta}$  which is also the ball orbital velocity:

$$I\dot{\omega}_1 = G_1$$

$$I\dot{\omega}_2 - I\omega_3\dot{\theta} = G_2$$

$$I\dot{\omega}_3 + I\omega_2\dot{\theta} = G_3$$

Where  $I$  is the ball moment of inertia,  $\vec{\omega}$  is the angular velocity and  $\vec{G}$  is the applied moment vector.

If, for instance, the applied moment is zero, then  $\omega_1$  will be constant and  $\omega_2$  and  $\omega_3$  will be governed by

$$\dot{\omega}_2 - \omega_3\dot{\theta} = 0$$

$$\dot{\omega}_3 + \omega_2\dot{\theta} = 0$$

or  $\ddot{\omega}_3 + \omega_3\dot{\theta}^2 = 0$  assuming  $\dot{\theta}$  to be constant and also  $\ddot{\omega}_2 + \omega_2\dot{\theta}^2 = 0$ .

Thus both  $\omega_2$  and  $\omega_3$  will have a cyclic variation with a frequency of  $\dot{\theta}$ . The nature of the applied moment  $\vec{G}$  and its dependence on ball angular velocity will of course greatly influence the ultimate motion of the balls.

As will be discussed in the next section, a knowledge of all of the above characteristic motions is necessary if any constraints on the ball motion are considered. In particular the knowledge of differences between the various components will be very useful and two classes of problems may be considered:

Class I: All frequencies are of the same general order

Class II: There is a distinct difference between the "very low" and "very high" frequency components.

Class I will be relevant for a relatively large bearing operating at very high speeds and Class II will apply to most small to moderate size bearings in a wide operating environment and large bearings operating at very low speeds, such as the DMA bearings. For the Class I system a generalized motion of each element must be determined while certain constraints can be imposed on Class II systems depending on the frequency range of interest. Also, some constraints may apply to class I system if the amplitudes of motion of certain components are very small compared to other components. A more extensive discussion of this subject is presented in the next section in terms of the modifications to the computer program DREB.

### 3.0 DREB MODIFICATIONS AND RAPIDREB DEVELOPMENTS

The available Dynamics of Rolling Element Bearings (DREB) computer program has been enhanced for several added capabilities for ball bearing performance simulation. The roller bearing capabilities of DREB have been suppressed in this enhanced version named RAPIDREB. All program modifications are centered around speeding up the computation and examining the low frequency behavior in the generalized performance simulation. Hence the modifications fall in two categories:

1. Suppression of High Frequency Content
2. Improved integrating algorithms.

Aside from the above, a minor modification to extend the program capabilities to treat ball guided cages for DMA bearings has also been made. This section of the report briefly discusses all these program enhancements.

#### 3.1 Suppression of High Frequency Content

As discussed in the preceding section there are certain high frequency characteristics present in the general performance simulation of ball bearings. A careful suppression of these frequencies is necessary to efficiently simulate the low frequency phenomenon specially because the time step size in the numerical integration algorithm is determined by the highest frequency present in the system. DREB is modified in two ways to suppress the high frequency motion, e. g., ball motion constraints and suitable damping.

##### 3.1.1 Ball Motion Constraints

The very high frequency motion results from ball vibration between the two races. Both the elastic contact frequency and the kinematic frequency represent the motion of ball mass center relative to the supporting races, as discussed in the preceding section. If the applied loads on the bearing are free of any high frequency vibrational loads, the amplitudes of the ball vibration are generally small and the resulting changes in contact loads are fairly insignificant when compared with the nominal loads. Thus it may be reasonable to constrain the ball such that the ball center follows a definite path which satisfies equilibrium of all normal contact forces acting on the ball including the centrifugal forces. The traction forces,

being quite small compared to the normal forces, may be neglected in the equilibrium equations. Also an equilibrium of forces is carried out on the inner race and its motion is constrained to satisfy such an equilibrium. Such constraints are reasonable for all static applied loads and constant races speeds. They are also applicable to time varying loads and speeds provided the frequency of such variations is very small compared to the characteristic ball/race vibration frequencies. Thus moderate race accelerations and synchronous loading due to unbalance can be satisfactorily treated within the realm of such equilibrium constraints.

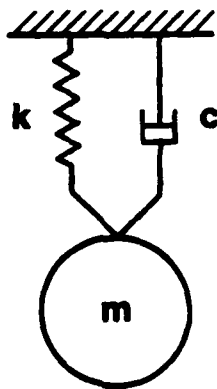
It is true that the process of imposing the above constraints is similar to obtaining the conventional quasi-static solutions at each time step and hence a set of non-linear algebraic equations has to be solved. This may appear to be quite time consuming but even for relatively large steps, allowable by ball/race traction phenomenon, the changes in the equilibrium conditions are rather small and therefore the convergence of the equilibrium equations is very rapid. Thus in spite of the additional effort of solving the equilibrium equations at each step, the equilibrium constraints result in a substantial reduction in the overall computational effort, primarily due to the relatively large time step size permissible by suppressing the very high frequency motion.

### 3.1.2 Damping Considerations

There may be some damping considerations which can assist in eliminating certain high frequencies. It is true that actual damping at any contact interface in the bearing is quite small and therefore the introduction of any damping will be "fictitious" with the prime objective of eliminating the high frequency response without significantly altering the very low frequency behavior.

Any contact interface can be modeled in terms of a spring with stiffness  $k$  (N/M) and a dashpot with damping  $C$  (NS/M) as shown in Figure 3-1. The contact stiffness will be known from the Hertzian contact parameters at the particular contacts and the damping coefficient will be the required input. Perhaps specification of damping will be best in terms of a damping ratio  $C/C_c$ , where  $C_c$  is called critical damping [7] corresponding to the





812820

Fig. 3-1 Simple Spring and Damper Model for any Contact Interface

undamped natural frequency of the system.

$$\text{Damping ratio } \zeta = C/C_c$$

$$\text{Where } C_c = 2m\omega_n$$

$$\omega_n = \sqrt{\frac{k}{m}}$$

Thus  $\zeta$  can be specified for the ball/race, ball/cage and cage/race interfaces. For the purpose of "real" damping  $\zeta$  will be very small for most steels but for certain nonmetals used for fabricating the cages it may be appreciable. In any event any non-zero value of  $\zeta$  will only effect the general response in the neighborhood of the undamped natural frequency  $\omega_n$  [7] and the response at very low frequencies will be practically unchanged.

Each contact interface in the bearing is modeled in terms of the above simplified vibration model and the computer program DREB is modified accordingly.

### 3.2 Integrating Algorithms

Algorithms used to integrate a system of first order differential equations may be either of implicit or explicit type. The implicit algorithms are better known as the predictor corrector formulae and such schemes can be very efficient if no discontinuities and high frequency oscillatory motions are present. These methods make use of a set of existing solutions to extrapolate to an expected solution at the current time step and this is called the prediction step. With the predicted values the derivatives are computed and corrections to the predicted values are applied in an iterative manner. Normally two to three correction iterations are enough for most non-stiff systems. If no high frequency motion exists in the bearing and if there are no discontinuities in the solutions the predictor-corrector process can provide a relatively large time step and therefore speed up the computation in the desired time domain. However, if discontinuities are present, such as ball/cage or race/cage collisions, the extrapolation process may not be realistic and the integration process as a whole will exhibit stability problems. For such cases an explicit formula, better known as the Runge-Kutta method, which makes use of only one solution to march to the

next step will probably be the best choice.

DREB is modified to incorporate both implicit and explicit methods, with appropriate step changing criterion. The step changing process generally depends on the local truncation error at each step. An estimate of this error is quite straight forward for an implicit method but it may be quite difficult for an explicit method. On the other hand treatment of variable size steps is trivial for an explicit scheme while considerable complications arise in the extrapolation process of the predictor. A special predictor-corrector formula in terms of a divided difference notation is therefore developed to efficiently carry out the extrapolation. Some suitable explicit Runge-Kutta methods are then reviewed with particular emphasis on error estimates and step changing rationale.

### 3.2.1 Adams Type Predictor-Corrector in Divided Differences

A predictor-corrector algorithm for a differential equation with one dependent variable is developed in this section. The extension of the algorithm to a system is quite obvious. Let the governing differential equation be written as:

$$\frac{\partial y}{\partial x} = f(x, y), \quad (1)$$

with initial condition  $y_0 = y(x_0)$ .

It will be further assumed that solutions in the domain  $0 \leq x \leq x_n$  have been obtained by some explicit algorithm and the predictor-corrector formula, to be developed here, will advance the solution from  $x_n$  to  $x_{n+1}$ . The process can be written as:

$$y_{n+1} = y_n + \int_{x_n}^{x_{n+1}} f(x, y) dx \quad (2)$$

With certain polynomial approximations to  $f(x, y)$ , the required algorithm can be developed. The formulation presented below is very similar to the conventional Adams-Bashford-Moulton formulae.

#### 3.2.1.1 Predictor Formula

Let the solutions  $(y_n, y_{n-1}, \dots, y_{n-N})$  and the derivatives  $(f_n, f_{n-1}, \dots, f_{n-N})$  be available at the  $(N+1)$  points  $(x_n, x_{n-1}, \dots, x_{n-N})$  and for any  $x$ , let the

derivative  $f(x)^*$  be a Nth order polynomial passing through the points  $(x_n, x_{n-1}, \dots, x_{n-N})$ , i.e.:

$$f(x) = f(x_n) + \sum_{i=1}^N (x-x_n)(x-x_{n-1}) \dots (x-x_{n-i+1}) f[x_n, x_{n-1}, \dots, x_{n-i}] \\ + (x-x_n)(x-x_{n-1}) \dots (x-x_{n-N}) f[x_n, x_{n-1}, \dots, x_{n-N}, \xi] \quad (3)$$

Where  $x_{n-N} \leq \xi \leq x_{n+1}$  and the conventional divided difference notation [8] is used. The divided difference notation will be convenient for step size change and will eliminate the need for interpolation to points spaced uniformly with a constant grid spacing.

The predictor formula is obtained by substituting the polynomial approximation, equation (3), in equation (2). Thus

$$y_{n+1} = y_n + \sum_{i=0}^N f[x_n, x_{n-1}, \dots, x_{n-i}] \sum_{j=0}^{i-1} \frac{x_{n+1} - x_n}{(j+1)} \cdot A_j \\ + f[x_n, x_{n-1}, \dots, x_{n-N}, \xi] \sum_{j=0}^{N-1} \frac{x_{n+1} - x_n}{(j+1)} \cdot A_j \quad (4)$$

Where  $A_j$  are the coefficients of the polynomial

$$(x-x_n)(x-x_{n-1}) \dots (x-x_{n-i}) \equiv A_0 + A_1 x + A_2 x^2 + \dots + A_{i+1} x^{i+1}$$

Note that estimate of  $\xi$  will be required in order to estimate the truncation error term of equation (4). It will be reasonable to assume  $\xi = x_{n+1}$  and the corresponding solution as the predicted value.

From computational standpoint, it may be noted that as the order N increases, the term multiplying the polynomial coefficient  $A_j$  may experience a round off problem, which can be eliminated by scaling the independent variable as

---

\* Note the change in notation: the derivative is actually a function of y also, notation used here is  $f(x) = f(x, y)$ .

$$S \equiv \frac{x - x_p}{x_{p+1} - x_p} = \frac{x - x_p}{\Delta_p} \quad (5)$$

so that the polynomial

$$(x - x_n)(x - x_{n-1}) \dots (x - x_{n-j}) \equiv \Delta_p^{j+1} (S - x_n^*)(S - x_{n-1}^*) \dots (S - x_{n-j}^*)$$

where  $x_j^* = (x_j - x_p)/\Delta_p$

Also if  $p=n$ , the integral of equation (2) takes the convenient form:

$$\begin{aligned} \int_{x_n}^{x_{n+1}} \{(x - x_n) \dots (x - x_{n-j})\} dx &= \Delta_n^{j+2} \int_0^1 \{(S - x_n^*)(S - x_{n-1}^*) \dots (S - x_{n-j}^*)\} dS \\ &= \Delta_n^{j+2} \sum_{k=0}^{j+1} \frac{A_k^*}{k+1} \end{aligned} \quad (6)$$

Where  $A_k^*$  are coefficients of the polynomial

$$(S - x_n^*) \dots (S - x_{n-j}^*) \equiv A_0^* + A_1^* S + \dots + A_{n-j+1}^* S^{n-j+1}$$

Substituting (5) and (6) in equation (4) gives the final predictor formula

$$\begin{aligned} y_{n+1} = y_n + \sum_{i=0}^N f[x_n, x_{n-1}, \dots, x_{n-i}] \Delta_n^{i+1} \sum_{j=0}^i \frac{A_j^*}{j+1} \\ + f[x_n, x_{n-1}, \dots, x_{n-N}, x_{n+1}] \Delta_n^{N+2} \sum_{j=0}^{N+1} \frac{A_j^*}{j+1} \end{aligned} \quad (7)$$

It can easily be seen from equation (5) that the coefficients  $A_j^*$  will only have to be computed if the grid in  $x$  is non-uniform.

### 3.2.1.2 Corrector Formula

For the general corrector formula, let  $f(x)$  be a polynomial of degree  $M$ , passing through the  $(M+1)$  points  $(x_{n+1}, x_n, x_{n-1}, \dots, x_{n-M+1})$ . Again using the divided difference notations

$$\begin{aligned} f(x) = f(x_{n+1}) + \sum_{i=0}^{M-1} (x - x_{n+1})(x - x_n) \dots (x - x_{n-i+1}) f[x_{n+1}, x_n, x_{n-1}, \dots, x_{n-i}] \\ + (x - x_{n+1})(x - x_n) \dots (x - x_{n-M+1}) f[x_{n+1}, x_n, \dots, x_{n-M+1}, \xi] \end{aligned} \quad (8)$$

Substitution of (8) in equation (2) gives the required corrector formula.

$$y_{n+1} = y_n + \sum_{i=-1}^{M-1} f[x_{n+1}, x_n, \dots, x_{n-i}] \sum_{j=0}^{i+1} \frac{x_{n+1}^{j+1} - x_n^{j+1}}{(j+1)} B_j \\ + f[x_{n+1}, x_n, \dots, x_{n-M+1}, \xi] \sum_{j=0}^{M+1} \frac{x_{n+1}^{j+1} - x_n^{j+1}}{(j+1)} B_j \quad (9)$$

Where  $B_j$  are coefficients of the polynomial

$$(x - x_{n+1})(x - x_n)(x - x_{n-1}) \dots (x - x_{n-i}) \equiv B_0 + B_1 x + \dots + B_{i+2} x^{i+2}$$

Again an estimate of the truncation error will require the value of  $\xi$  which may be assumed as  $x_{n-M}$ , which demands that one additional data point is available. This demand is easily met if  $M \leq N$ .

Scaling the independent variable again, as done for the predictor formula will give the final corrector algorithm:

$$y_{n+1} = y_n + \sum_{i=-1}^{M-1} f[x_{n+1}, x_n, \dots, x_{n-i}] \Delta_n^{i+2} \sum_{j=0}^{i+1} \frac{B_j^*}{j+1} \\ + f[x_{n+1}, x_n, \dots, x_{n-M+1}, x_{n-M}] \Delta_n^{M+2} \sum_{j=0}^{M+1} \frac{B_j^*}{j+1} \quad (10)$$

As for the predictor formula, the coefficients  $B_j^*$  will only have to be computed for non-uniform grid. Also it can be easily seen that the truncation error will employ the last term in the divided difference table and it will be proportional to  $\Delta_n^{M+2}$ .

### 3.2.1.3 Computation of Coefficients

In order to implement equations (7) and (10) a formula for computing the coefficients of the polynomial

$$P \equiv (x - x_n)(x - x_{n-1}) \dots (x - x_{n-p})$$

will be required.

By expanding the polynomial for  $p = 1, 2, 3, 4$  and by noting the algebraic similarities in the expansions, the polynomial can be written in the following general form:

$$P \equiv x^{p+1} + \sum_{k=1}^{p+1} x^{p-k+1} (-1)^k \sum_{i_1=1}^{p-k+2} x_{n-i_1+1} \sum_{i_2=i_1+1}^{p-k+3} x_{n-i_2+1} \dots \sum_{i_j=i_{j-1}+1}^{p-k+j+1} x_{n-i_j+1} \dots$$

$$\dots \sum_{i_k=i_{k-1}+1}^{p+1} x_{n-i_k+1} \quad (11)$$

The above formula can be coded once the maximum value of  $p$  is assigned.

#### 3.2.1.4 Step Changing Criterion

The step size can be changed at any time in the above formulation by knowing the truncation error at the preceding step size and the allowable limit. Let us assume that the order of corrector is equal to that of the predictor ( $M=N$ ) and hence the above algorithm is a  $(N+1)$  step process. The truncation error of the predictor-corrector step will now be given by the truncation error of the corrector step only [9]. Thus error committed in arriving at  $x_{n+1}$ , from  $x_n$  is given by:

$$\frac{E_{n+1}}{\Delta_n^{N+2}} = f[x_{n+1}, x_n \dots x_{n-N}] \sum_{j=0}^{N+1} \frac{B_j^*}{j+1} \quad (12)$$

An estimate of step  $\Delta_{n+1}$  in going from  $x_{n+1}$  to  $x_{n+2}$  can be obtained from the relation:

$$\Delta_{n+1} = \frac{\Delta_n}{C} \left( \frac{\epsilon}{E_{n+1}} \right)^{\frac{1}{N+2}} \quad (13)$$

Where  $\epsilon$  is the allowable truncation limit and  $C (> 1)$  is a constant, which arbitrarily reduces the computed step size with the expectation that the tolerance criterion will be met at  $x_{n+2}$ . The value of  $C$  may be selected primarily by experience, it may vary from 1.2 to 2.0. Also it should be noted that any time the step size is changed all coefficients will have to be computed for  $N+1$  steps (assuming that no step change occurs within these steps) and hence this added work may outweigh the savings in increased step size. It is therefore recommended that the step size be changed only if the following conditions is met:

$$\frac{\Delta_{n+1}}{\Delta_n} > a \quad (14)$$

Where  $a$  is a constant, again selected by experience; it may be assumed as 1.25 as a first approximation.

Equation (13) can also be used to reduce the step size at any time, if the truncation limit is not met.

From a practical standpoint, upper and lower limits to the step size are assigned and the objective of the step changing rationale is to keep the step size to a maximum within this range. Also if the truncation limit is not met for a specified number of steps then further integration should be terminated.

#### 3.1.2.5 Change of Order

A criterion for change of order is not very clear and generally a trial and error approach is used. At a given time, solutions with the order reduced and increased by one are computed and the order giving minimum truncation is selected. Similar to the step size the maximum and minimum bounds on the order should also be assigned. The maximum order can generally be determined by examining the divided differences which will generally decrease with increase of order. However, the computed values may show an increasing trend at very high order, which will commonly be due to machine round off errors. Thus the maximum order should be limited by this phenomenon. Selection of minimum order will primarily be by experience with the problem being investigated.

#### 3.1.2.6 Computational Considerations

In developing a computer code for implementing the above formulation, certain considerations will be helpful:

1. Set a maximum limit on the order and hence the number of solutions to be stored.
2. Compute divided differences of derivatives at the first call and upgrade table at subsequent calls by adding the latest solution and deleting the earliest solution.



3. Check grid uniformity and compute coefficients (in subsequent calls) only in case of non-uniformity resulting from step size change.
4. Check maximum allowable order by examining the divided difference table and make sure that the current order is less than this maximum.
5. Store the entire divided difference table in disc file at the end of the run for subsequent restarts of the program.

### 3.2.2 Explicit Runge-Kutta Type Algorithms

As discussed earlier an explicit formula is required for two purposes. First for integrating the equations in the domain of time where there are either discontinuities or large cyclic variations at relatively high frequency. Secondly an explicit formula is required to start the implicit predictor-corrector process. Also it is required that some estimate of the local truncation error be available in order to establish some criterion for changing the step size.

The existing DREB program employs a Runge-Kutta-Merson method [9] which does estimate the truncation error. It is a fourth order process and requires an additional function evaluation for estimating the error. Hence a total of five function evaluations per step are used. There have been some questions about the accuracy of the error estimate provided by this method particularly when the equations are non-linear. Hence methods due to Scranton and England have appeared in the literature [10]. The Scranton method also uses five function evaluation but the error estimate is only realistic for a single equation and its validity to a system of equations is questionable. The England method attempts to resolve this problem by an additional function evaluation per step and it is therefore a six stage process. More recently Fehlberg [11] has provided another six stage formula which has been of considerable use in recent years. Since the selection of a method really depends on the problem under consideration, which in the case of a ball bearing can be quite complicated by the operating conditions, both the formulae due to England and Fehlberg are incorporated in the RAPIDREB version of DREB.

All of the explicit formulae can be best summarized in terms of tabular notation [12]. Thus with given solution  $y_n$  at the  $n$ th step, the solution  $y_{n+1}$  at  $(n+1)$ th step is given by

$$y_{n+1} = y_n + \sum_{i=1}^n \gamma_i k_i \quad (15)$$

where

$$k_i = h f(y_n + \sum_{j=1}^{i-1} \beta_{ij} k_j) \quad i = 1, \dots, n \quad (16)$$

and the estimate of local truncation error  $E_{n+1}$  is given by

$$E_{n+1} = \sum_{i=1}^n \gamma_i^* k_i \quad (17)$$

The values of  $\beta$ ,  $\gamma$  and  $\gamma^*$  for the three methods discussed above are given in Tables 3.1 to 3.3.

All of the above methods are fourth order. For improved accuracy a higher order method may sometimes be desirable, e.g., in a detailed simulation of one ball/cage collision. With this objective a fifth order Kutta-Nystrom method [10] and a sixth order (eight stage) Huta method [10] are also incorporated in the computer program. The coefficients of these methods are given respectively in Tables 3.4 and 3.5. For these methods since  $\gamma^*$  is not available a step doubling technique is used to compute the truncation error. In other words the computation at each step is done twice, first with the prescribed step size and then with half the prescribed step size. Thus the computation with these methods can be very expensive but the solutions obtained will be extremely accurate. Just for reference purposes the classical fourth order Runge-Kutta method, the fourth order Ralston-Runge-Kutta method, and the third and second order Runge-Kutta methods are also incorporated in the computer program. Again a step doubling technique is used in all these methods and hence considerable care must be exercised in their use. The coefficients for all these methods are fairly well known and they are summarized in Tables 3.6 to 3.9 for completeness.

TABLE 3.1  
COEFFICIENTS FOR THE RUNGA-KUTTA-MERSON METHOD

i	$\beta_{ij}$				$\gamma_i$	$\gamma_i^*$
1					$\frac{1}{6}$	$-\frac{1}{3}$
2	$\frac{1}{3}$				0	0
3	$\frac{1}{6}$	$\frac{1}{6}$			0	$-\frac{3}{2}$
4	$\frac{1}{8}$	0	$\frac{3}{8}$		$\frac{2}{3}$	$-\frac{4}{3}$
5	$\frac{1}{2}$	0	$-\frac{3}{2}$	2	$\frac{1}{6}$	$\frac{1}{6}$

TABLE 3.2  
COEFFICIENTS FOR THE RUNGA-KUTTA-ENGLAND METHOD  
 $n = 6$

i	$\beta_{ij}$					$\gamma_i$	$\gamma_i^*$
1						$\frac{1}{6}$	$-\frac{1}{8}$
2	$\frac{1}{2}$					0	0
3	$\frac{1}{4}$	$\frac{1}{4}$				$\frac{2}{3}$	$-\frac{2}{3}$
4	0	-1	2			$\frac{1}{6}$	$-\frac{1}{16}$
5	$\frac{7}{27}$	$-\frac{10}{27}$	0	$\frac{1}{27}$		0	$\frac{27}{56}$
6	$\frac{28}{625}$	$-\frac{1}{5}$	$\frac{546}{625}$	$\frac{54}{625}$	$-\frac{378}{625}$	0	$\frac{125}{336}$

TABLE 3.3  
COEFFICIENTS FOR THE RUNGA-KUTTA-FEHLBERG METHOD

$n = 6$

$i$	$\beta_{ij}$					$\gamma_i$	$\gamma_i^*$
1						$\frac{16}{135}$	$\frac{1}{360}$
2	$\frac{1}{4}$					0	0
3	$\frac{3}{32}$	$\frac{9}{32}$				$\frac{6656}{12825}$	$\frac{196992}{6579225}$
4	$\frac{1932}{2197}$	$-\frac{7200}{2197}$	$\frac{7296}{2197}$			$\frac{28561}{56430}$	$\frac{41743}{1429560}$
5	$\frac{439}{216}$	- 8	$\frac{3680}{513}$	$-\frac{845}{4104}$		$-\frac{9}{50}$	$\frac{1}{50}$
6	$-\frac{8}{27}$	2	$-\frac{3544}{2565}$	$\frac{1859}{4104}$	$-\frac{11}{40}$	$\frac{2}{55}$	$\frac{2}{55}$

TABLE 3.4  
COEFFICIENTS FOR THE FIFTH ORDER KUTTA-NYSTROM METHOD

$n = 6$

$i$	$\beta_{ij}$					$\gamma_i$
1						$\frac{23}{192}$
2	$\frac{1}{3}$					0
3	$\frac{4}{25}$	$\frac{6}{25}$				$\frac{125}{192}$
4	$\frac{1}{4}$	- 3	$\frac{15}{4}$			0
5	$\frac{2}{27}$	$\frac{10}{9}$	$-\frac{50}{81}$	$\frac{8}{81}$		$-\frac{27}{64}$
6	$\frac{2}{25}$	$\frac{12}{25}$	$\frac{2}{15}$	$\frac{8}{75}$	0	$\frac{125}{192}$

TABLE 3.5  
COEFFICIENTS FOR THE SIXTH ORDER (EIGHT STAGE) HUTTA METHOD

$n = 8$

$i$	$B_{ij}$							$\gamma_i$
1								$\frac{41}{840}$
2	$\frac{1}{9}$							0
3	$\frac{1}{24}$	$\frac{1}{8}$						$\frac{9}{35}$
4	$\frac{1}{6}$	$-\frac{1}{2}$	$\frac{2}{3}$					$\frac{9}{280}$
5	$-\frac{5}{8}$	$\frac{27}{8}$	$-3$	$\frac{3}{4}$				$\frac{34}{105}$
6	$\frac{221}{9}$	$-109$	$\frac{289}{3}$	$-\frac{34}{3}$	$\frac{1}{9}$			$\frac{9}{280}$
7	$-\frac{183}{48}$	$\frac{113}{8}$	$-\frac{53}{6}$	$-\frac{11}{8}$	$\frac{10}{6}$	$\frac{1}{16}$		$\frac{9}{35}$
8	$\frac{358}{41}$	$-\frac{2079}{82}$	$\frac{501}{41}$	$\frac{417}{41}$	$-\frac{227}{41}$	$-\frac{9}{82}$	$\frac{36}{41}$	$\frac{41}{840}$

TABLE 3.6  
COEFFICIENTS OF THE CLASSICAL FOURTH ORDER  
RUNGA-KUTTA METHOD

$n = 4$

$i$	$B_{ij}$			$\gamma_i$
1				$\frac{1}{6}$
2	$\frac{1}{2}$			$\frac{1}{3}$
3	$\frac{1}{2}$	$\frac{1}{2}$		$\frac{1}{3}$
4	1	0	1	$\frac{1}{6}$

TABLE 3.7

COEFFICIENTS OF THE FOURTH ORDER RALSTON-RUNGA-KUTTA METHOD

$n = 4$

$i$	$\beta_{ij}$			$\gamma_i$
1				0.17476028
2	0.40			- 0.55148053
3	0.29697760	0.15875966		1.20553547
4	0.21810038	- 3.05096470	3.83286432	0.17118478

TABLE 3.8

COEFFICIENTS OF THE THIRD ORDER RUNGA-KUTTA METHOD

$n = 3$

$i$	$\beta_{ij}$		$\gamma_i$
1			$\frac{1}{4}$
2	$\frac{1}{3}$		0
3	0	$\frac{2}{3}$	$\frac{3}{4}$

TABLE 3.9

COEFFICIENTS OF THE SECOND ORDER RUNGA-KUTTA METHOD $n = 2$ 

$i$	$\beta_{ij}$	$\gamma_i$
1		$\frac{1}{2}$
2	1	$\frac{1}{2}$

### 3.3 Modifications for Ball/Cage Guidance in DMA Bearings

An analytical model for the ball guided cages has been presented earlier [13]. The model assumes a conical end on a cylindrical pocket as shown in Figure 3-2. It is really a purely geometric interaction model in the sense that the ball center is located with respect to the center of the cone base. This is shown as vector  $\vec{r}_{bp}^p$  in the pocket frame in Figure 3-2.

In order to determine the magnitude of interaction with the conical surface, it will be convenient to transform  $\vec{r}_{bp}^p$  into cylindrical coordinates  $(r, \theta, z)$  such that

$$\begin{aligned} r &= \sqrt{(\tilde{r}_{bp_1}^p)^2 + (\tilde{r}_{bp_2}^p)^2} \\ \theta &= \arctan(-\tilde{r}_{bp_1}^p / \tilde{r}_{bp_2}^p) \\ z &= \tilde{r}_{bp_3}^p \end{aligned} \tag{17}$$

The angle  $\theta$  measured as positive rotation about the  $z$  axis from the  $y$  axis will also denote the contact angle for the cage cone contact. It should be noted that if the cone exists on the inner diameter of cage the positive  $z$  axis will be pointing radially inwards and the  $y$  axis will also be rotated by  $180^\circ$ .

From simple geometry it may be shown that a unit vector along the normal to the conical surface from the center of the ball is given by

$$\vec{e}_{bp}^p = \begin{pmatrix} \cos\phi \sin(\theta + \theta') \\ \cos\phi \sin(\theta + \theta') \\ \sin\phi \end{pmatrix} \tag{18}$$

where  $\phi$  is the cone angle and the angle  $\theta$  is measured from the line denoting maximum interaction. Thus  $\theta' = 0$ , will correspond to the unit vector along maximum interaction.

The interaction  $\delta_{bp}$  is given by



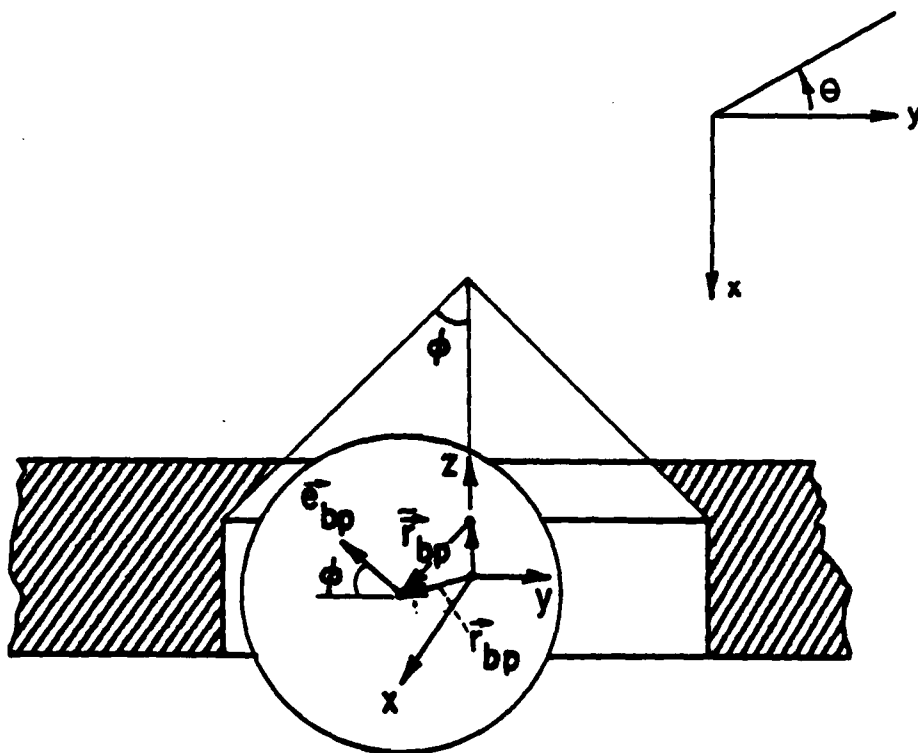


Fig. 3-2 Exaggerated Pocket Geometry For a Ball Riding Cage

812825

$$\delta_{bp}(\theta') = \left(\frac{d}{2} + \Delta_{bp}\right) \cos\phi - \vec{r}_{bp}^p \cdot \vec{e}_{bp}^p - \frac{d}{2} \quad (19)$$

It may be noted that since  $\vec{e}_{bp}^p$  is a function of  $\theta'$ , the interaction will depend on  $\theta'$  and it will be necessary to determine the range of  $\theta'$  for which  $\delta_{bp}$  is negative. This range will also determine the length of interaction. Also by straightforward geometry, the relative position of the ball center and the length of the conical surface will determine if the vector  $\vec{e}_{bp}^p$  falls on the given surface or not. The interaction analysis will only be performed when the vector  $\vec{e}_{bp}^p$  falls on the given cage surface. Once the point of contact has been established the relative slip velocity can be readily defined in terms of the ball and cage velocities.

For the computed geometric interference, the normal load is approximated by either a Hertzian point or line contact, depending on the contact arc length. This is certainly an approximation because the contact between a sphere and a cone is not really Hertzian and the true solution will require a generalized three-dimensional elastic contact analysis. The tractive forces are computed by substituting the calculated slip velocities in the prescribed traction-slip relation. For the line contact the contact arc is divided into several incremental areas and an integration is performed to compute the normal and traction forces.

#### 3.4 Recommendations for Using the RAPIDREB Version of DREB

All of the above enhancements are incorporated into the DREB program to create the new version RAPIDREB. In addition, with the objective of making the program efficient for ball bearings, the roller bearing parts and some special output options of DREB have been eliminated. Depending on the operational conditions, the computation effort in RAPIDREB may be significantly reduced if proper options are exercised. Some useful guidelines to this effect are therefore presented here:

1. If elastohydrodynamic lubrication exists it is recommended that a few time steps be run on the original DREB program and typical traction curves be printed out. Thus a ball to ball variation in traction

may be studied and a judgement can be made if the traction behavior can be approximated by a single curve and thereby eliminating all EHD computations at each step. If so, such a curve must be approximated for RAPIDREB.

2. For purely thrust loaded bearings the ball constraints can be set such that the load computation is performed only once. This will significantly effect the computational effort.
3. Bearings with a combined radial and thrust load may also employ ball/race constraints by performing an equilibrium analysis at each time step. This may result in an increase in the computational effort per step but the total effort will be greatly reduced by permitting the maximum step size to be much larger in absence of any high frequency motions.
4. Considerable care must be exercised in selecting the integration method. By extensive running of RAPIDREB it is found that the predictor-corrector scheme performs very well for cageless bearings with ball/race constraints. Hence this method is not recommended for most bearings with cage, where large discontinuities in the solutions may be present. The Fehlborg and England formulae do sometimes provide an increase in permissible step size but an increased function evaluation at every step adds to the effort per step. The benefit of these methods may only be investigated for prescribed application by a few trial runs. Any of the higher order methods provide extreme accuracy but they may be very time consuming and hence these methods should only be used in very small time domains.
5. For investigating the effects of small perturbations in the operating conditions, a steady state solution under nominal conditions must be obtained first and it should be used for determining the initial conditions for subsequent parametric runs.

6. Proper error processing control must be used to process time limit errors in order to store all the generated data files in the event an CP time limit is encountered. This is normally done by using the EXIT control statement on the CDC systems.

Appendix A contains the description of the input data to the RAPIDREB versions of both the main program RDREB and the plotting program RDREBP. The plot program is almost identical to the original version except for a few enhancements for handling large quantities of data and properly truncating the curves if they exceed the plot limits. This can be easily understood from the input description in Appendix A.

#### 4.0 PERFORMANCE SIMULATION OF DMA BEARINGS

Ball bearings used in DMA (Despun Mechanical Assembly) systems are generally very large bearings operating at very low pure thrust loads and speeds. However, they are designed for a long time of continuous operation (of the order of ten years). The lubricant is sealed into the bearing at the time of assembly and hence lubricant degradation or starvation is not an uncommon problem. Also the nature of friction at ball/cage interface has been a suspect for cage instability in such applications.

Simulation of the dynamic performance of such bearings can be obtained for extended time domains by using the equilibrium constraints on ball motion in the RAPIDREB version of the computer program. This basically eliminates the ball/race natural vibration and thereby allows a substantially large time step to integrate the differential equations of motion over more than a shaft revolution. Such simulations are the subject of this section.

#### 4.1 Bearing Geometry

Two different geometrical configurations of the DMA bearings are investigated. Figure 4-1 shows the geometrical details of a 100 mm bore angular contact bearing with the cage guided on the inner race and Figure 4-2 displays the design of a 150 mm bore ball bearing with the cage guided on the balls. The guidance surface is of a conical shape and it is attached to the cylindrical pockets on the inner diameter of the cage. Details of the cage geometry are shown in Figure 4-3.

#### 4.2 Operating Conditions

Both bearings operate at relatively low pure thrust loads and speeds, which are typical of actual application. The operating condition assumed for the simulations to be presented here are:

100 mm bearing:	Thrust load	=	178 N
	Inner race speed	=	60 RPM
150 mm bearing:	Thrust load	=	534 N
	Inner race speed	=	62.5 RPM

[illegible]

ЭНД

## BEARINGS

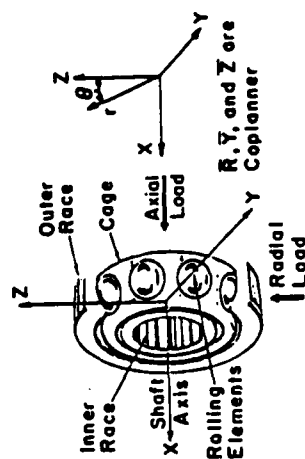
**TIME PERFORMANCE SIMULATION-  
(VERSION RAPIOREB.0)**

**PRADEEP K. GUPTA**  
**L TECHNOLOGY INCORPORATED**  
**ALRANY-SHAKER ROAD**  
**LATHAM, NEW YORK**  
**U. S. A.**

RPM 178N\*\*

## BEARING GEOMETRY

(M)	=	1.00000E-05
(M)	=	1.00000E-05
(M)	=	2.00000E-01
(M)	=	5.20000E-01
(M)	=	5.20000E-01
(M)	=	1.28532E-04
(M)	=	3.50000E-03
(M)	=	4.00000E-04
(M)	=	3.00000E-04



IND (M)	CAGE HALF WIDTH (M)
-03	1.30000E-02
-03	1.30000E-02

**Fig. 4-1 Geometrical Data for the 100 mm DMA Ball Bearing with Inner Race Guided Cage**

The outer race is assumed to be stationary in both cases and the operating temperature of both bearings is assumed to be 15°C. The motion of the cage is considered under the influence of gravity with the bearing axis oriented both along and normal to the direction of gravity. This is really the only factor which will promote cage motion and its interaction with the balls. The two orientations of the bearing with respect to the direction of gravity do represent laboratory conditions.

#### 4.3 Ball/Race Traction Models

Traction behavior of typical lubricants used in DMA bearings is not fully known and a number of assumptions in modelling the behavior are generally made. For the present application a lubricant called Apiezon C + 1.5% antioxidant [14, 15] is considered with the following properties under ambient pressure and at a reference temperature of 15°C.

Viscosity =	0.38425 Pa.S
Pressure-Viscosity Coefficient =	$8.4234 \times 10^{-9}$ 1/Pa
Temperature-Viscosity Coefficient =	6000°K
Thermal Conductivity =	0.10 N/S/°C

Since the traction parameters are not known, the following parameters, which actually correspond to a MIL-L-7808 type oil, are arbitrarily assumed for the Type I traction model discussed by Gupta et al [16].

Viscosity Parameter, $\mu^*$	=	0.58889 Pa
Pressure-Viscosity Parameter, $\alpha^*$	=	$5.22136 \times 10^{-9}$ 1/Pa
Temperature Viscosity Parameter, $\beta^*$	=	$2.48550 \times 10^{-2}$ 1/°K

Also typical of the DMA bearing environment a lubricant starvation factor (distance of lubricant meniscus from the edge of the Hertzian contact zone divided by the major contact half width) of 2 is assumed.

With the above lubricant parameters and the operating conditions outlined earlier the computed elastohydrodynamic traction coefficients for the two bearings are fairly linear with the slide-to-roll ratio, in the range of 0 to 0.10, as shown in Figure 4-4. The lubricant film thicknesses are

[illegible]

# RAPID SIMULATION OF THE

## DYNAMICS OF ROLLING ELEMENT BEARINGS

--A REAL TIME PERFORMANCE SIMULATION-  
(VERSION RAPIDREB.0)

**PRADEEP K. GUPTA**  
**MECHANICAL TECHNOLOGY INCORPORATED**  
**968 ALBANY-SHAKER ROAD**  
**LATHAM, NEW YORK**  
**U. S. A.**

BEARING TYPE -- BALL  
SPEC CODE -- 150MM-DMA-BRG BG-CAGE 62.5RPM 534N\*\*\*

## BEARING GEOMETRY

RORE	(M) = 1.50000E-01	OUTER RACE SHRINK FIT	(M) = 1.00000E-05
OUTSIDE DIAMETER	(M) = 2.25000E-01	INNER RACE SHRINK FIT	(M) = 1.00000E-05
SHAFT INNER DIA	(M) = 1.37000E-01	HOUSING OUTER DIA	(M) = 2.44000E-01
BALL DIAMETER	(M) = 2.22250E-02	NUMBER OF BALLS	16
PITCH DIAMETER	(M) = 1.87500E-01	OUTER RACE CUR FACTOR	= 5.20000E-01
CONTACT ANGLE	(DEG) = 1.80000E+01	INNER RACE CUR FACTOR	= 5.30000E-01
END PLAY	(M) = 6.86790E-04	DIAMETRAL PLAY	(M) = 1.08777E-04
CAGE OUTER DIA	(M) = 1.97104E-01	CAGE OUTER DIA CLS	(M) = 3.98780E-03
CAGE INNER DIA	(M) = 1.77165E-01	CAGE INNER DIA CLS	(M) = 4.28600E-04
EFF CAGE WIDTH	(M) = 3.35280E-02	DIA RF/CAGE CLEARANCE	(M) = 4.06400E-04
RE/CAGE CONE ANG	(DEG) = 3.75000E+01	RE/CAGE CONE HEIGHT	(M) = -3.18353E-03

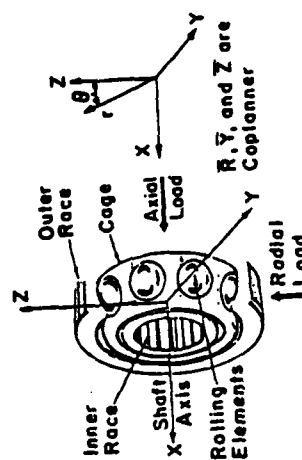
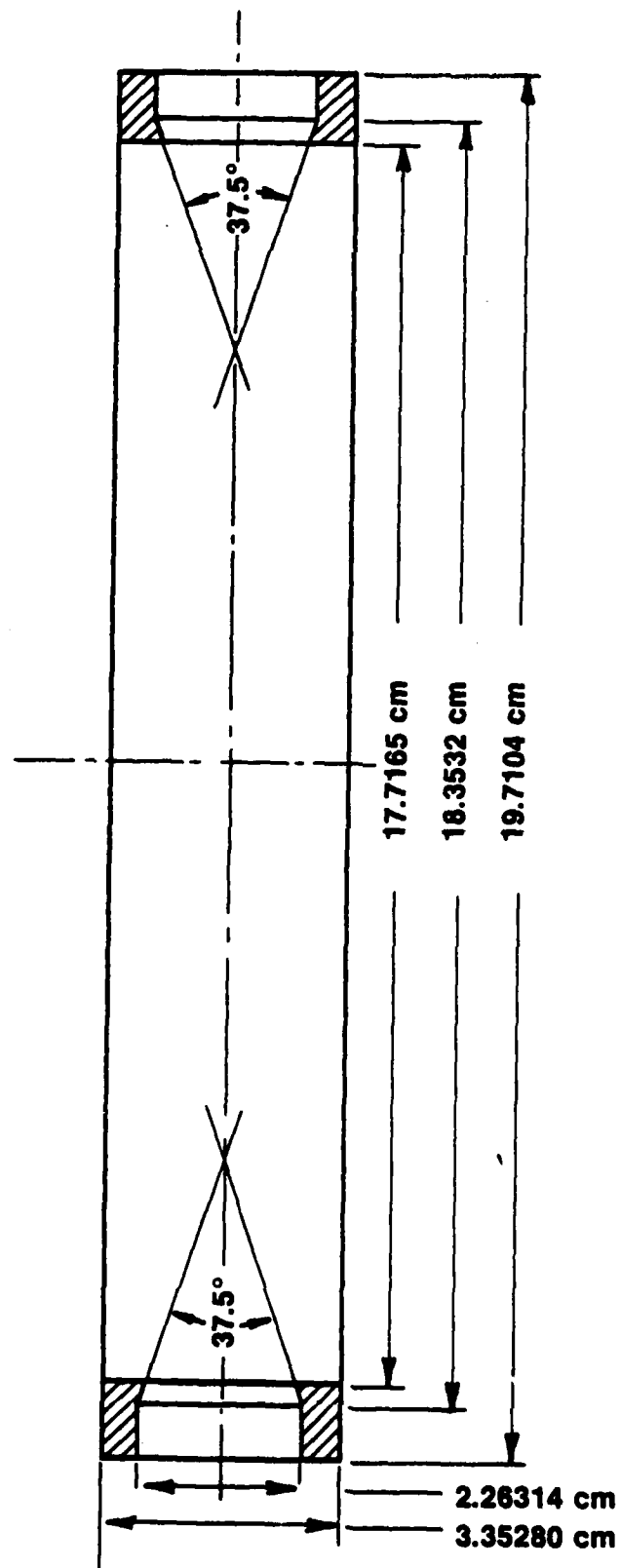


**Fig. 4-2 Geometry of the 150 mm DMA Ball Bearing with Ball Guided Cage**





812822

Fig. 4-3 Geometry of the Ball Guided Cage

also listed in the figure and from these numbers it may be concluded that the assumption of full film elastohydrodynamic lubrication even under starved conditions may be fairly reasonable. If the data of Figure 4-4 is plotted as a function of the sliding speed or slip velocity, then all of the data lies on one line with a slope of 0.0410 S/M; this is because the roll speed is different for each line in Figure 4-4. Thus a linear traction curve with a slope of 0.0410 S/M is assumed for both bearings.

Friction at ball/cage and cage/race contacts is another unknown and for the present investigation a constant friction coefficient of 0.010 is arbitrarily assumed.

#### 4.4 Performance Simulations of 100 mm DMA Bearing

The first simulation with the RAPIDREB program is obtained for the 100 mm, inner race guided DMA ball bearing operating with gravity oriented along the bearing axis. In such a orientation the cage moves axially and rests on all the balls to balance its own weight. Typical ball/cage force variation is shown in Figure 4-5. The mean force is approximately equal to the cage weight. What is interesting to notice is the settling in of the ball/cage contact angle. The observed distinct frequency in this pattern is about 44.6 Hz and it is probably related to some kinematic phenomenon in the bearing; it is really much lower than the ball/cage contact frequency which is of the order of 1 kHz. Such a cyclic variation also gets transmitted to the cage angular acceleration about the bearing axis as shown in Figure 4-6, and hence to the skid parameter  $\lambda_2$  as shown in Figure 4-7. The parameter  $\lambda_2$  is defined as:

$$\lambda_2 = \frac{\text{Cage Angular Velocity}}{\text{Race Angular Velocity}}$$

From Figure 4-7 it is also seen that the cage does not experience any significant whirl. This is indicated by the parameter  $\lambda_1$  in Figure 4-7 which is defined as:

$$\lambda_1 = \frac{\text{Cage Mass Center Whirl}}{\text{Cage Angular Velocity}}$$

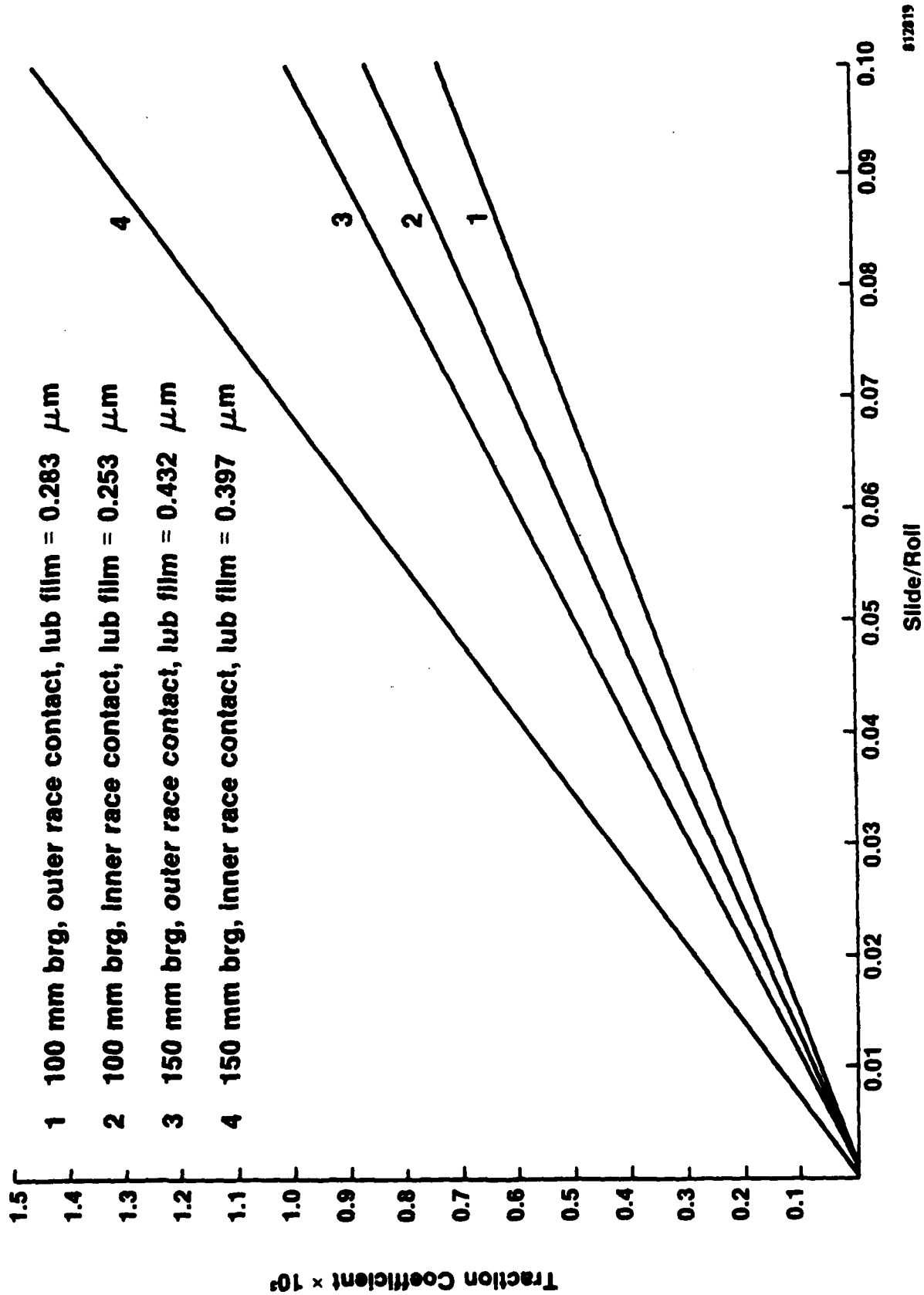


Fig. 4-4 Ball/Race Traction Characteristics for the DMA Bearings

812819

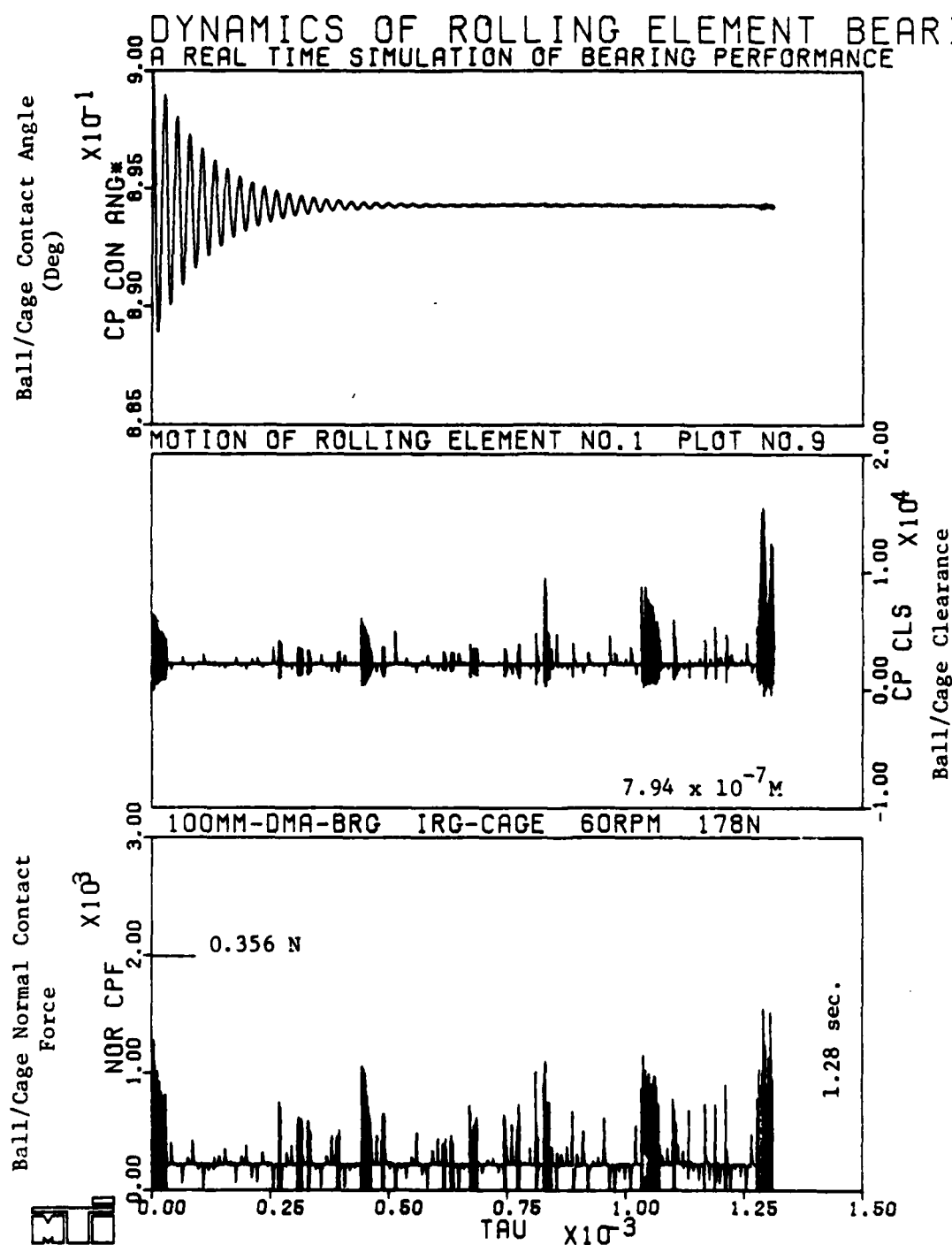


Fig. 4-5 Ball Cage Interaction for the 100 mm DMA Ball Bearing

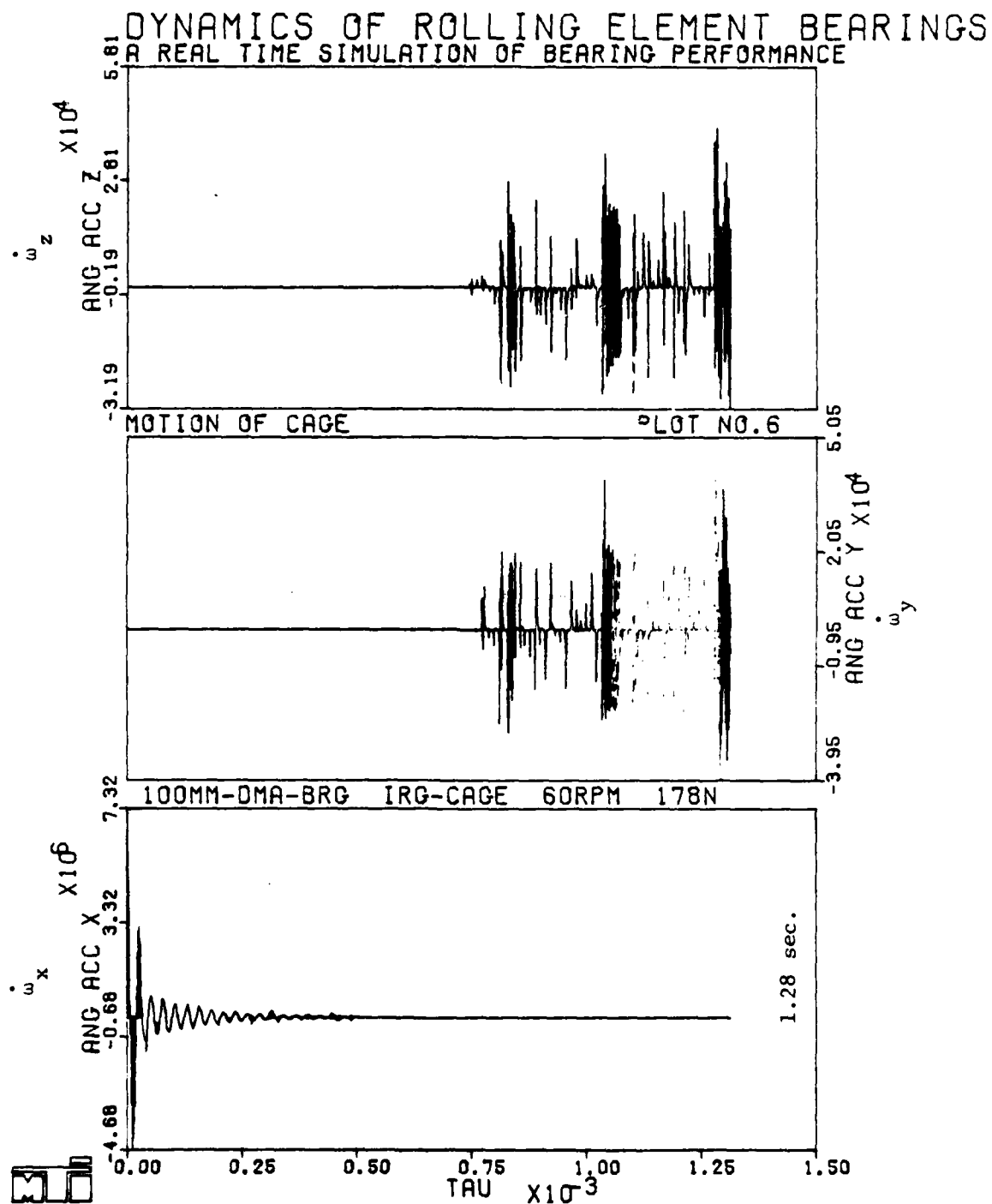


Fig. 4-6 Dimensionless Cage Angular Accelerations for the 100 mm DMA Bearing with Gravity Acting Along the Bearing Axis. Scale =  $1.319 \times 10^7$  RPM/S.

# DYNAMICS OF ROLLING ELEMENT BEARINGS A REAL TIME SIMULATION OF BEARING PERFORMANCE

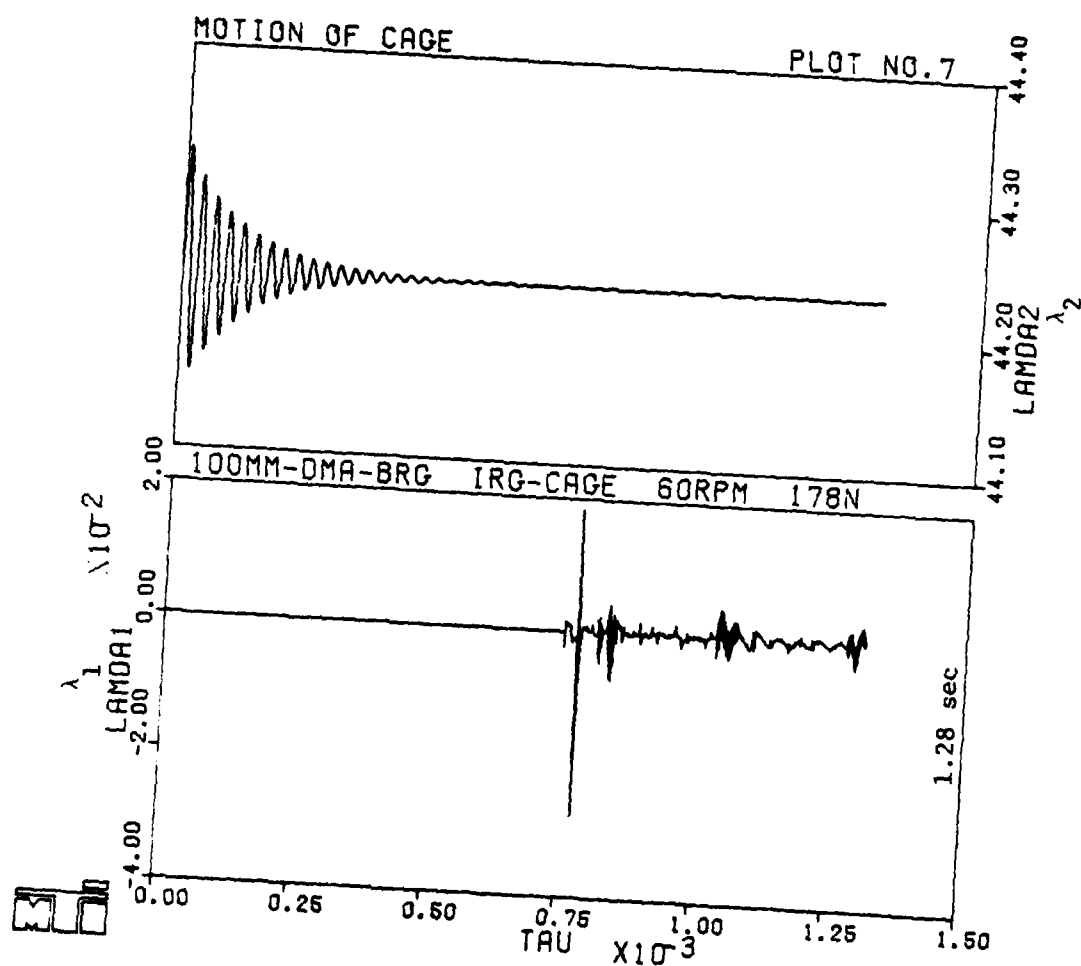


Fig. 4-7 Cage Whirl and Skid Parameters for the 100 mm DMA Bearings

The sudden change from zero whirl to some vibratory motion indicates cage radial motion beyond a certain machine round off threshold set in RAPIDREB. In reality the entire whirl pattern will look like what is seen in steady state in Figure 4-7, but the magnitude of the radial motion for all practical purposes will be negligible and no interaction with the guiding race will be seen. The bearing torque variations are seen in Figure 4-8. Again the cyclic variation corresponding to about 44.6 Hz is seen in both the outer and inner race torque. The damping of the cyclic variation is due to ball/race and ball/cage friction. Under actual laboratory conditions such cyclic torque variations may exist in steady state since the bearing is constantly subjected to subtle disturbances which may be adequate to continually excite the cyclic motion.

The ball motion indicates that the conventional race-control hypotheses do not hold when the ball/race friction is quite low as in the present case. As shown in Figure 4-9 the angular velocity vector tends to orient itself along the bearing axis and hence the x component continually increases while the z component decreases. Also a small component about the y axis is developed indicating gyroscopic slip. The resulting spin-to-roll ratios are shown in Figure 4-10. Such deviations of ball velocity from the race-control hypothesis have also been observed earlier [17].

When the bearing is oriented vertically such that the cage weight now acts in a plane perpendicular to the bearing axis, the cage tends to move radially and this causes substantial variations in ball/cage interactions as the ball travels around its orbit. Also significant interaction with the guiding race is observed and some coning motion (rotation about transverse axes of the cage) is also noted. Figure 4-11 shows the ball/cage force variation. The high frequency content is generally the ball/cage elastic contact frequency and the low frequency variation corresponds to the ball orbital velocity; the simulation time in Figure 4-11 corresponds to about one shaft revolution or approximately half of ball orbit. The cage/race forces are shown in Figure 4-12. The steady magnitude of the force is of the order of cage weight although not exactly equal to it since the ball/cage forces also enter in the cage equilibrium. Although not very clear

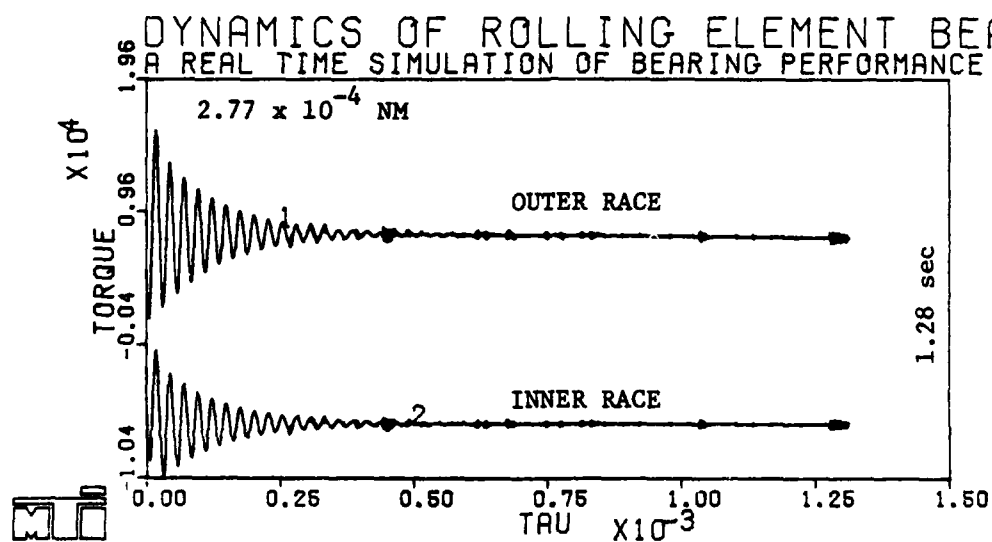


Fig. 4-8 Bearing Torque Variations for the 100 mm DMA Bearing with Gravity Acting Along the Bearing Axis



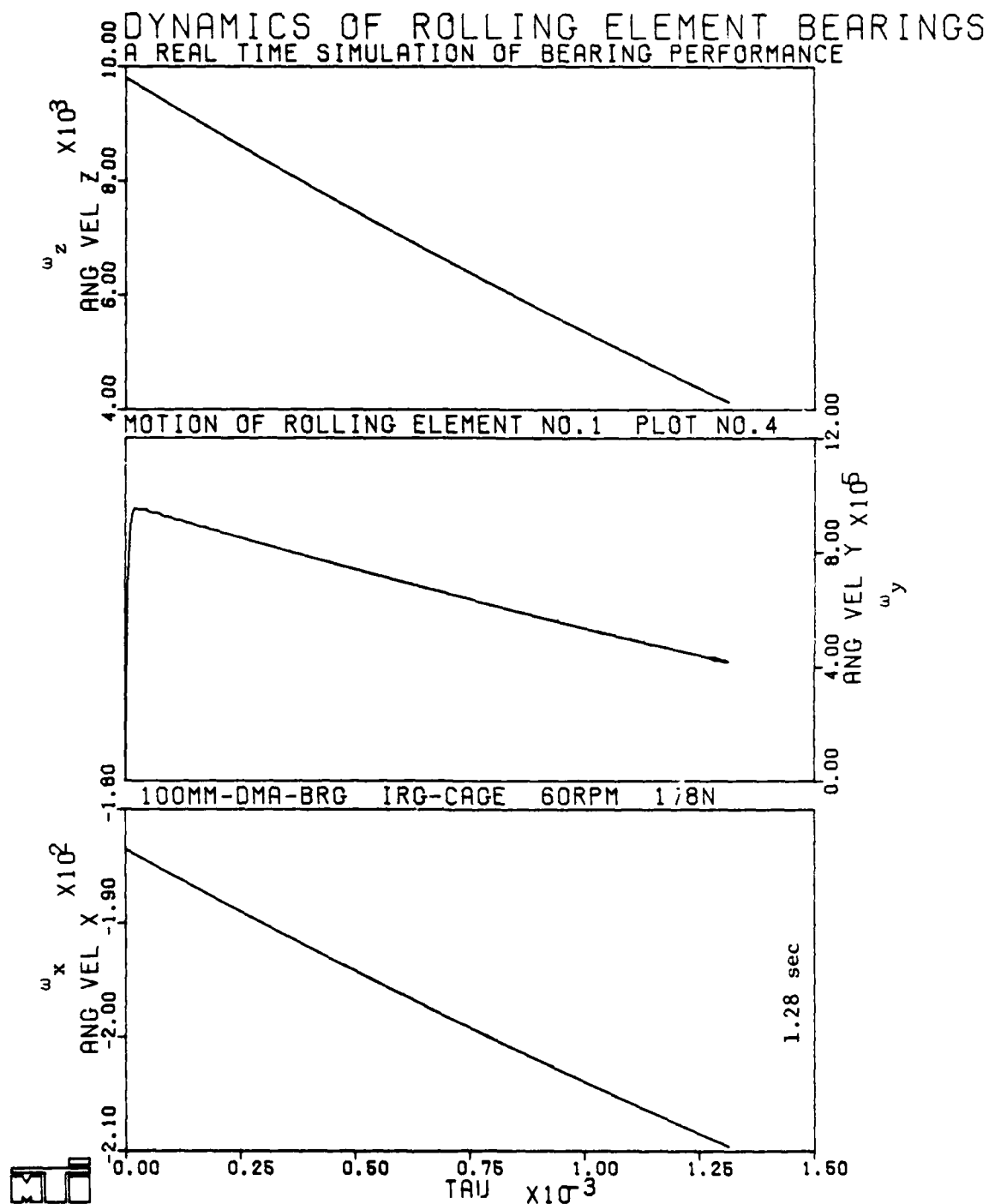


Fig. 4-9 Dimensionless Ball Angular Velocity for the  
100 mm Bearing. Scale =  $1.22 \times 10^4$  RPM

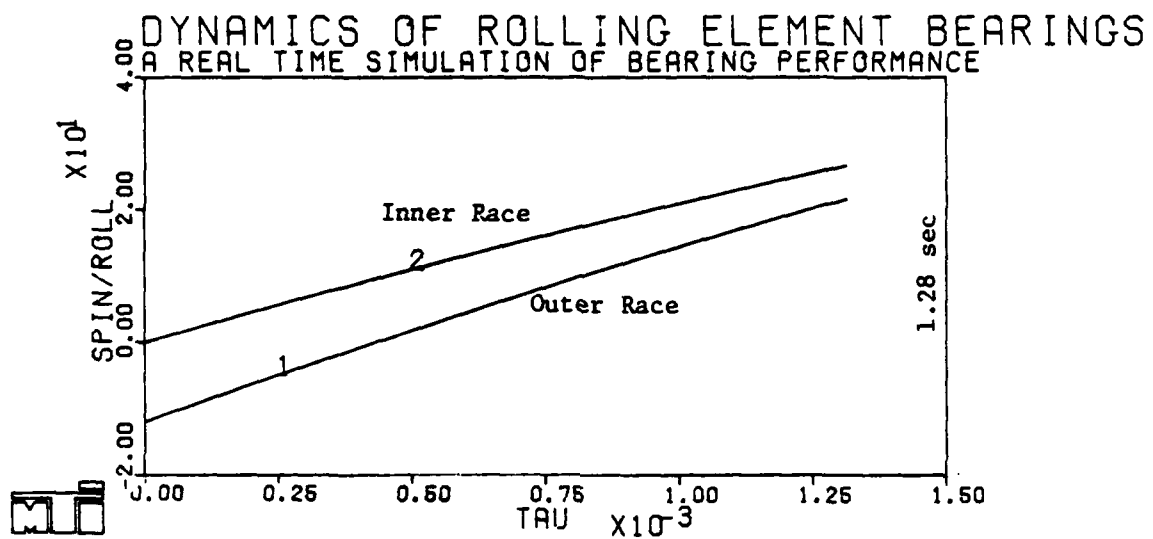


Fig. 4-10 Ball/Race Spin-to-Roll Ratio for the 100 mm DMA Bearing

# DYNAMICS OF ROLLING ELEMENT BEARINGS A REAL TIME SIMULATION OF BEARING PERFORMANCE

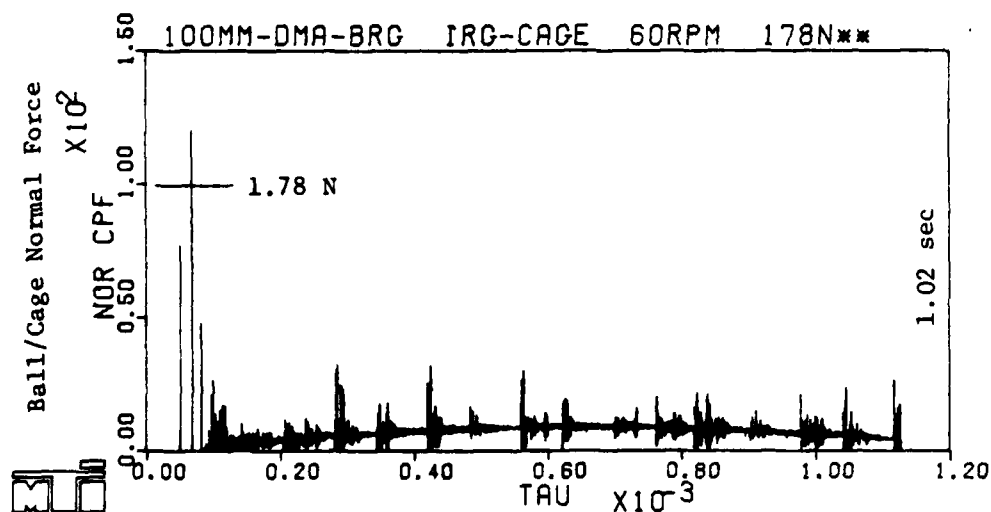


Fig. 4-11 Ball/Cage Force Variation for the 100 mm Bearing with Gravity Acting Normal to the Bearing Axis

# DYNAMICS OF ROLLING ELEMENT BEARINGS A REAL TIME SIMULATION OF BEARING PERFORMANCE

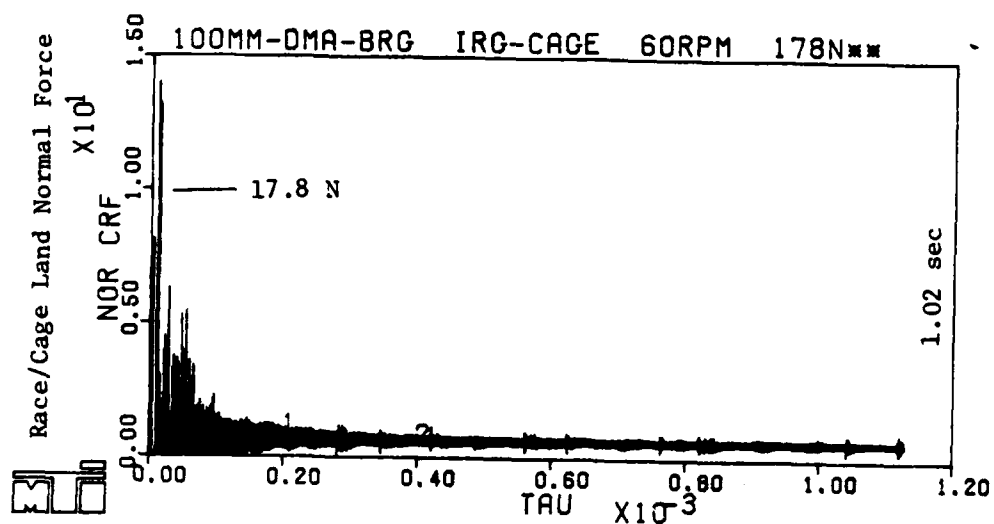


Fig. 4-12 Normal Contact Force at the Cage/Race Interface When Gravity Acts Normal to the Bearing Axis in the Case of the 100 mm DMA Bearing

from Figure 4-12, there is an appreciable difference between the contact forces at the two land<sup>2</sup>, which is due to the coning motion of the cage. This is better seen in Figure 4-13 where the cage angular accelerations are plotted. Most of this motion is clearly cyclic and it has both the high and low frequency content present in it. The high frequency corresponds to the ball/cage and cage/race elastic contacts while the low frequency is similar to what is seen earlier in Figure 4-5. Both the y and z components do show the low frequency but it is more clear in Figure 4-14, where the angular velocities are plotted. The magnitude of this low frequency is about 76.4 Hz compared to the frequency of 44.6 Hz shown earlier with the bearing more symmetrically oriented.

In spite of the complicated motion the cage does seem to be fairly stable with practically no whirl in steady-state as indicated by  $\lambda_1$  in Figure 4-15. Also seen in this figure is the skid parameter  $\lambda_2$ , which is also fairly stable. The bearing torque variations are shown in Figure 4-16. These variations do contain both the high and low frequency cyclic variations, although they are not very clear in the figure. The ball angular velocities, as seen in Figure 4-17, are similar to those seen earlier. Also, the deviations from the race-control hypothesis are clear in terms of the spin-to-roll ratios plotted in Figure 4-18. In addition to this it may be interesting to note the ball orbital acceleration pattern shown in Figure 4-19. The noise in the ball orbital acceleration correlates well with the noise observed earlier in the skid parameter  $\lambda_2$  in Figure 4-15. Again the high frequency content comes from the ball/cage elastic collisions, which are now continually varying as the ball travels around its orbit.

#### 4.5 Performance Simulations of the 150 mm DMA Bearing

The general behavior of the 150 mm DMA bearing with ball guided cage is relatively more noisy than the 100 mm bearing. With the gravity oriented along the bearing axis the ball/cage pocket force variation is shown in Figure 4-20. Once again the mean force balances the cage weight and the ball/cage contact angle demonstrate some cyclic variations as is seen for the 100 mm bearing (Figure 4-5). The frequency of this component is now 37.4 Hz which is not very different from 44.6 Hz observed with the 100 mm bearing. The resulting cage motion is, however, substantially noisier.

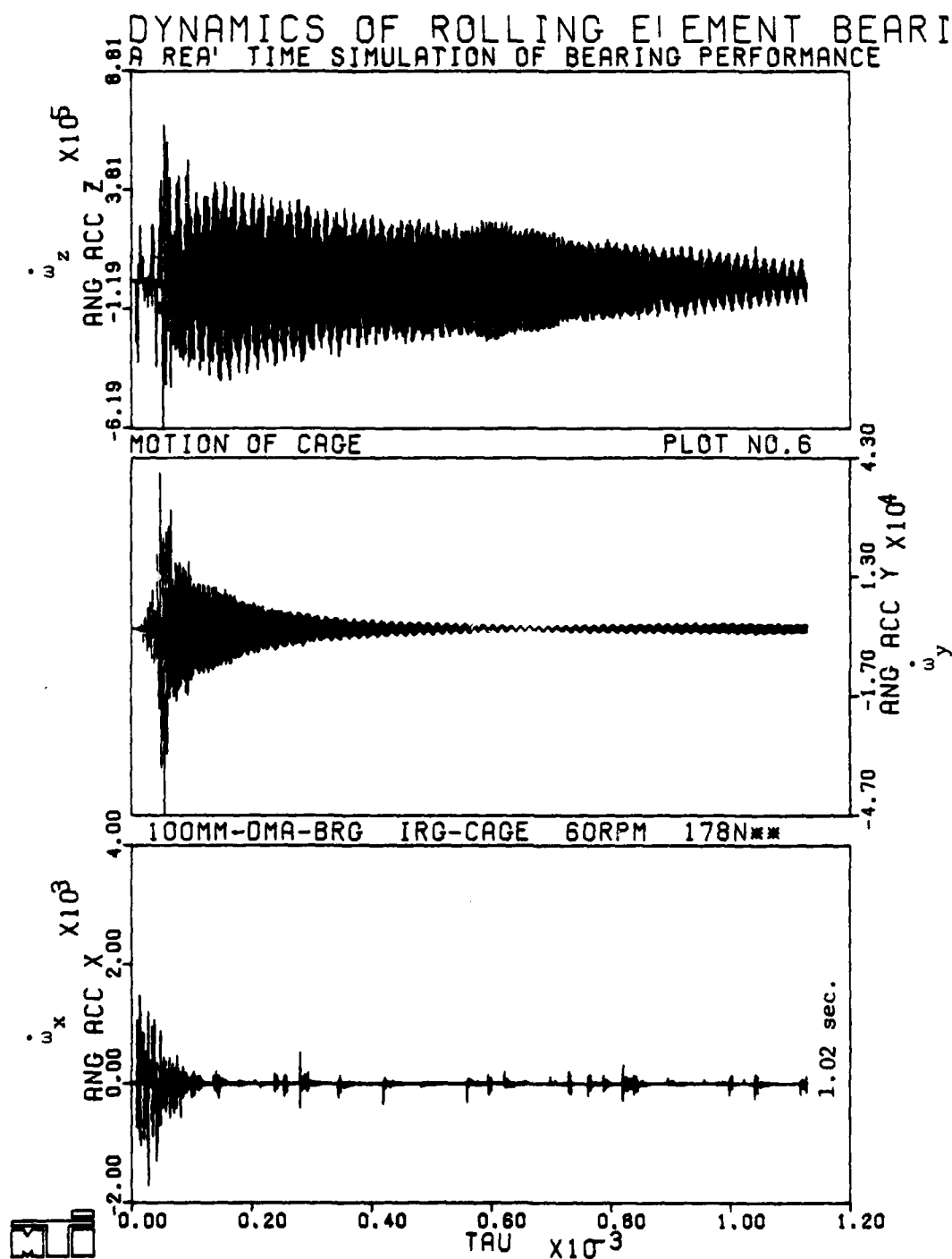


Fig. 4-13 Dimensionless Angular Accelerations of the 100 mm Bearing Cage When Gravity Acts Normal to the Bearing Axis. Scale =  $1.319 \times 10^7$  RPM/S

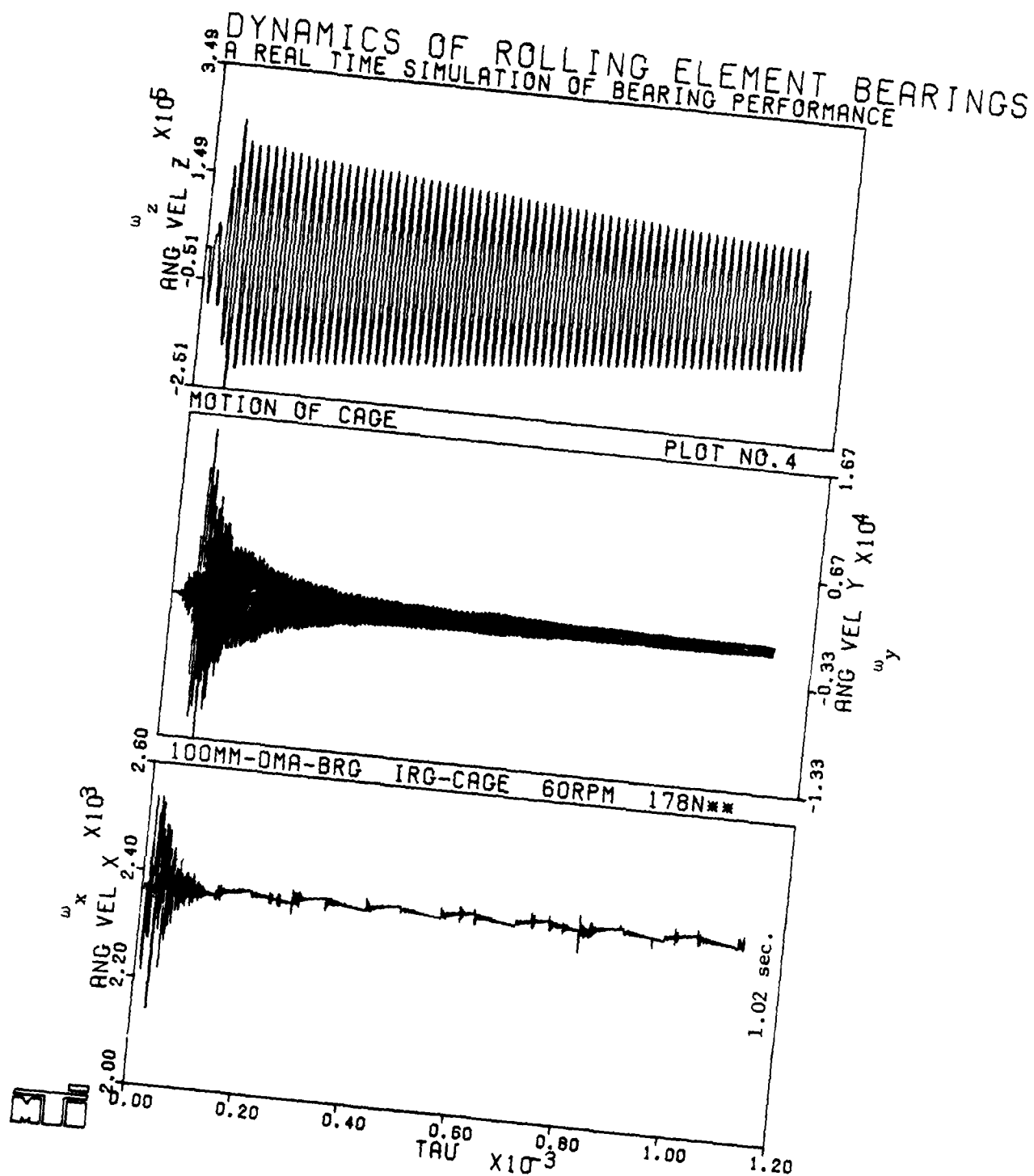


Fig. 4-14 Dimensionless Ball Angular Velocity for the 100 mm Bearing with Gravity Acting Normal to the Bearing Axis

# DYNAMICS OF ROLLING ELEMENT BEARINGS A REAL TIME SIMULATION OF BEARING PERFORMANCE

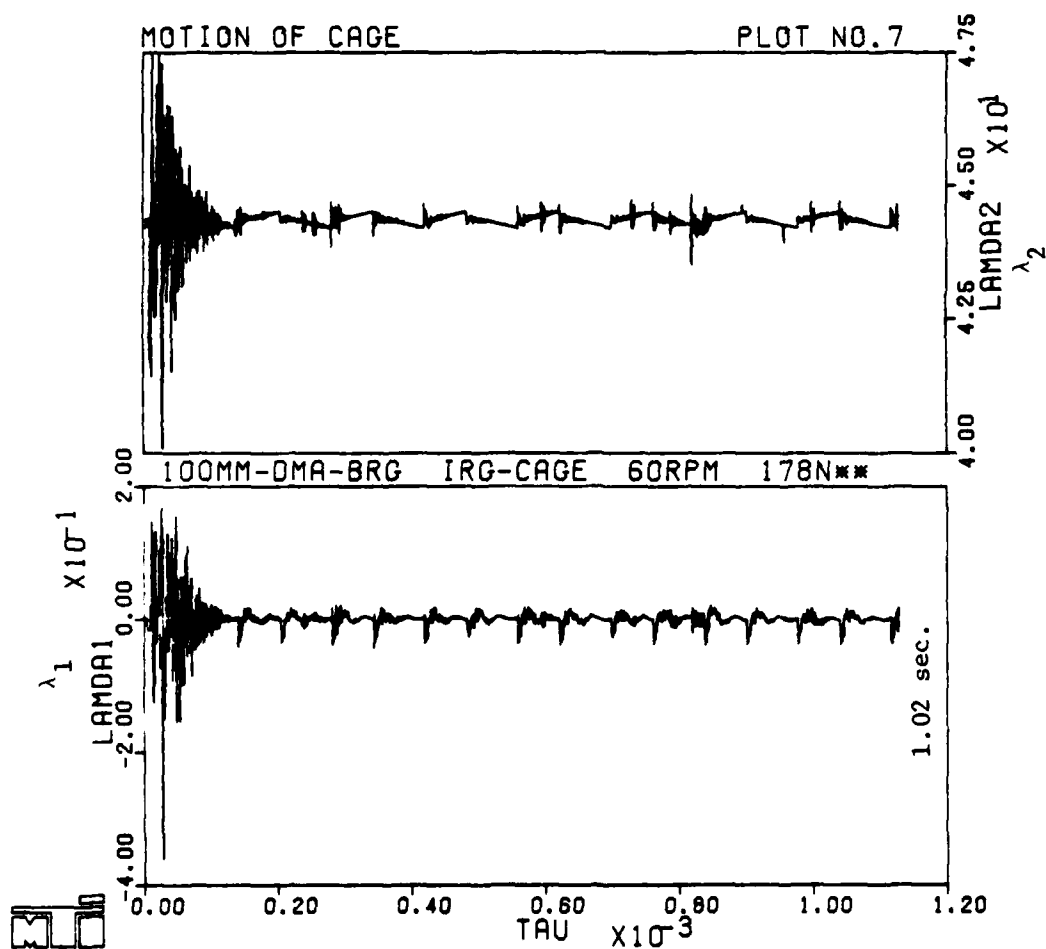


Fig. 4-15 Cage Whirl and Skid Parameters for the 100 mm Bearing with Gravity Acting Normal to Bearing Axis



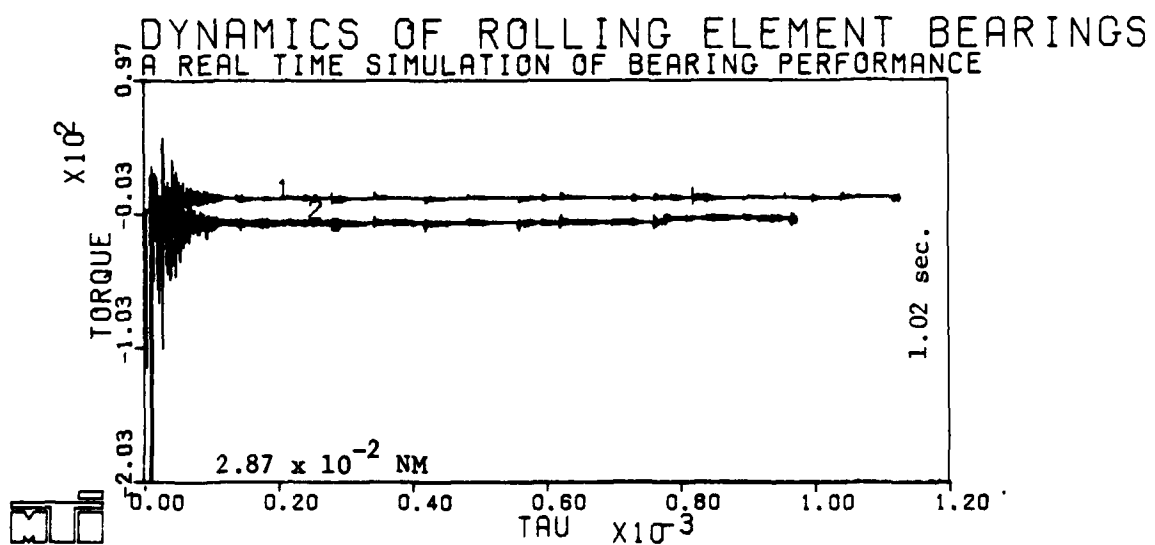


Fig. 4-16 Variation in Bearing Torque in Case of the 100 mm Bearing with Gravity Acting Normal to the Bearing Axis

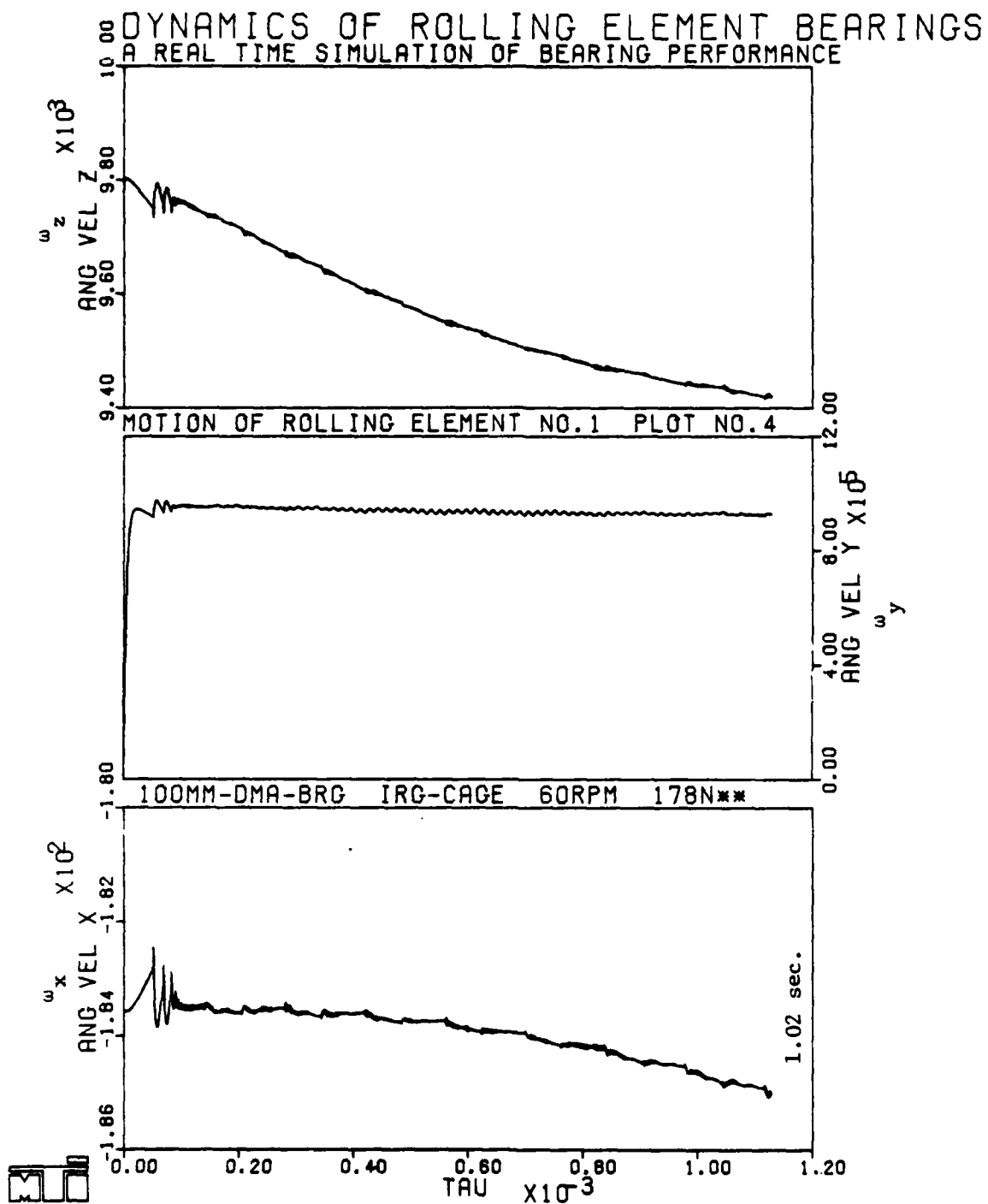


Fig. 4-17 Dimensionless Ball Angular Velocity Variation  
for the 100 mm DMA Bearing with Gravity  
Oriented Normal to the Bearing Axis

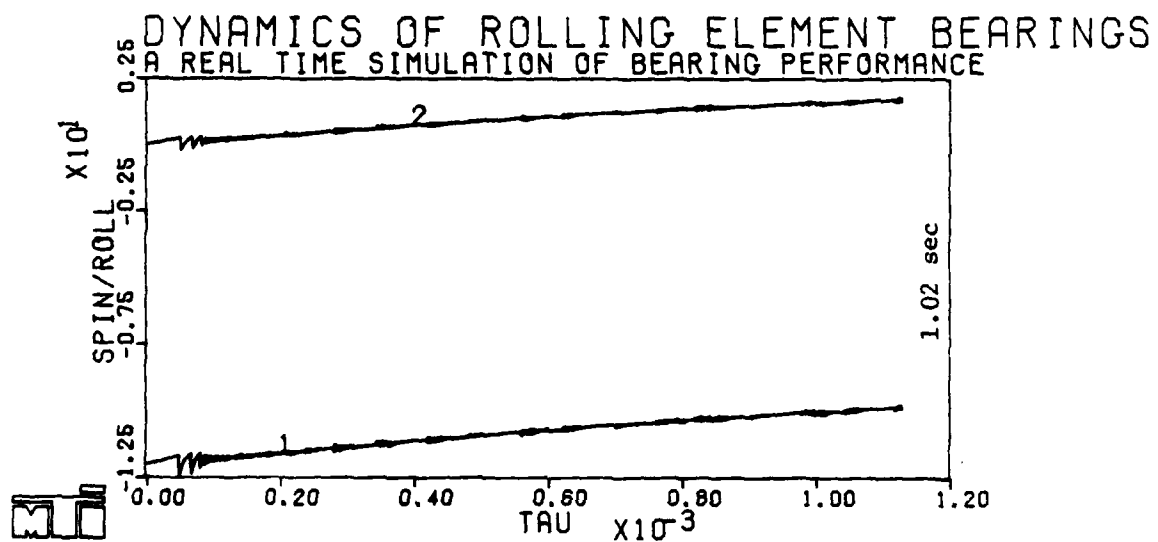


Fig. 4-18 Ball/Race Spin Variation for the 100 mm Bearing  
with Gravity Acting Normal to Bearing Axis

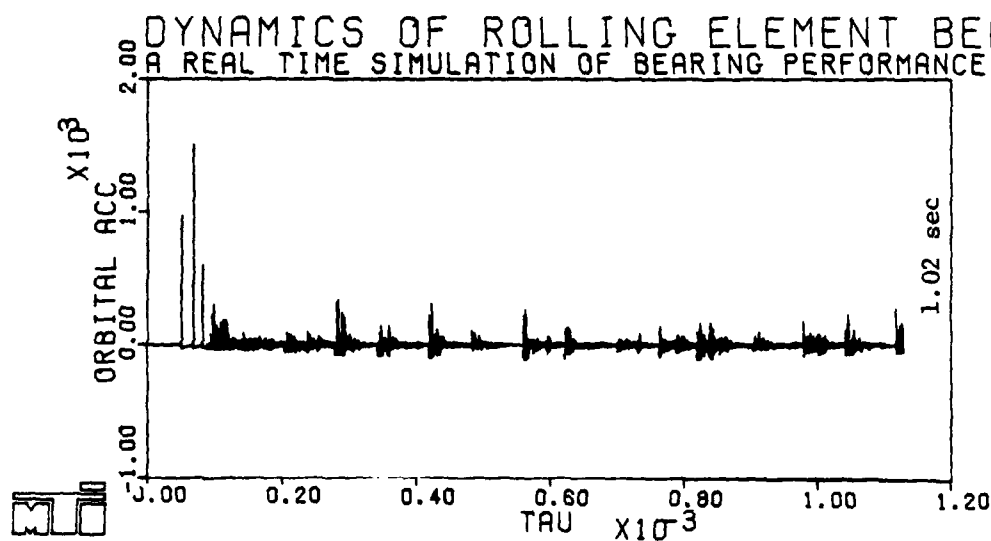


Fig. 4-19 Ball Orbital Acceleration Resulting from the Ball/Cage Collision due to Eccentric Cage in the 100 mm Bearing with Gravity Normal to Bearing Axis

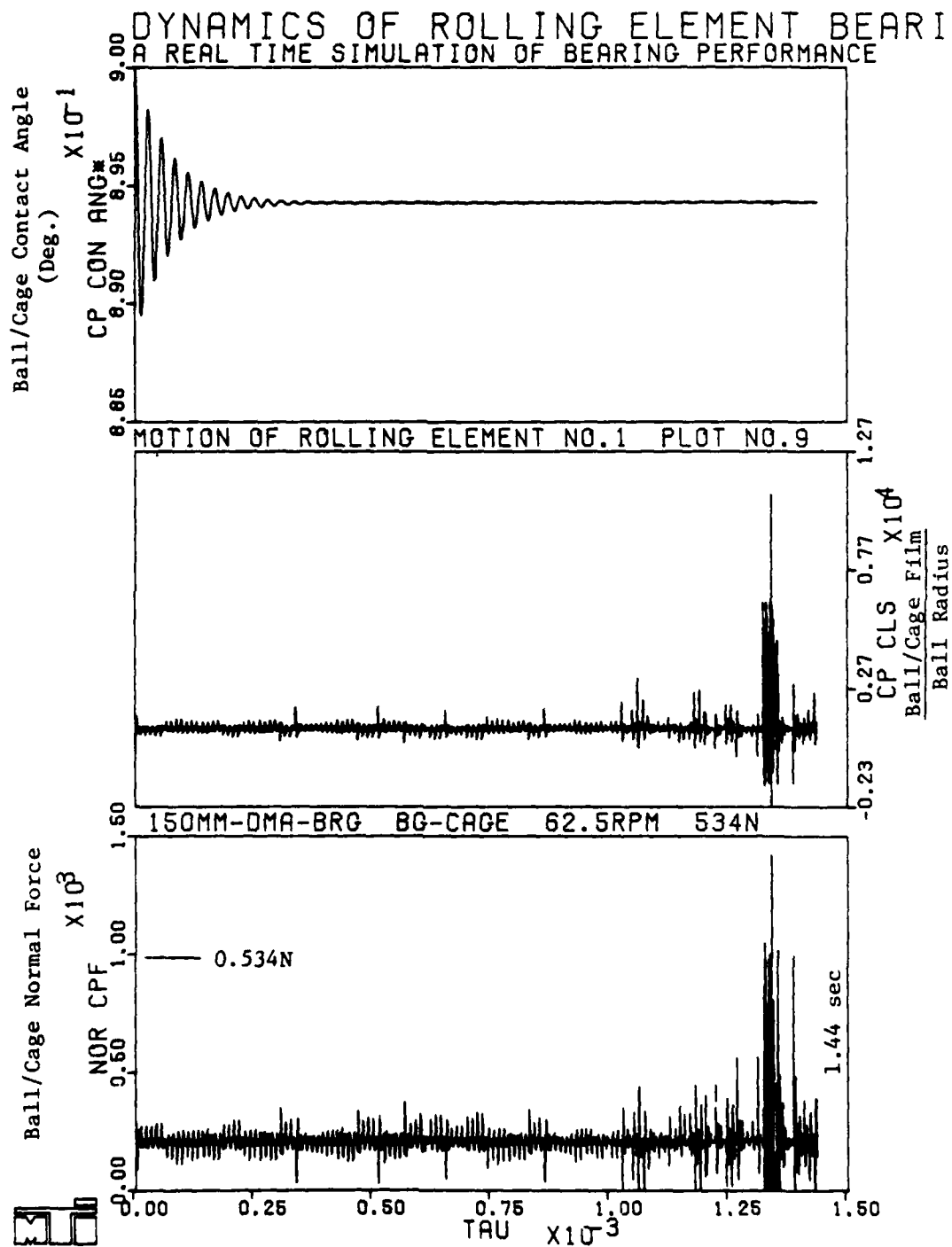


Fig. 4-20 Ball/Cage Interaction in the 150 mm Bearing With Ball Guided Cage Operating Horizontal with Gravity Acting Along the Bearing Axis

Figure 4-21 shows cage mass center accelerations. It is clear that both radial and orbital components develop beyond the threshold of machine round off errors. Although the resulting whirl motion is substantial in terms of angular velocity, the whirl radius is still small and no appreciable interaction with the pocket cone takes place. The cage whirl is indicated by  $\lambda_1$  variation in Figure 4-22. It is easily seen that once the cage starts whirling the whirl velocity oscillates by large magnitudes; this may indicate some form of instability. Cage angular velocity, indicated by  $\lambda_2$ , is, however, fairly steady after the dampening of the initial cyclic variations. The bearing torque variations are very similar to those for the 100 mm bearing, as seen in Figure 4-23.

The general motion of the ball is almost identical to that observed in the 100 mm bearing. The ball angular velocity vector, see Figure 4-24, tends to line up with the bearing axis and the race-control hypotheses do not hold, as seen by the spin-to-roll ratios in Figure 4-25.

When the 150 mm bearing with ball-guided cage is run with gravity oriented normal to the bearing axis, significant noise in the performance simulations is produced by the repeated collisions in the cage pocket. Figure 4-26 shows typical collisions with the cylindrical part of the pockets and Figure 4-27 shows interaction at the conical guidance surface. Such repeated collisions produce considerable noise in both the ball and cage motions. The ball angular velocity variations are shown in Figure 4-28 and the orbital accelerations of the ball from the repeated impacts is shown in Figure 4-29. The angular velocity of the cage indicates substantial coning motion as seen by the y and z components in Figure 4-30. The noise generated from the ball-cage collisions is also transmitted to the cage mass center accelerations as shown in Figure 4-31. Excessive cyclic whirl of the cage is produced although no significant steady whirl is observed over the short time of this performance simulation. This is seen by the  $\lambda_1$  variation in Figure 4-32. As may be expected the skid parameter,  $\lambda_2$ , does pick up the influence of the excessive ball/cage collisions.

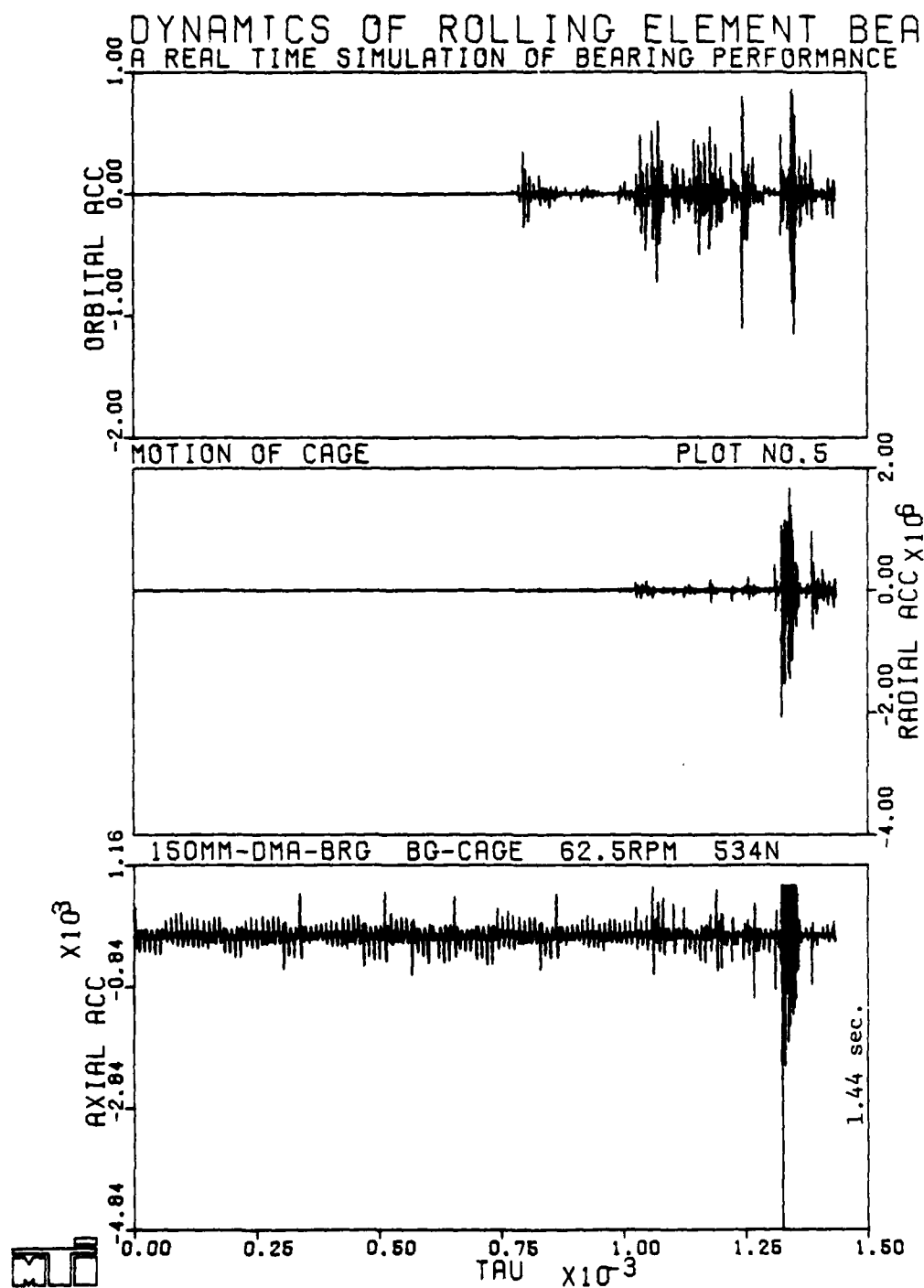


Fig. 4-21 Dimensionless Cage Mass Center Accelerations  
Resulting From the Noisy Ball/Cage Interaction  
for the 150 mm Bearing. Scale =  $1.198 \times 10^4 \text{ M/S}^2$ ,  
 $1.03 \times 10^7 \text{ RPM/S}$

# DYNAMICS OF ROLLING ELEMENT BEARINGS

## A REAL TIME SIMULATION OF BEARING PERFORMANCE

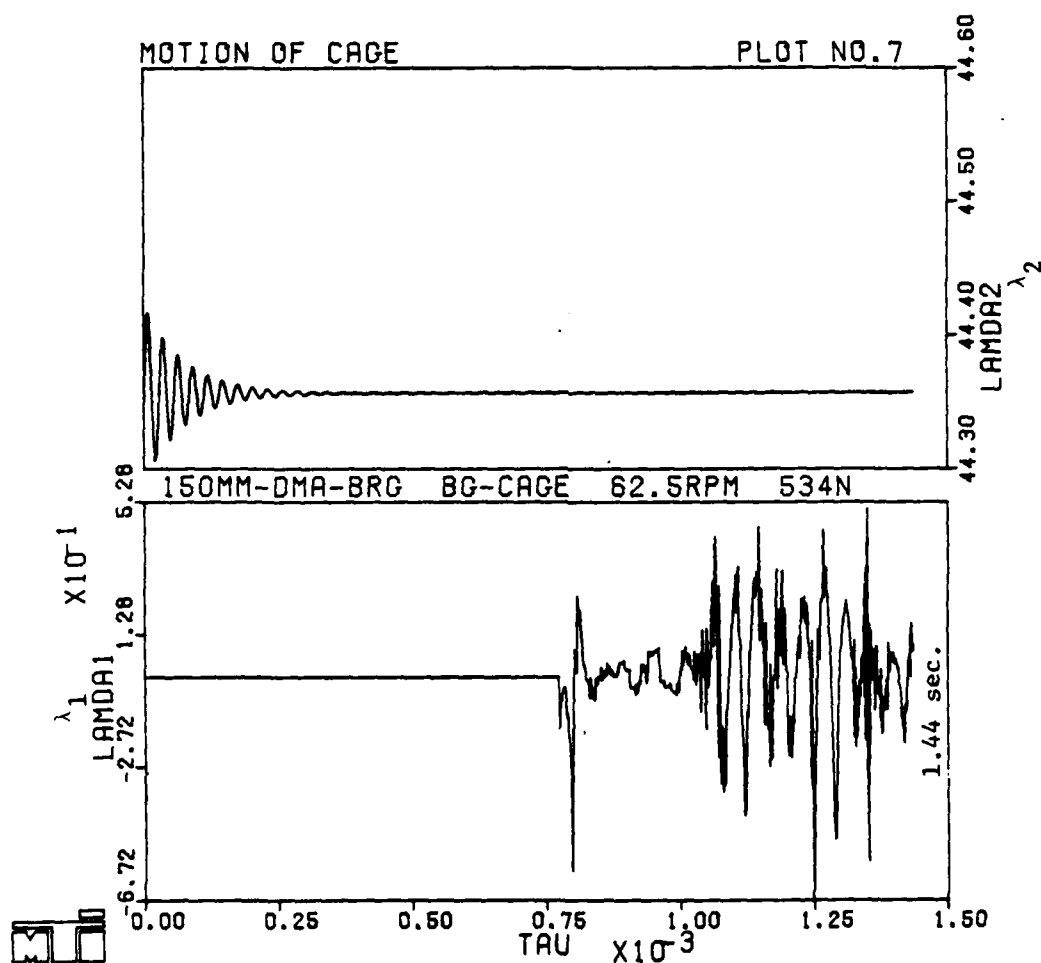


Fig. 4-22 Cage Whirl and Skid Parameter for the 150 mm DMA Bearing



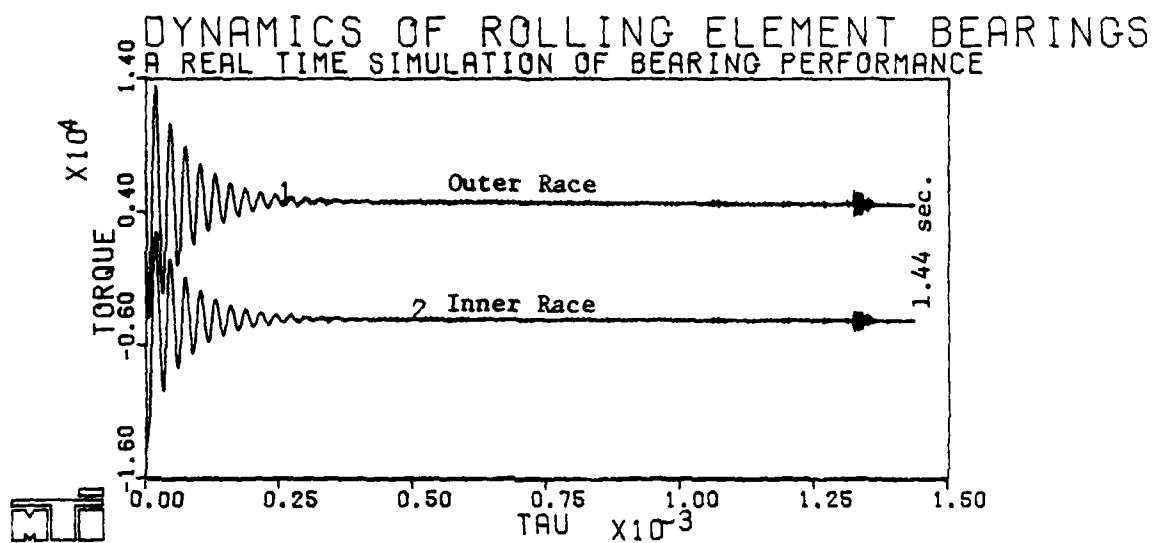


Fig. 4-23 Bearing Torque Variation for the 150 mm Bearing  
with Gravity Acting Along the Bearing Axis

# DYNAMICS OF ROLLING ELEMENT BEARINGS

## A REAL TIME SIMULATION OF BEARING PERFORMANCE

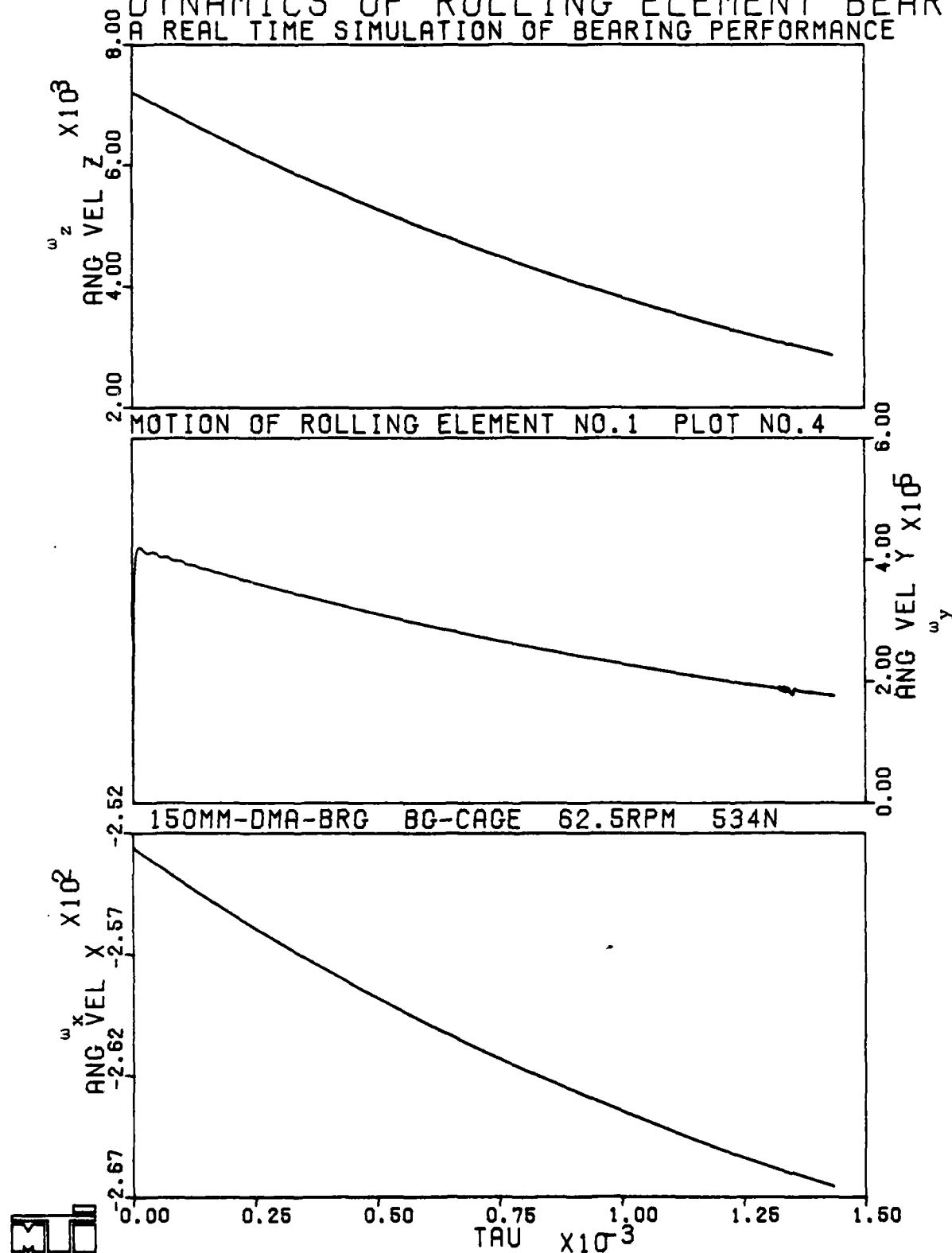


Fig. 4-24 Dimensionless Angular Velocities of the Ball in the 150 mm DMA Bearing. Scale =  $9.918 \times 10^3$  RPM

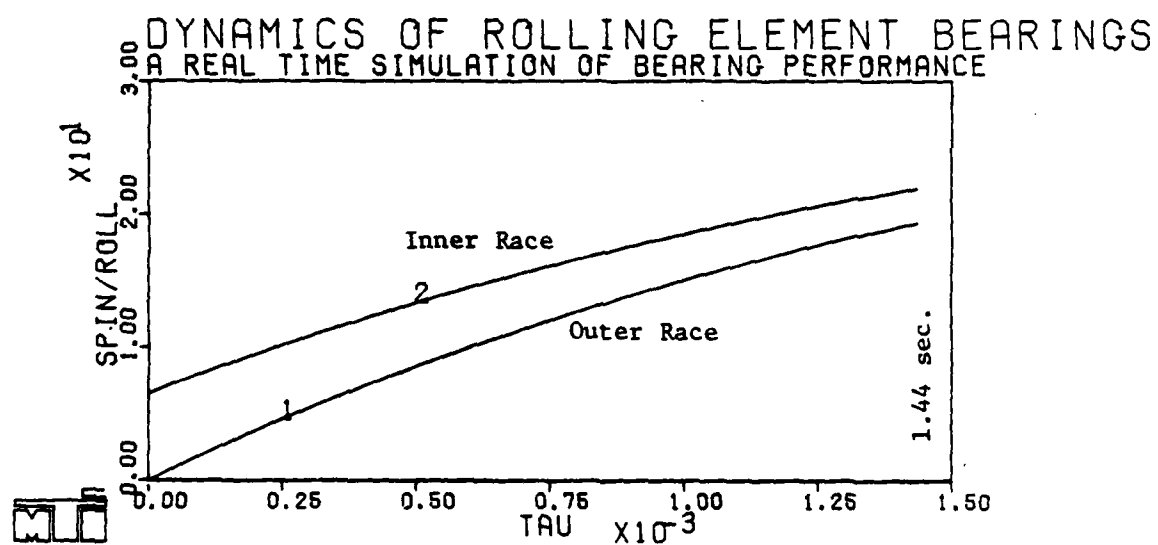


Fig. 4-25 Ball/Race Spin for the 150 mm DMA Bearing

# DYNAMICS OF ROLLING ELEMENT BEARINGS

## A REAL TIME SIMULATION OF BEARING PERFORMANCE

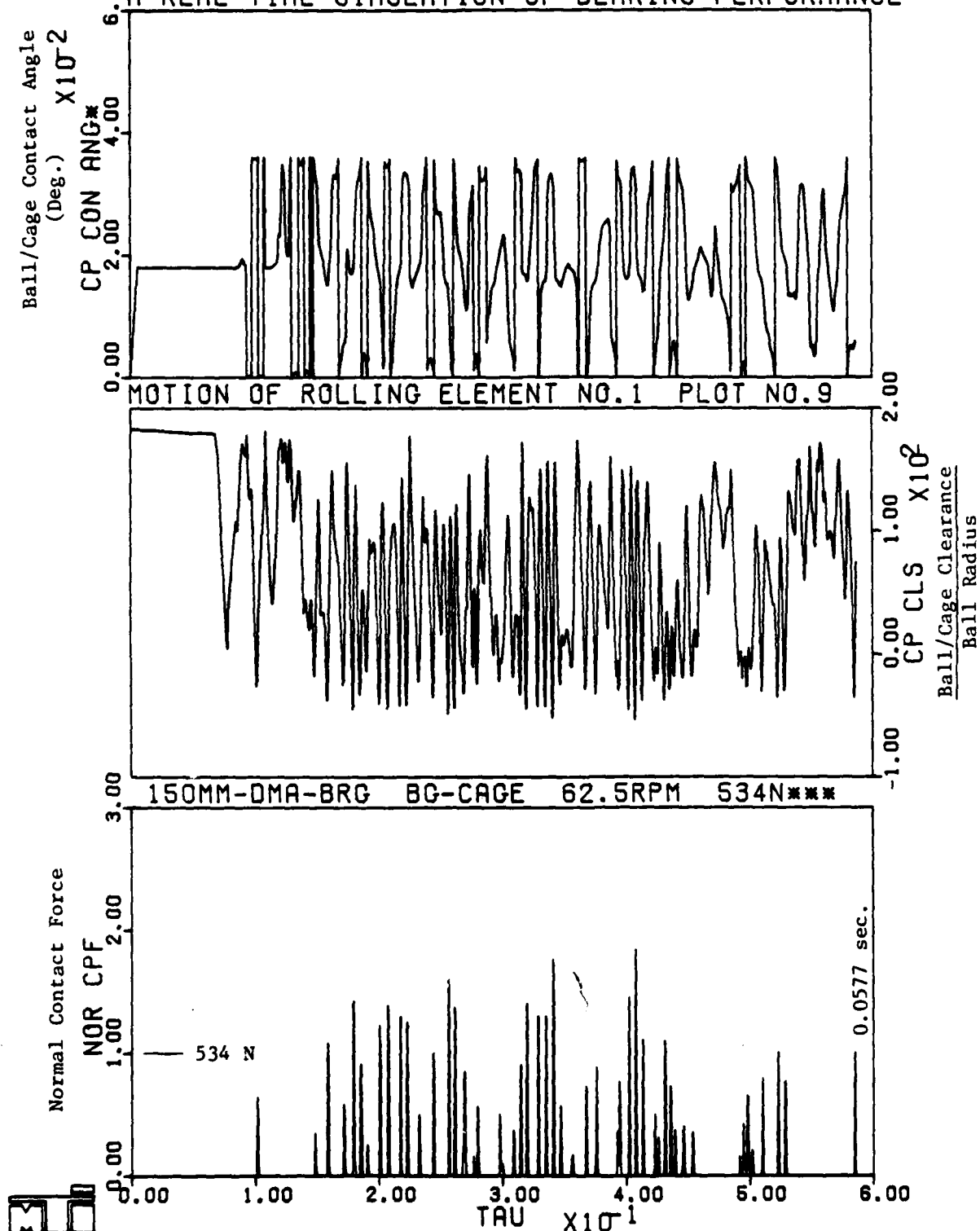


Fig. 4-26 Ball/Cage Interaction at the Cylindrical Pocket Surface for the 150 mm Bearing with Gravity Acting Normal to the Bearing Axis

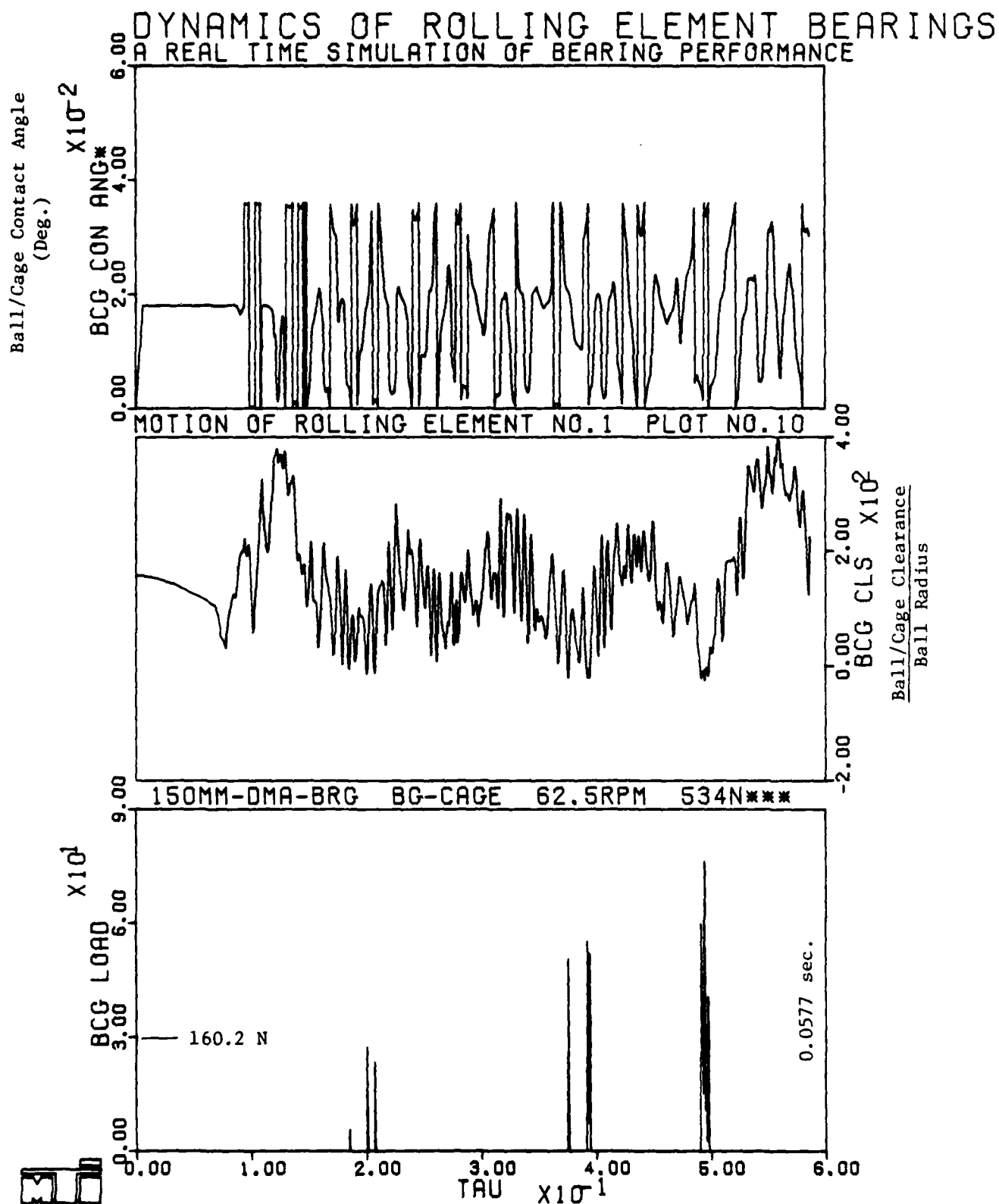


Fig. 4-27 Ball/Cage Interaction at the Conical Guidance Surface for the 150 mm Bearing with Gravity Acting Normal to Bearing Axis

# DYNAMICS OF ROLLING ELEMENT BEARINGS A REAL TIME SIMULATION OF BEARING PERFORMANCE

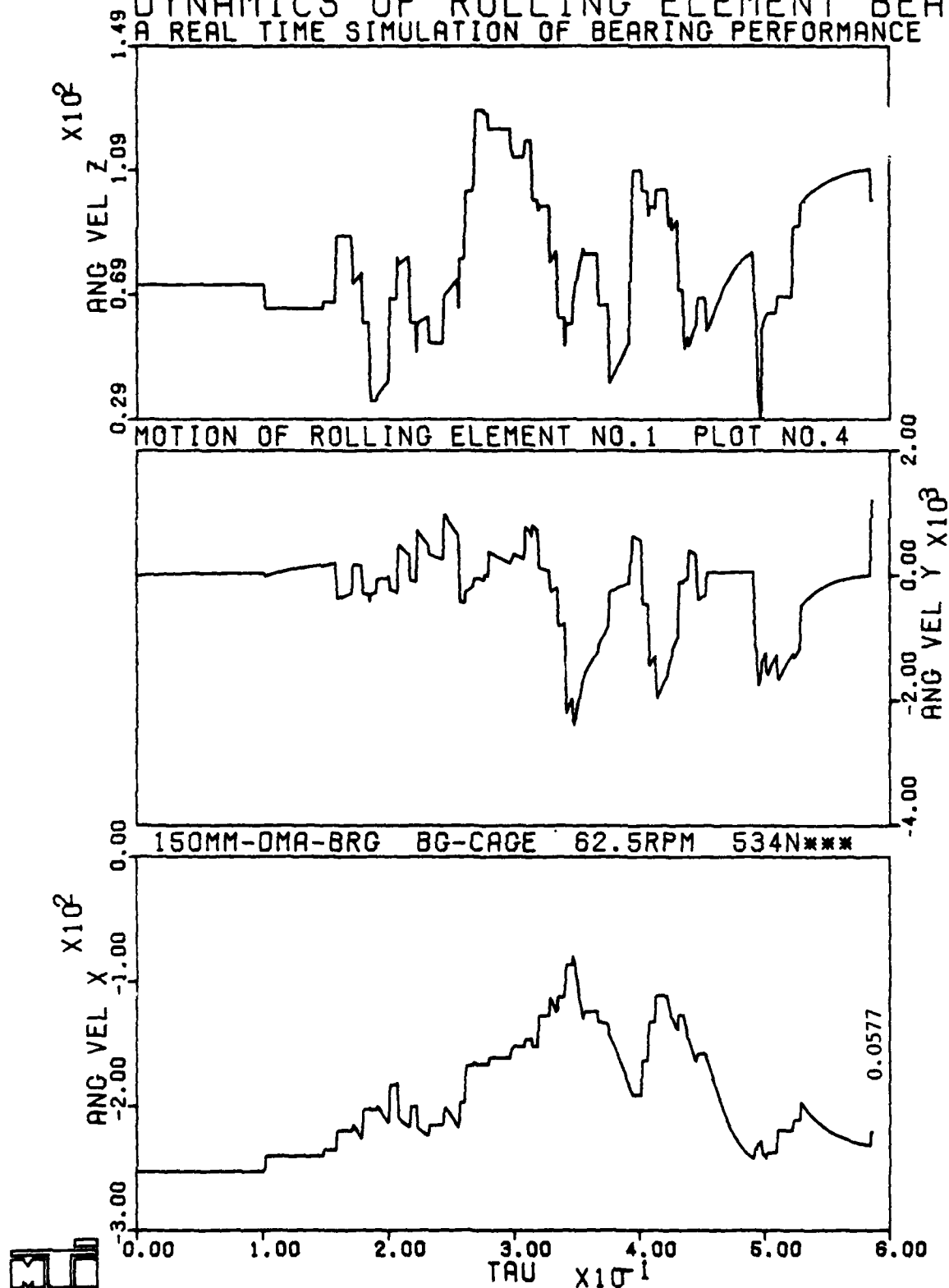


Fig. 4-28 Dimensionless Angular Velocity of the Ball  
for the 150 mm Bearing with Ball Guided  
Cage. Scale =  $9.918 \times 10^3$  RPM

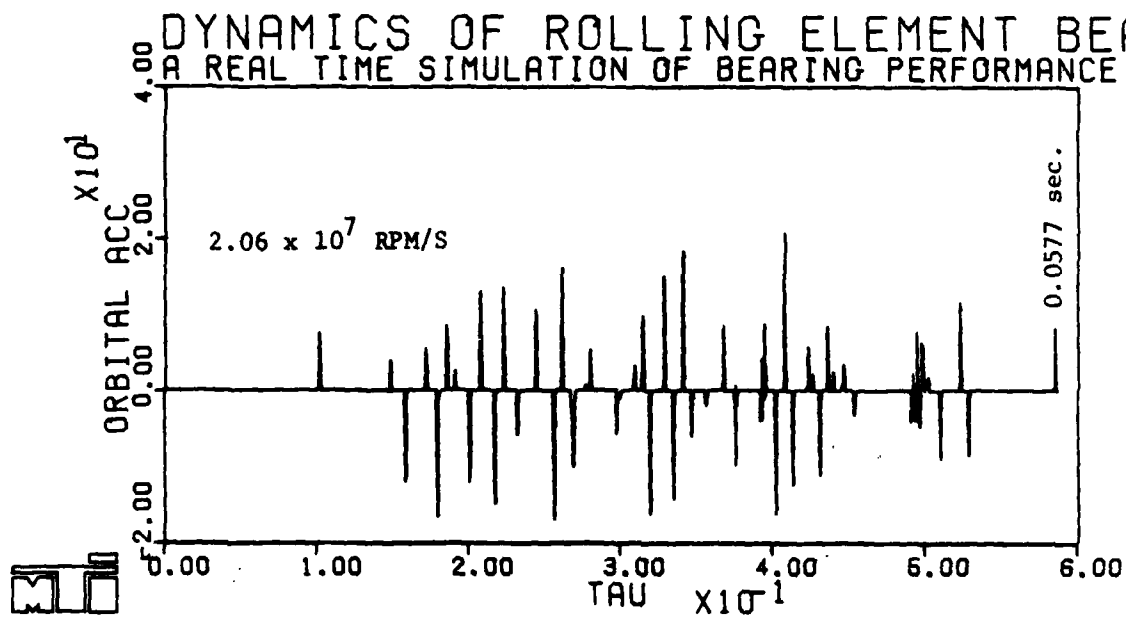


Fig. 4-29 Ball Orbital Accelerations Resulting From the Excessive Ball/Cage Interaction for the 150 mm DMA Bearing

# DYNAMICS OF ROLLING ELEMENT BEARINGS A REAL TIME SIMULATION OF BEARING PERFORMANCE

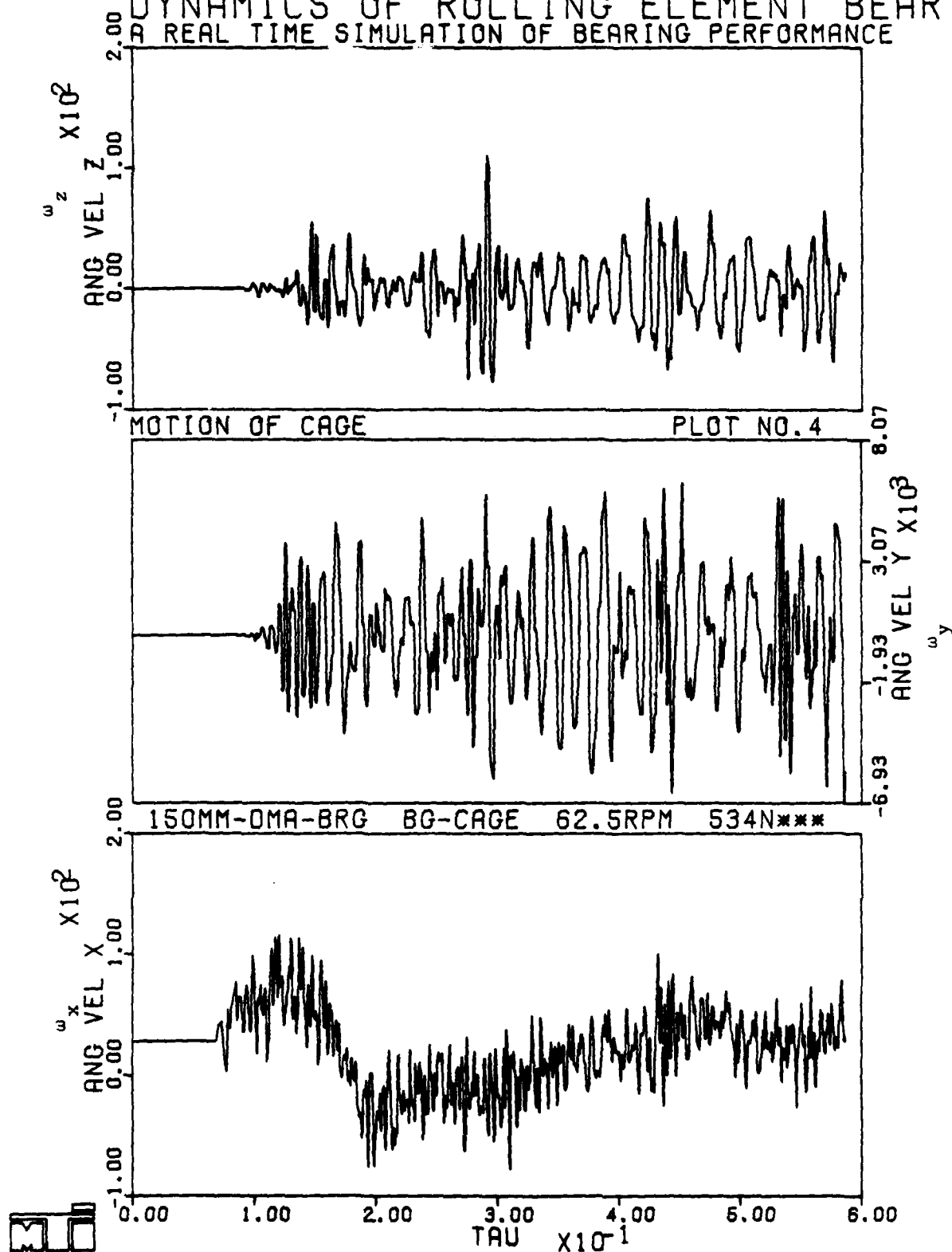


Fig. 4-30 Dimensionless Angular Velocity of the Ball Guided Cage in the 150 mm Bearing with Large Ball/Cage Interaction. Scale =  $9.918 \times 10^3$  RPM



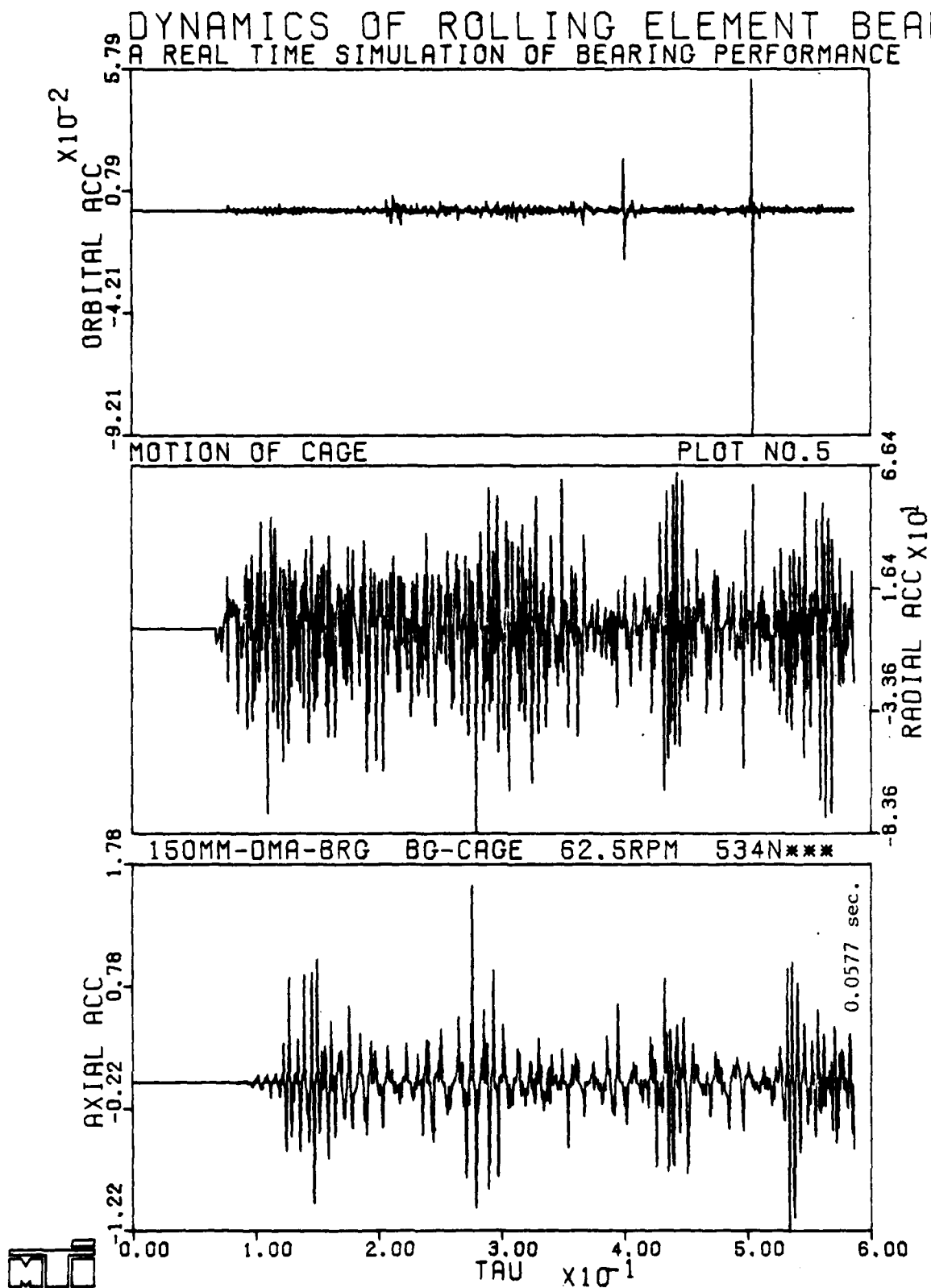


Fig. 4-31 Dimensionless Cage Mass Center Accelerations Resulting From the Excessive Ball/Cage Interaction in the 150 mm Bearing with Gravity Acting Normal to the Bearing Axis  
Scale =  $1.199 \times 10^4 \text{ M/sec}^2$ ,  $1.030 \times 10^3 \text{ RPM/sec}$

# DYNAMICS OF ROLLING ELEMENT BEARINGS

## A REAL TIME SIMULATION OF BEARING PERFORMANCE

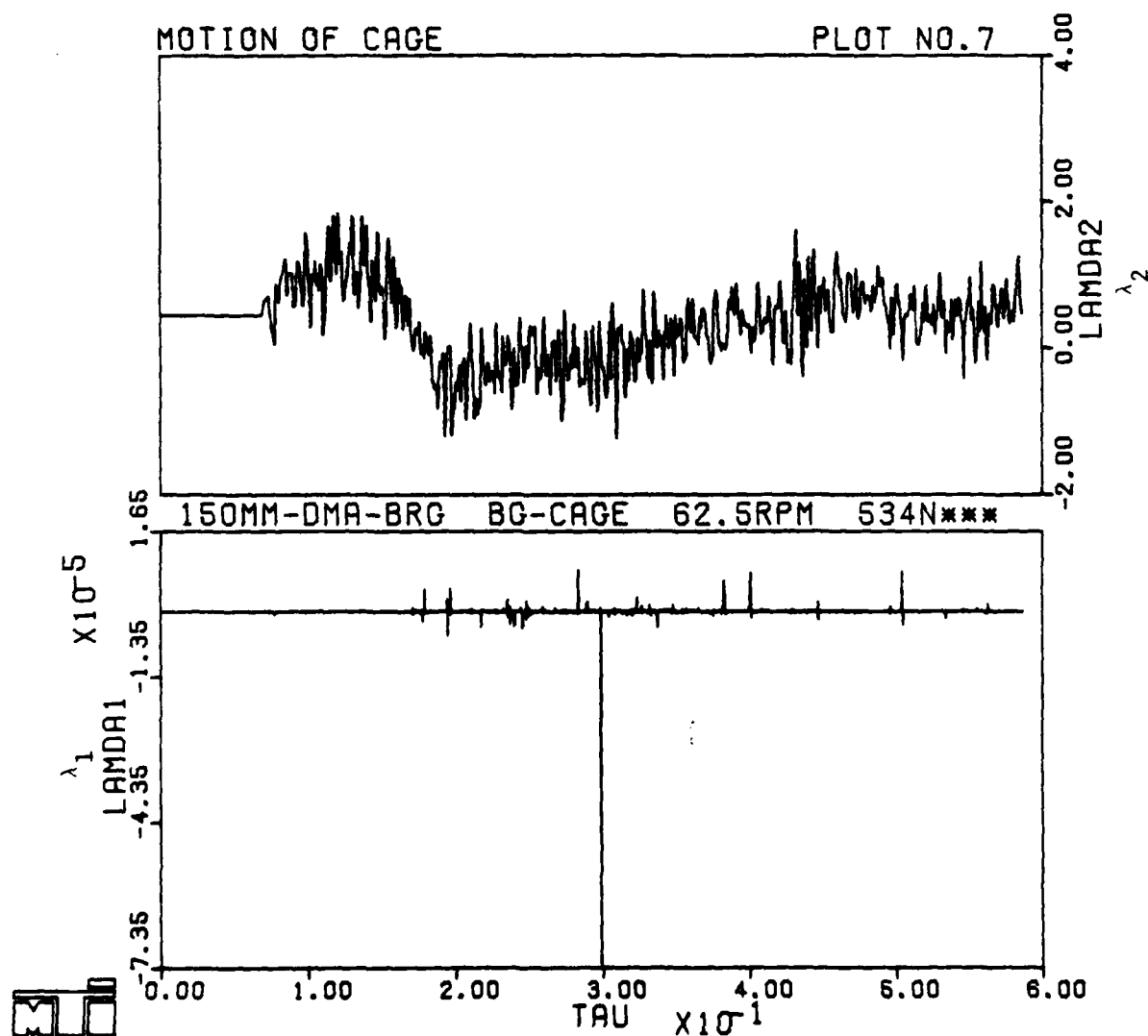


Fig. 4-32 Cage Whirl and Skid Parameters for the 150 mm Bearing with Ball Guided Cage and with Gravity Acting Normal to the Bearing Axis

## 5.0 ENGINE BEARING PERFORMANCE SIMULATIONS

The enhanced capabilities of RAPIDREB also apply to the high-load and high-speed engine bearings by providing bearing performance simulation over several shaft revolutions. For a given bearing and a set of operating conditions some typical performance simulations are presented in this section.

### 5.1 Bearing Geometry

The geometry of the bearing is shown in Figure 5-1. It is a 100 mm bore ball bearing with a steel cage guided on the inner race. The design corresponds to an actual test bearing at the Air Force Propulsion Laboratories.

### 5.2 Lubricant Traction Models

Conventional lubricant with the MIL-L-7808 specification is assumed. The traction behavior of this lubricant has been studied fairly extensively and the model in the original DREB program has been demonstrated to show a reasonable fit with the experimental data. The model is also built into RAPIDREB and appropriate input option is exercised to select the MIL-L-7808 model.

For the ball/cage and cage/race interfaces a hypothetical traction model (see Appendix C) is used to compute the friction forces when a metal contact takes place.

### 5.3 Operating Conditions

To simulate typical test conditions, the following operating conditions are assumed:

Axial load =	18,000 N
Radial load =	4,500 N
Inner race speed =	20,000 RPM
Outer race speed =	0
Operating temperature =	330°K

Gravity acts normal to the bearing axis, but in this case it really plays no appreciable role because the applied forces are quite high. Radial and axial equilibrium constraints on ball motion are assumed to eliminate the high frequency ball/race vibrations. Also the quasi-static solutions are used to determine the initial conditions.



#### 5.4 Performance Simulations

Performance simulations for the engine bearing at the above conditions are obtained over seven shaft revolutions and hence definite steady state behavior can be easily understood. Typical initial parameters are illustrated in the computer output presented in Appendix C.

As might be expected in case of combined axial and radial load, the ball load and contact angles go through a cyclic variation with a frequency corresponding to the ball orbital velocity. This is seen in Figure 5-2, where over three wavelengths of variations corresponding to over seven shaft revolutions are shown. It is also seen in this figure that the race-control hypotheses do not hold here also and definite spin velocities on both races develop in steady-state. Ball angular velocities demonstrate an interesting effect, see Figure 5-3. Since the initial quasi-static solutions do not allow gyroscopic slip and exact equilibrium of moments is not satisfied, the ball immediately tends to slip about the transverse y axis due to the gyroscopic moments. This alters the x and z components also and it takes approximately two shaft revolutions for the angular velocities to develop some steady state pattern and satisfy the gyroscopic slip as permitted by the lubricant characteristics. The ball cage interactions show that about one collision in each pock takes place per revolution of the cage and the ball drives the cage (ball/cage contact angle of  $180^\circ$ ) for part of the revolution and gets driven by the cage (contact angle of zero) for the remaining part. This is seen in Figure 5-4. The ball/cage forces seen in this figure are really the collision forces and the hydrodynamic forces, being very small compared to the collision forces, are not seen in the figure. However, the ball/cage approach relative to the radial pocket clearance clearly demonstrates the transition from hydrodynamic to metal contact.

The race/cage interaction is very dynamic and interesting to note. Figure 5-5 shows the race/cage force variations at the two lands (labelled 1 and 2) on either side of the balls. Initially both lands show identical collision forces but when appreciable coning motion of the cage develops, the forces on the two lands begin to differ; this is more clear from the traction

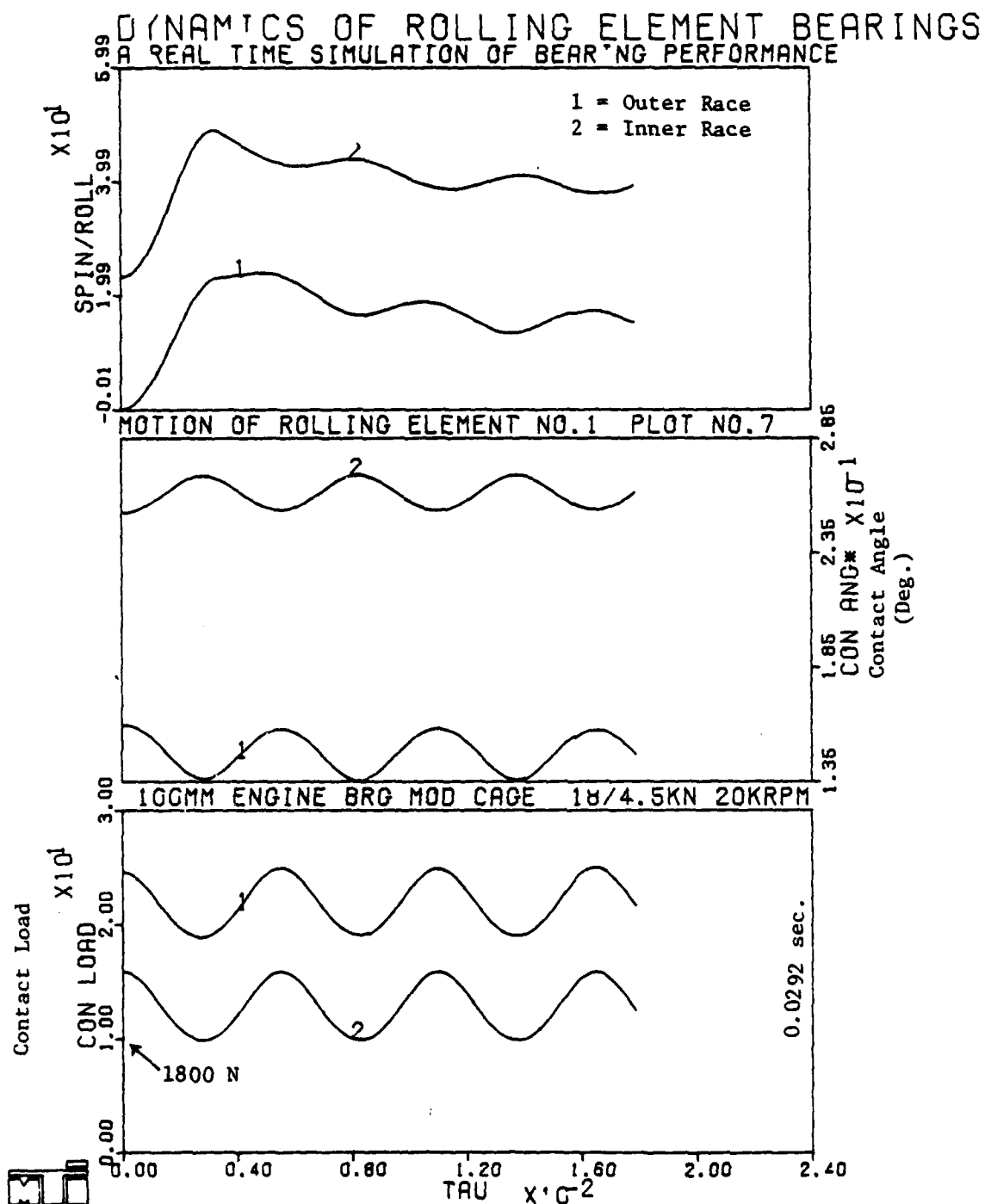


Fig. 5-2 Variations in Ball/Race Load, Contact Angle and Spin-to-Roll for the 100 mm Engine Bearing

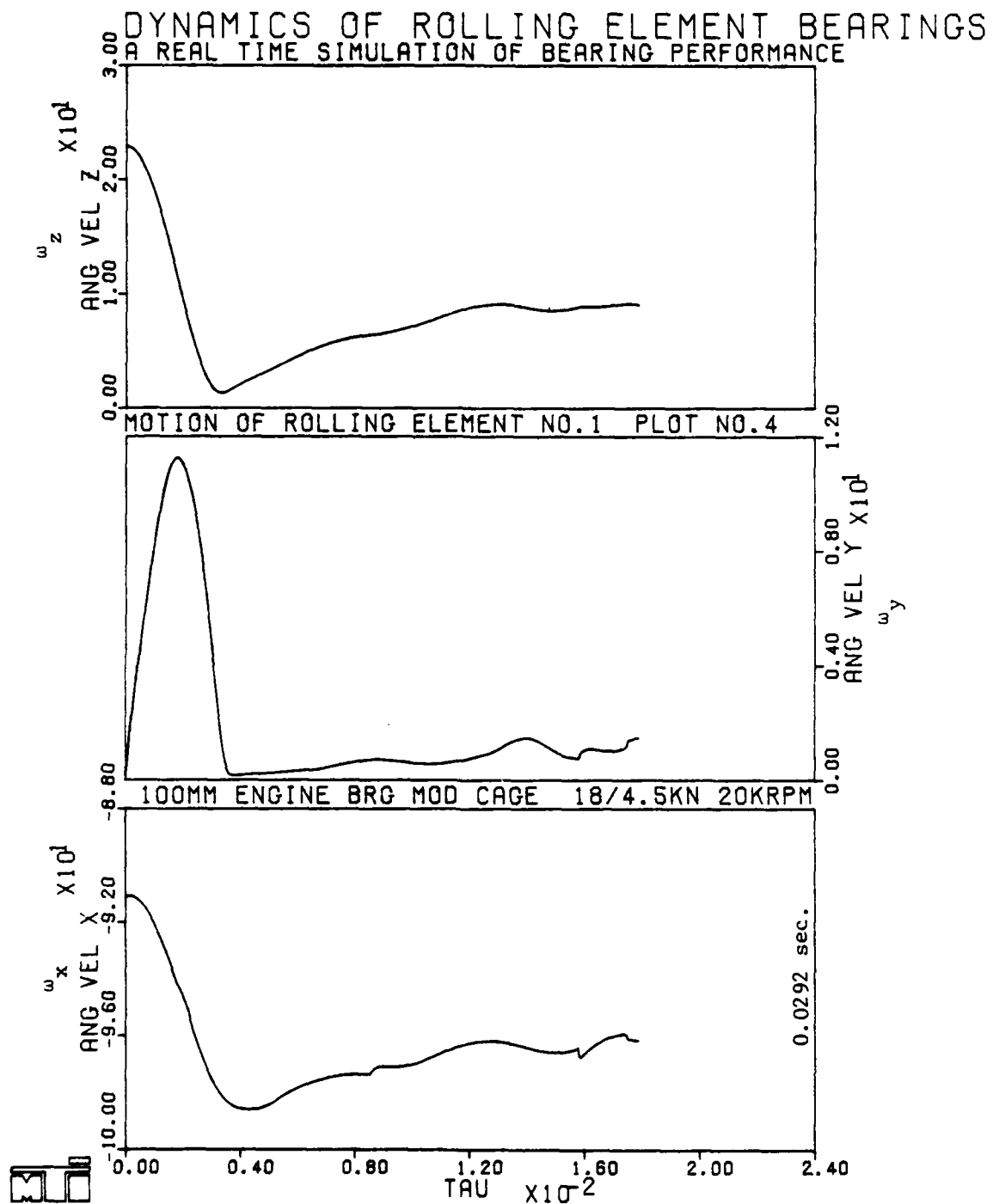


Fig. 5-3 Dimensionless Ball Angular Velocity Variation for the 100 mm Engine Bearing. Scale =  $7.84 \times 10^4$  RPM

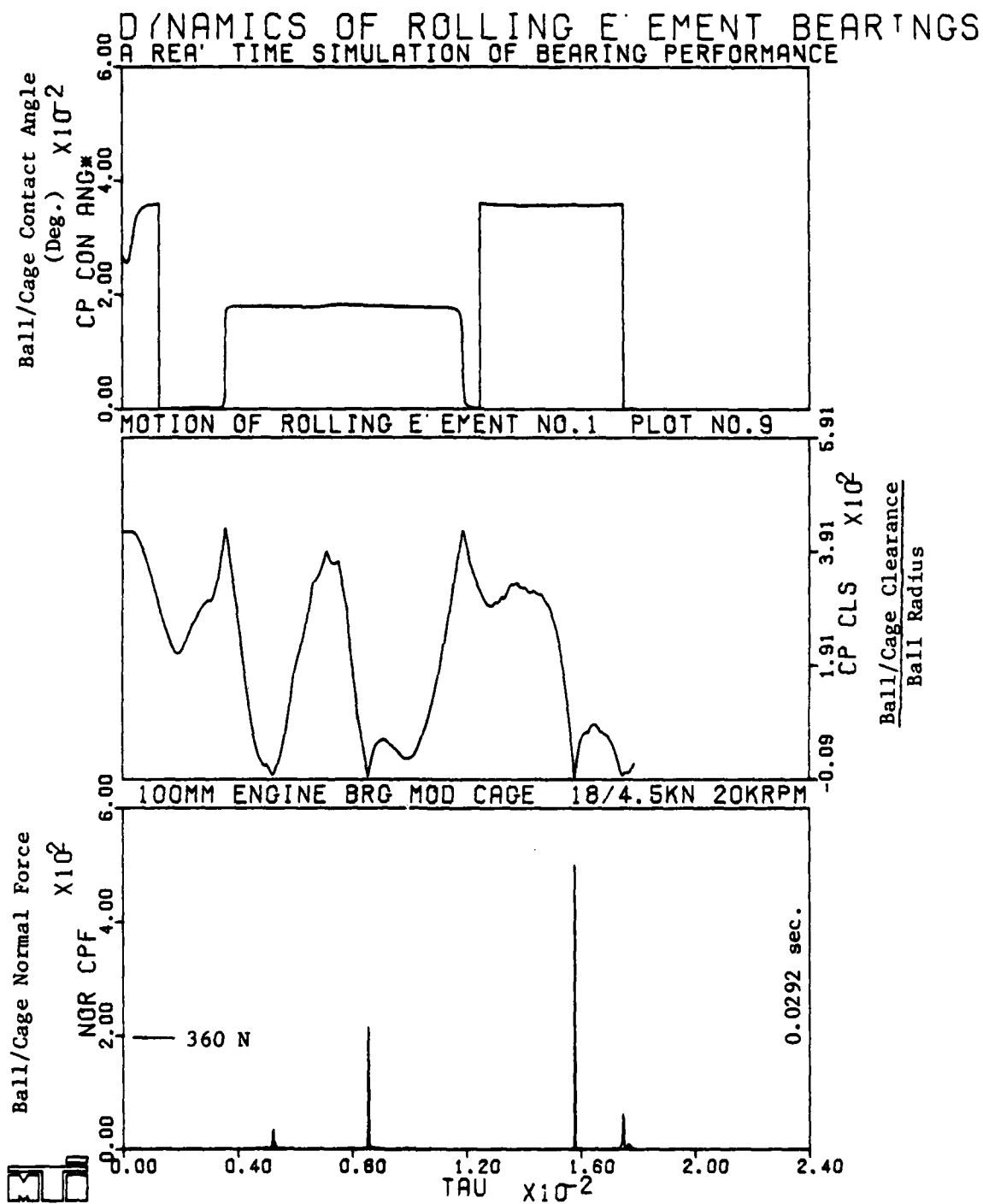


Fig. 5-4 Ball/Cage Interaction for the 100 mm Engine Bearing



# DYNAMICS OF ROLLING ELEMENT BEARINGS A REAL TIME SIMULATION OF BEARING PERFORMANCE

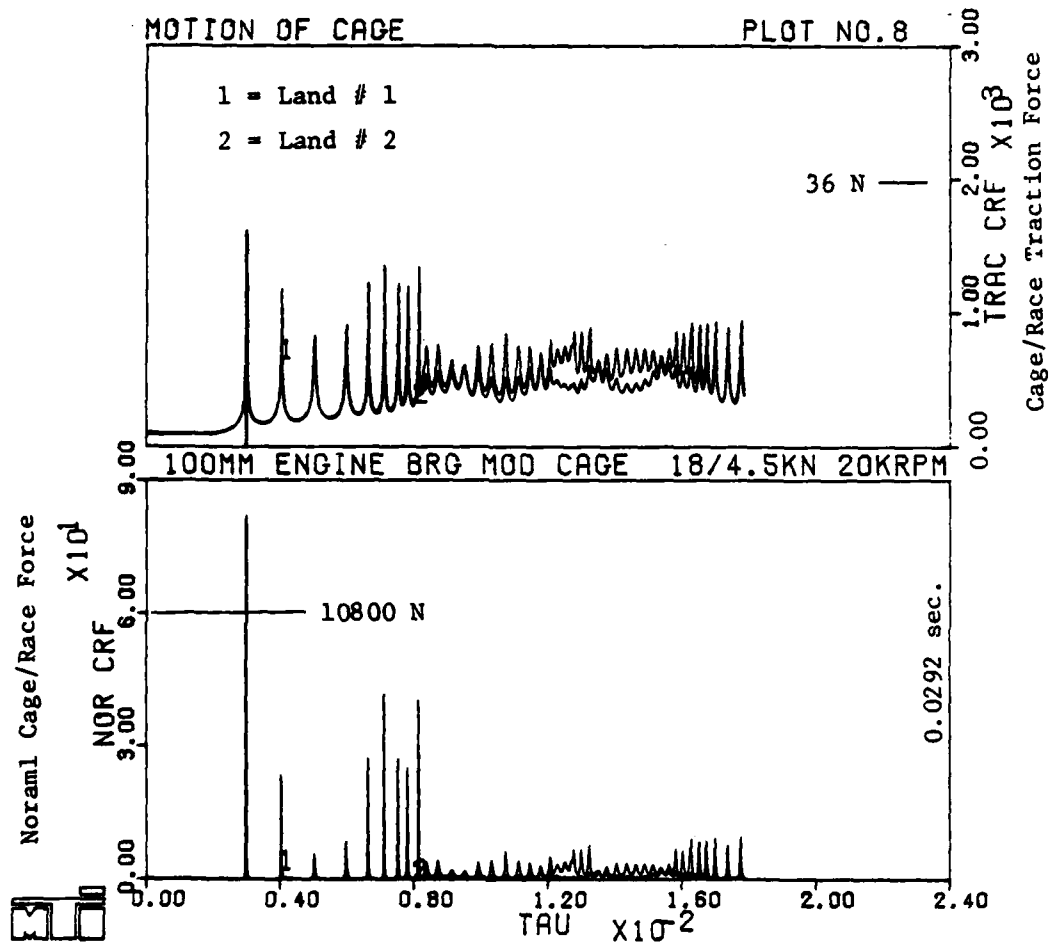


Fig. 5-5 Repeated Cage/Race Collisions in the 100 mm Engine Bearing

force curves. The ultimate behavior to note is that the race/cage collisions are really very close together in time in steady state. Also the magnitude of the force is fairly large ( $\sim 1800$  N). This means that the cage will steadily be in contact with the race with a relatively large force, and some cage wear problems may be expected. This is seen by the steady circular orbit of the cage mass center in Figure 5-6 with the orbit radius equal to the cage/race radial clearance. This effect has indeed been confirmed experimentally [18] and the experimental results will soon be documented elsewhere [19].

Corresponding to the above race/cage collisions considerable radial chatter of the cage mass center is observed, as shown in Figure 5-7 in terms of the cage mass center velocities. Excessive whirl is indicated by the increased orbital velocity. The coning motion is demonstrated by the angular velocity variations in Figure 5-8. The deviation of cage angular velocity from the initial epicyclic angular velocity (see component x) indicates substantial skid in the bearings due to excessive rubbing of the cage at the cage/race interracial. Both cage whirl and skid are better understood in terms of the parameters  $\lambda_1$  and  $\lambda_2$  respectively, as shown in Figure 5-9.

Finally, the variations of bearing torque, power loss, and the cumulative load slip integral are shown in Figure 5-10. The initial bump in the torque curves correspond to the gyroscopic slip of the balls as discussed above and the steady noise is a result of the ball/cage and race/cage collisions.

# DYNAMICS OF ROLLING ELEMENT BEARINGS

## A REAL TIME SIMULATION OF BEARING PERFORMANCE

100MM ENGINE BRG MOD CAGE 18/4.5KN 20KRPM  
MOTION OF CAGE PLOT NO.9

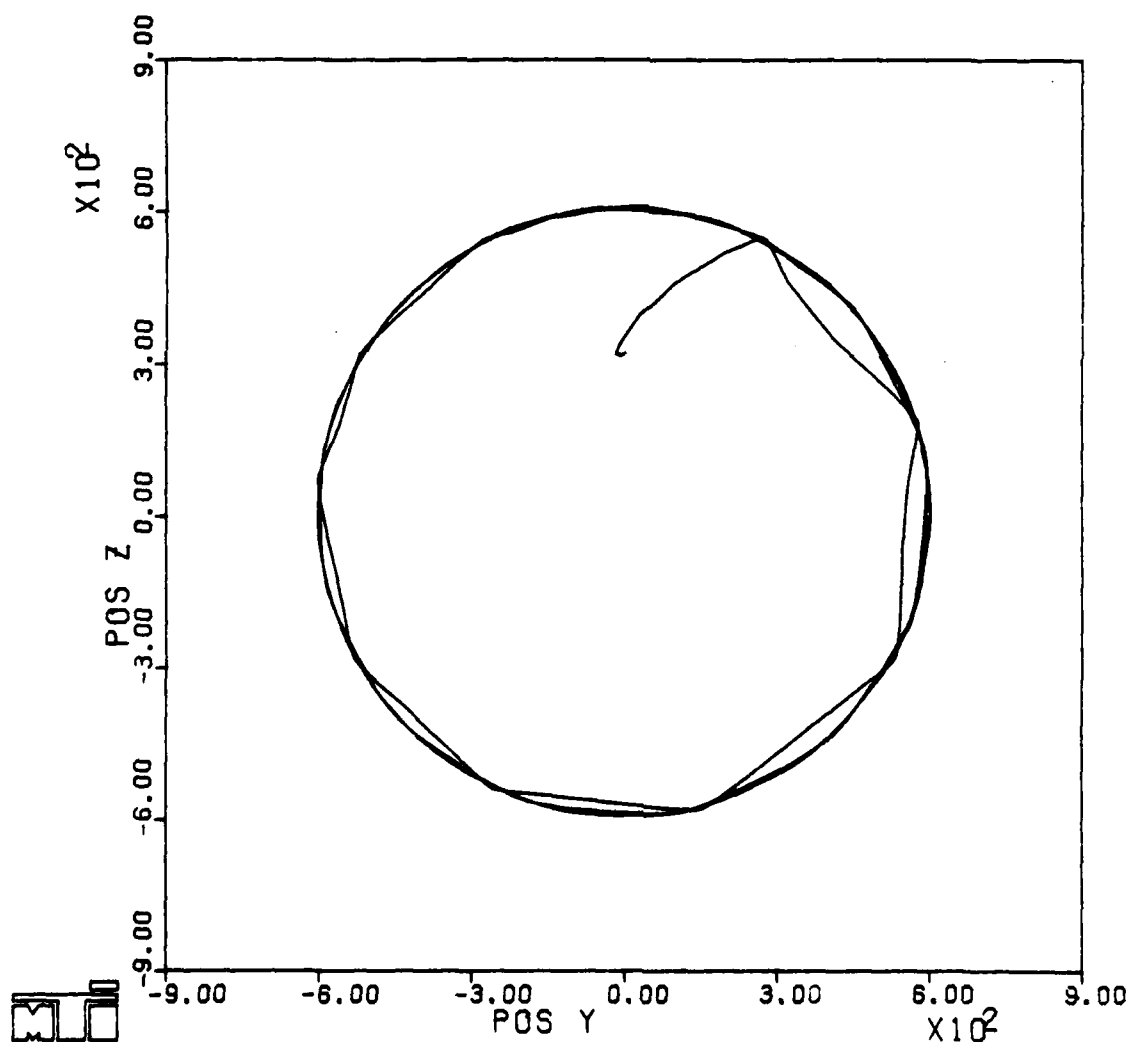


Fig. 5-6 Steady Orbit of the Cage Mass Center for the 100 mm Engine Bearing. Scale = 0.009525 M

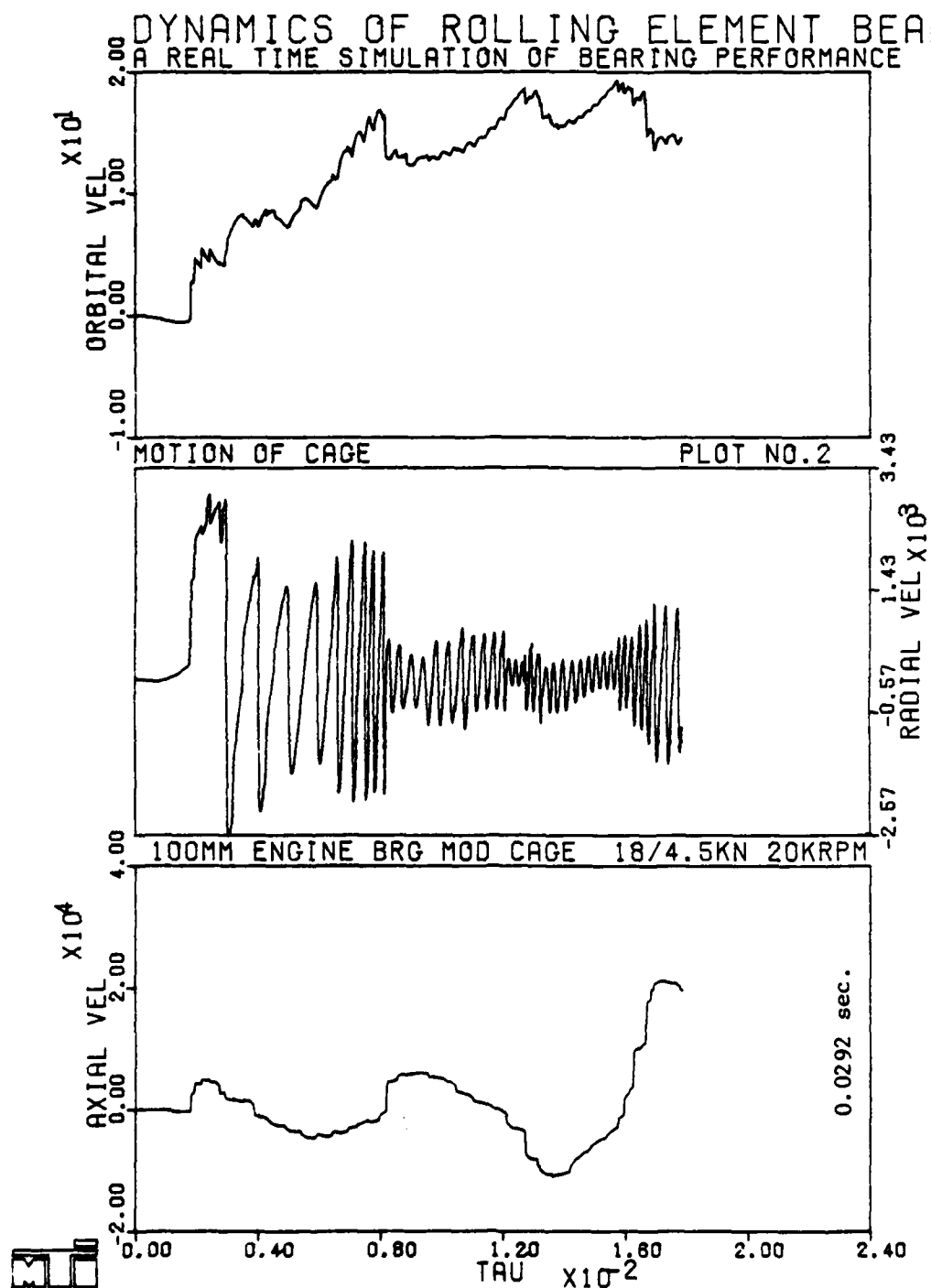


Fig. 5-7 Dimensionless Velocity of Cage Mass Center for the 100 mm Engine Bearing. Scales = 78.17 M/Sec,  $7.84 \times 10^4$  RPM

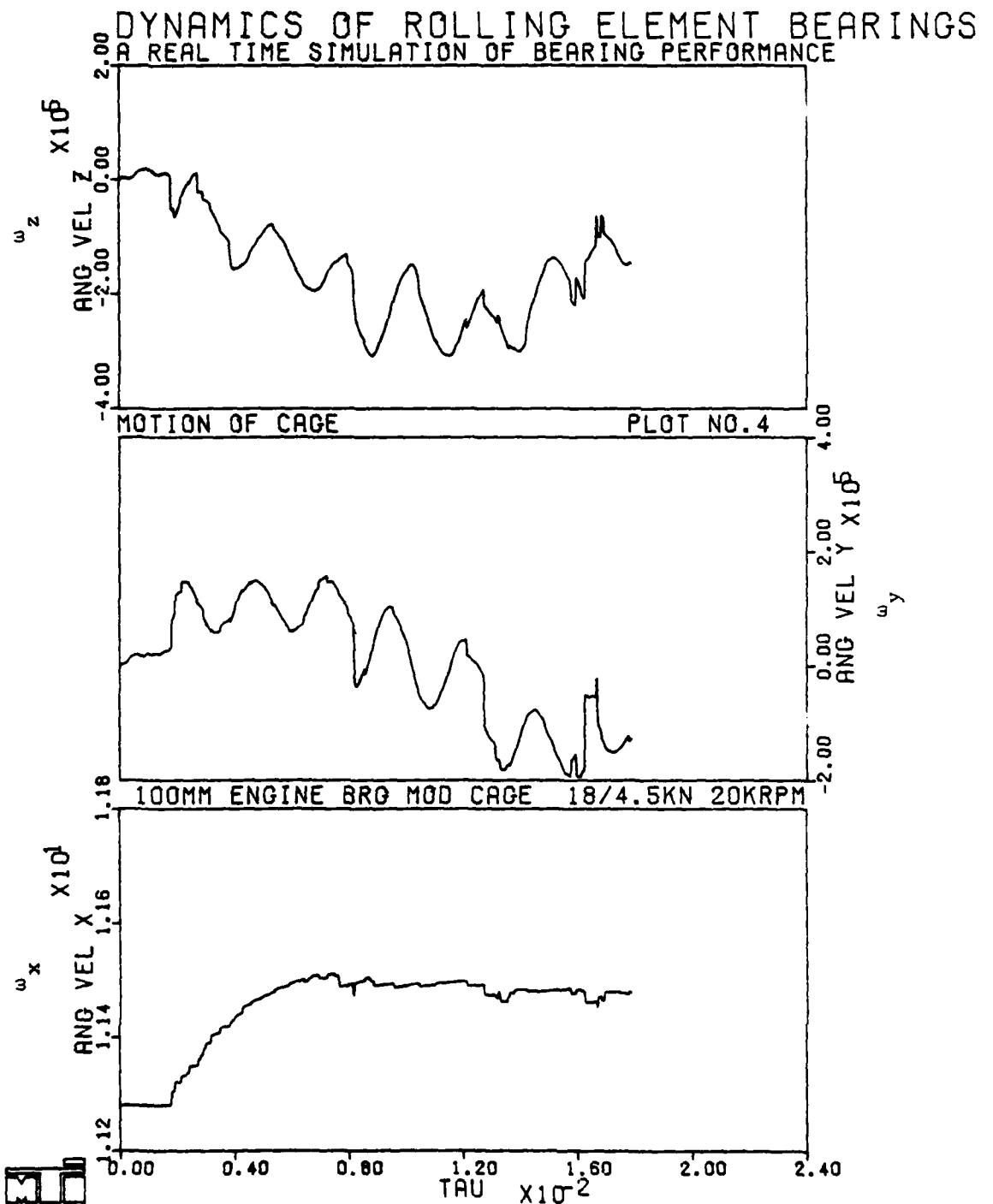


Fig. 5-8 Dimensionless Angular Velocity of a Ball in the 100 mm Engine Bearing. Scale =  $7.84 \times 10^4$  RPM

# DYNAMICS OF ROLLING ELEMENT BEARINGS A REAL TIME SIMULATION OF BEARING PERFORMANCE

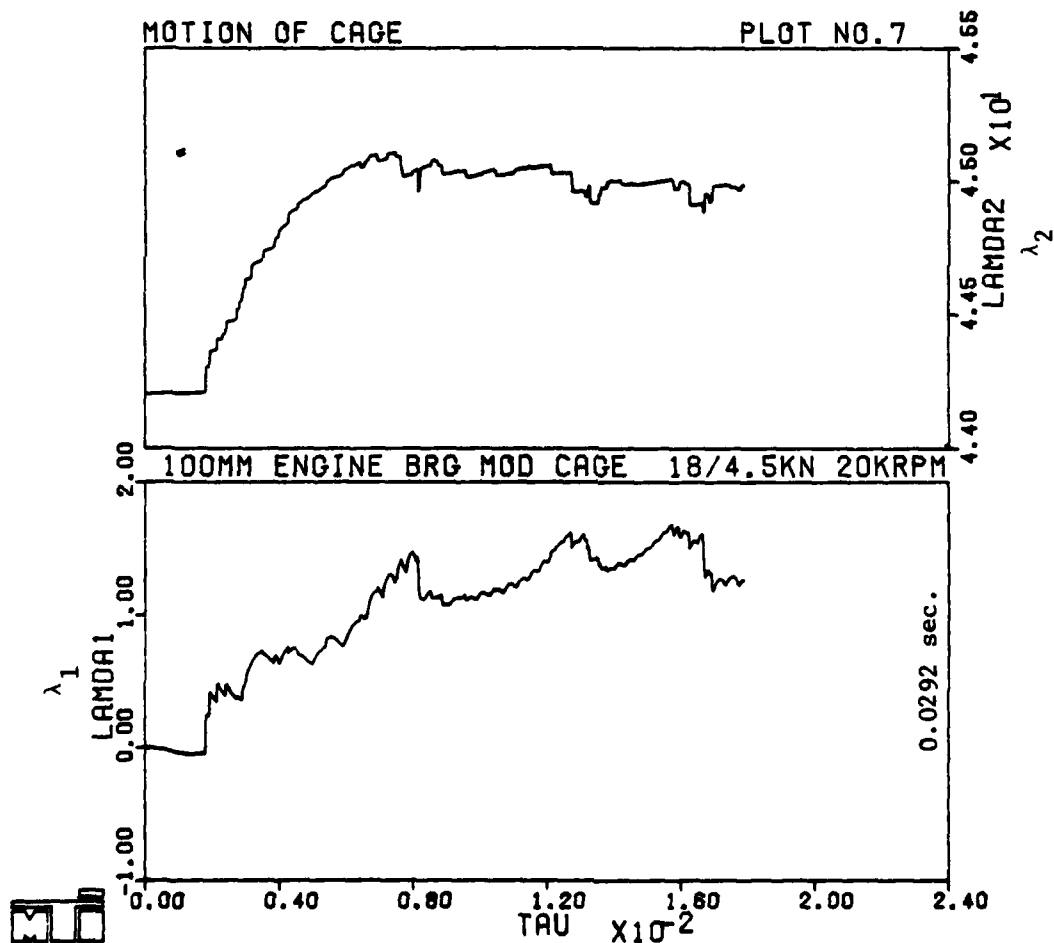


Fig. 5-9 Cage Whirl and Skid Parameters for the 100 mm Engine Bearing

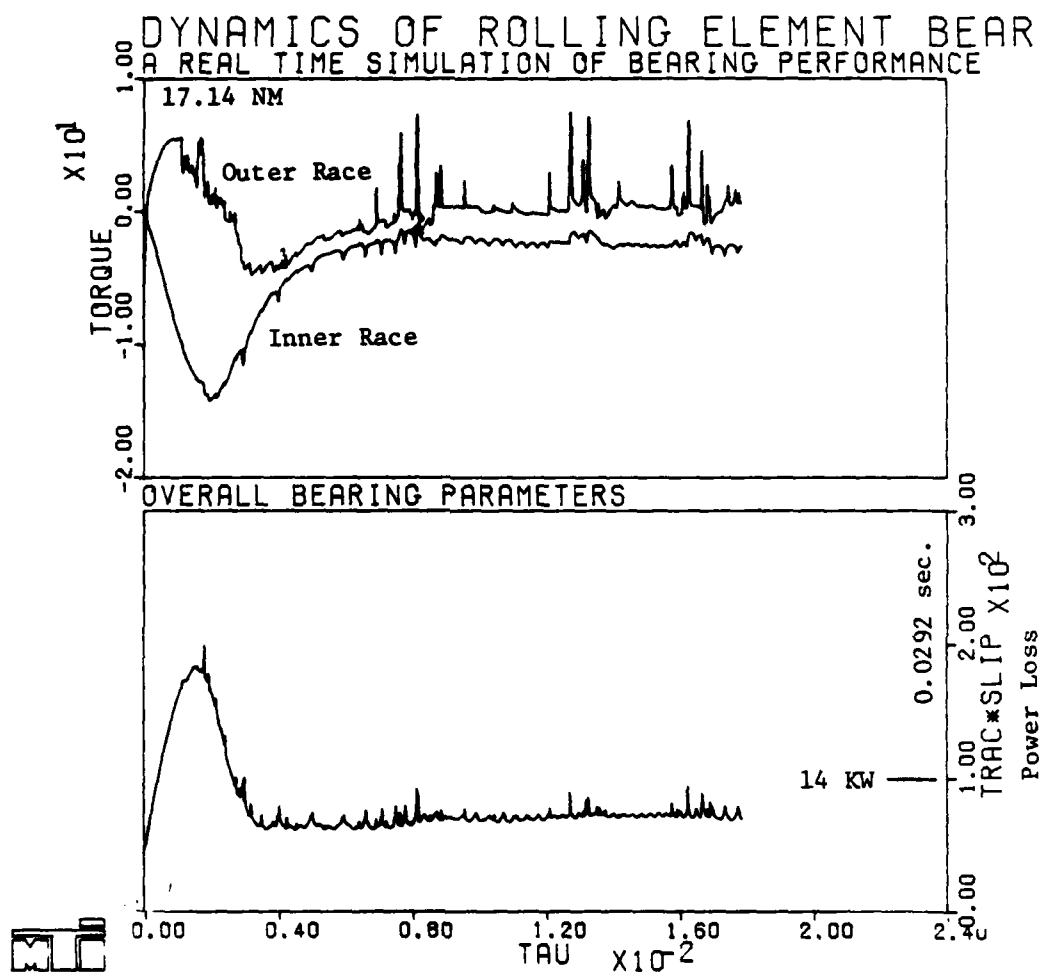


Fig. 5-10 Bearing Torque and Power Loss Variations in the 100 mm Engine Bearing

## 6.0 CONCLUSIONS AND RECOMMENDATIONS

The existing Dynamics of Rolling Element Bearings (DREB) computer program has been enhanced to selectively suppress the very high frequency vibratory motion of the balls in an angular contact ball bearing and thereby provide the added capability of investigating the low frequency phenomena in some depth. With such an enhancement a considerable increase in the maximum permissible time step size has led to bearing performance simulation over several shaft revolutions within reasonable computing effort. The updated program version is referred to as RAPIDREB. Some of the essential RAPIDREB capabilities include:

1. Radial and axial equilibrium constraints on the balls to eliminate the high frequency ball/race vibration.
2. Introduction of fictitious damping at each contact interface to selectively damp the high frequencies.
3. Incorporation of a number of Runge-Kutta type explicit formulae.
4. A predictor-corrector algorithm for conditions under which no substantial cyclic components and discontinuities in the solutions exist.
5. Option to change the integrating algorithm at any point in time.
6. Treatment of ball guided cages for very low speed ball bearings.
7. Built in options for synchronous radial loading due to unbalance or any rotating loads.

Any of the above options can be selected or the program can be run in a completely generalized mode identical to the original DREB program. It is shown that depending on the operating conditions substantial computing effort can be saved by properly selecting the constraints and the integrating method. By exercising RAPIDREB over a number of trial runs it is concluded that the predictor-corrector type of formula is only suitable when there are no discontinuities and high frequency vibratory motions in the system. Thus after suppressing the very high frequencies, the



predictor-corrector schemes offer the benefit of very large step sizes, only for the cases where no discontinuities associated with ball/cage or race/cage collisions are present. This is because extrapolation past a discontinuity results in larger errors in the prediction process. Thus these schemes are useful only for bearings either without cage or with basically hydrodynamic interaction at the ball/cage and race/cage interfaces. Considerable care in selecting the integrating method is therefore necessary.

RAPIDREB is used to produce performance simulations of two very low speed, lightly loaded DMA (Despun Mechanical Assembly) ball bearings and a typical high-load, high-speed ball bearing for engine applications. The DMA bearings have pure thrust load and therefore gravity is the only dominant factor as far as the cage is concerned. Hence both bearings are oriented such that gravity is either parallel or perpendicular to the bearing axis. The first of the DMA bearings is a 100 mm bore ball bearing with inner race guided cage. The steady state performance simulation obtained by integrating the equations of motion over more than a shaft revolution indicate that when gravity acts along the bearing axis the cage contacts all the balls and balances its own weight against the balls. No substantial cage whirl is observed in the simulation and the bearing operation is generally stable. When weight of the cage acts normal to the bearing axis variable ball/cage and cage/race interactions are observed as the balls travel in their orbit. This is basically due to the eccentric location of the cage. An appreciable coning motion of the cage is also observed in this case but again no appreciable cage whirl or skid is observed and the operation is generally stable. The second of the DMA bearings is a 150 mm bore ball bearing with a ball guided cage with a conical guidance surface attached to the nominally cylindrical pocket. Again the first symmetric case when the gravity acts along the bearing axis is similar to the 100 mm bearing and the weight of the cage is balanced against the ball/cage forces. However, large variations in cage whirl velocity are observed indicating some element of instability. The bearing performance worsens as the cage is allowed to move eccentricly under its own weight acting normal to the bearing axis. In this case large interactions at both the cylindrical and

conical parts of the cage pocket are observed. This results in a large amount of noise and greatly erratic motion of the cage.

The engine bearing performance simulations are obtained with a combined thrust and radial load (thrust to radial load ratio of 4) over more than seven shaft revolutions. The test example consists of a 100 mm bore ball bearings operating at 20,000 rpm with a thrust load of 18000 N and a radial load of 4500 N. The bearing uses a steel cage guided on the inner race. It is shown that for such an operating environment the cage develops appreciable whirl velocity and in steady state a continued metal contact at the guiding land is established. Hence a definite possibility of cage wear at the guiding surface is predicted.

Since RAPIDREB easily provides bearing performance simulations over several shaft revolutions and the prediction of steady state performance is possible with great confidence, several recommendations for future development may be listed:

1. The steady state performance predictions should be validated experimentally, particularly in terms of the cage motion. This will greatly strengthen the predictive capability of RAPIDREB and thereby enhance its value as a design tool.
2. Since solutions over relatively large time domains are now possible a graphic simulation of the various component motions in the bearing will contribute to greater understanding of the various instabilities and the dynamic behavior of the bearing as a whole. This will essentially require the development of a sophisticated graphics program replacing the current plot program.
3. RAPIDREB can be very useful in establishing direct correlations of bearing life and dynamic stability with both geometrical and operational variables. Hence it can be a very useful tool in guiding accelerated life cycle tests for long life bearings

AD-A112 009

MECHANICAL TECHNOLOGY INC LATHAM N Y

F/G 13/9

INTERACTIVE GRAPHIC SIMULATION OF ROLLING ELEMENT BEARINGS. PHA--ETC(U)

NOV 81 P K GUPTA

F33615-80-C-5152

UNCLASSIFIED

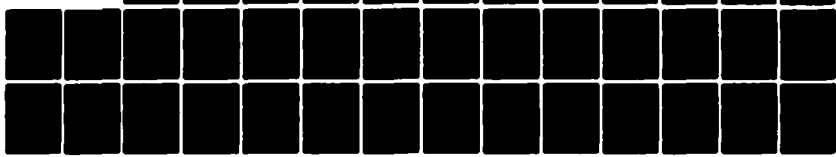
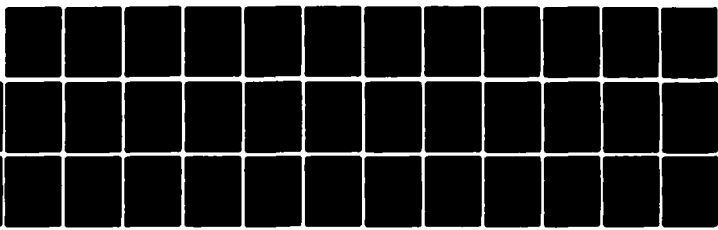
MTI-81TR66

AFWAL-TR-81-4148

NL

2 x 2

00000000



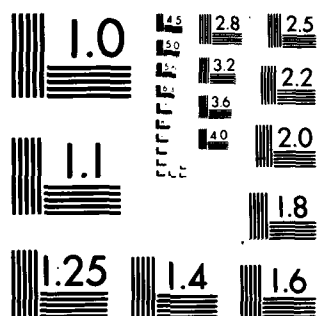
END

DATE

FILED

4-82

DTIC



MICROCOPY RESOLUTION TEST CHART

NATIONAL BUREAU OF STANDARDS-1963-A

such as the DMA bearings. A parametric study to establish such correlations and the development of guidelines for accelerated bearing life tests is therefore recommended.

#### REFERENCES

1. Gupta, P. K., "Dynamics of Rolling Element Bearings - Part I: Cylindrical Roller Bearing Analysis", Trans. ASME, J. Lub. Tech., Vol. 101, No. 3, July 1979, pp. 293-304.
2. Gupta, P. K., "Dynamics of Rolling Element Bearings - Part II: Cylindrical Roller Bearing Results", Trans. ASME, J. Lub. Tech., Vol. 101, No. 3, July 1979, pp 305-311.
3. Gupta, P. K., "Dynamics of Rolling Element Bearings - Part III: Ball Bearing Analysis", Trans. ASME, J. Lub. Tech., Vol. 101, No. 3, July 1979, pp 312-318.
4. Gupta, P. K., "Dynamics of Rolling Element Bearings - Part IV: Ball Bearing Results", Trans. ASME, J. Lub. Tech., Vol. 101, No. 3, July 1979, pp 319-326.
5. Gupta, P. K., "Dynamics of Rolling Element Bearings - DREB Computer Program", MTI Computer Software, July 1977.
6. Gupta, P. K., Winn, L. W. and Wilcock, D. F., "Vibrational Characteristics of Ball Bearings, J. Lub. Tech., ASME Trans., 99F #2, pp 284-289, (1977).
7. Den Hartog, J. P., MECHANICAL VIBRATIONS, McGraw Hill Book Company 1956.
8. Hildebrand, F. B., INTRODUCTION TO NUMERICAL ANALYSIS, McGraw Hill Book Company, 1956.
9. Gear, C. W., NUMERICAL INITIAL VALUE PROBLEMS IN ORDINARY DIFFERENTIAL EQUATIONS, Prentice Hall, 1971.
10. Lambert, J. D., COMPUTATIONAL METHODS IN ORDINARY DIFFERENTIAL EQUATIONS, John Wiley, 1973.
11. Shampine, L. F. and Allen, R. C., NUMERICAL COMPUTING: An Introduction, W. B. Saunders Company, 1973.
12. Forsythe, G. E., Malcolm, M. A. and Moler, C. B., COMPUTER METHODS FOR MATHEMATICAL COMPUTATIONS, Prentice Hall, 1977.
13. Gupta, P. K., "Analysis of Cage Motion", Air Force Report AFAPL-TR-76-28, Wright Patterson Air Force Base, Ohio, December 1975.
14. Tyler, J. C., Carper, H. J., Brown, R. D. and Ku, P. M., "An Analysis of Film Thickness Effects in Slow Speed Lightly Loaded Elastohydrodynamic Contacts - Part I: Development of Film Thickness Measurement Technique", Air Force Report AFML-TR-74-189 Part I, December 1974.

15. Gupta, P. K., "Simulation of Torque Variations in the DMA Ball Bearings", Trans. ASLE, Vol. 23, No. 3, July 1980, pp 315-325.
16. Gupta, P. K., Flamand, L., Berthe, D., and Godet, M., "On the Traction Behavior of Several Lubricants", J. Lub. Tech., ASME Trans., Vol. 103, No. 1, January 1981, pp 55-64.
17. Gupta, P. K., "Transient Ball Motion and Skid in Ball Bearings", J. Lub. Tech., ASME Trans., 97F, #2, pp 261-269, (1975).
18. Dill, J. F., Personal Communications.
19. Dill, J. F. and Gupta, P. K., "Experimental Validation of the DREB Computer Program in the Engine Bearing Operating Environment", to be published.

APPENDIX A

INPUT DATA DESCRIPTION FOR THE COMPUTER PROGRAMS

RDREB  
and  
RDREBP





```

C      7. IMPROVED COMPUTING SPEEDS. PROPER SELECTION OF CONS-    RDREB 59
C      TRAINTS AND INTEGRATING METHOD CAN EASILY REDUCE THE COM-   RDREB 60
C      PUTATION EFFORT BY A FACTOR OF FIFTEEN TO TWENTY WHEN-     RDREB 61
C      COMPARED WITH THE ORIGINAL DREB PROGRAM.                   RDREB 62
C                                                                    RDREB 63
C                                                                    RDREB 64
C      THE PROGRAM -RDREB- IS DESIGNED FOR BALL BEARINGS ONLY AND NO RDREB 65
C      TREATMENT OF ROLLER BEARINGS IS AVAILABLE.                 RDREB 66
C                                                                    RDREB 67
C                                                                    RDREB 68
C                                                                    RDREB 69
C      INPUT DATA                                                 RDREB 70
C      *****                                                    RDREB 71
C                                                                    RDREB 72
C      ALL INPUT DATA IS SUPPLIED ON DATA CARDS IN COLUMNS 11 TO 70. RDREB 73
C      THE FIRST AND THE LAST TEN COLUMNS ON EACH CARD ARE RESERVED FOR RDREB 74
C      IDENTIFICATION PURPOSES. THE USER MAY USE THESE COLUMNS FOR ANY RDREB 75
C      DESIRABLE INFORMATION. THE INFORMATION IS JUST READ IN AND RDREB 76
C      PRINTED OUT IN THE LIST OF DATA CARDS.                     RDREB 77
C                                                                    RDREB 78
C      THE PROGRAM ALLOWS FOR BOTH THE ENGLISH AND SI SYSTEMS OF UNITS. RDREB 79
C      ALL INPUT DATA MUST BE IN THE SYSTEM OF UNIT SELECTED BY THE USER. RDREB 80
C      THE FUNDAMENTAL UNITS AND THE ABBREVIATIONS USED IN THE TWO RDREB 81
C      SYSTEMS ARE DESCRIBED IN THE FOLLOWING TABLE --            RDREB 82
C                                                                    RDREB 83
C      QUANTITY              ENGLISH UNIT                SI UNIT          RDREB 84
C                                                                    RDREB 85
C      FORCE (F)             POUND FORCE (LRF)           NEWTON (N)         RDREB 86
C      LENGTH (L)           INCH (IN)                  METER (M)          RDREB 87
C      TIME (T)             SECOND (S)                 SECOND (S)          RDREB 88
C      MASS (MA)            POUND MASS (LRM)            KILOGRAM MASS (KGM) RDREB 89
C      TEMP (TM)            DEG RANKINE (DEG-R)          DEG KELVIN (DEG-K) RDREB 90
C                                                                    RDREB 91
C      APPROPRIATE UNITS FOR ALL THE PHYSICAL QUANTITIES CAN BE DERIVED RDREB 92
C      IN TERMS OF THE ABOVE FUNDAMENTAL UNITS. SIMPLY FOR CONVENIENCE RDREB 93
C      ALL ANGULAR VELOCITIES AND ANGULAR ACCELERATIONS ARE SPECIFIED IN RDREB 94
C      RPM AND RPM/SEC RESPECTIVELY. ALSO, ALL ANGLES ARE SPECIFIED IN RDREB 95
C      DEGREES.                                                     RDREB 96
C                                                                    RDREB 97
C      ALL INPUT VARIABLE NAMES BEGINNING WITH I, J, K, L, M AND N ARE RDREB 98
C      INTEGERS AND THE REMAINING ARE REAL NUMBERS. ALSO, IT WILL BE RDREB 99
C      IMPORTANT THAT ALL INTEGERS ARE RIGHT ADJUSTED IN THEIR FIELDS. RDREB100
C                                                                    RDREB101
C      AN ABBREVIATION -RE- IS USED FOR ROLLING ELEMENT IN THE FOLLOWING RDREB102
C      INPUT DESCRIPTION AND ALSO IN THE PRINT OUTPUT OF THE PROGRAM. RDREB103
C                                                                    RDREB104
C      THE VARIABLE NAMES, COLUMN FIELDS AND VARIABLE DESCRIPTIONS ARE RDREB105
C      DOCUMENTED BELOW FOR EACH INPUT DATA CARD.                 RDREB106
C                                                                    RDREB107
C      CARD 1                                                       RDREB108
C      -----                                                      RDREB109
C      MODE    11-12    SWITCH WITH FOLLOWING FUNCTIONS --        RDREB110
C                      DYNAMIC SOLUTION WITH NO                   RDREB111
C                      CHANGE IN OPERATING DATA = 0               RDREB112
C                      DYNAMIC SOLUTION WITH                        RDREB113
C                      MODIFIED OPERATING DATA ON                  RDREB114
C                      CARDS 13-19 = 1                               RDREB115
C                      DYNAMIC SOLUTION WITH ARBI-

```

C		TRARY INITIAL CONDITIONS = 2	RDRB116
C		AXIAL AND RADIAL BALL MOTION	RDRB117
C		CONSTRAINED BY QUASI-STATIC	RDRB118
C		EQUILIBRIUM AT EACH STEP = 3	RDRB119
C		CONSTRAINED AXIAL AND RADIAL	RDRB120
C		BALL MOTION UNDER PURE	RDRB121
C		THRUST LOAD AND CONSTANT	RDRB122
C		RACE SPEEDS = 4	RDRB123
C	IR 13-16	RECORD NUMBER FOR INITIAL CONDITIONS. IR=0 AT	RDRB124
C		START.	RDRB125
C	MONT 17-19	DATA MONITOR CODE. WHEN MODULUS OF (IQ-1), IQ	RDRB126
C		BEING THE STEP NUMBER, AND MONT VANISHES, THE	RDRB127
C		DIMENSIONLESS SOLUTION VECTOR WILL BE WRITTEN	RDRB128
C		IN THE MASTER DATA FILE.	RDRB129
C	NPRT 20-28	VECTOR OF LENGTH 3 CONTAINING THE PRINT CODES	RDRB130
C		WITH THE FOLLOWING SIGNIFICANCE --	RDRB131
C		NPRT(1) = 0, PRINT ALL ROLLING ELEMENT SOLUTIONS	RDRB132
C		N, SKIP " ROLLING ELEMENT SOLUTIONS	RDRB133
C		-N, SKIP ALL ROLLING ELEMENT SOLUTIONS	RDRB134
C		NPRT(2)=K SUCH THAT WHEN THE MODULUS OF (IQ-1),	RDRB135
C		IQ BEING THE STEP NUMBER, AND K	RDRB136
C		VANISHES, THE OUTPUT IS PRINTED AT	RDRB137
C		STEP IQ.	RDRB138
C		NPRT(3)=K SUCH THAT WHEN THE MODULUS OF (IQ-1),	RDRB139
C		IQ BEING THE STEP NUMBER AT WHICH OUT-	RDRB140
C		PUT IS PRINTED, AND K VANISHES, THE	RDRB141
C		DIMENSIONLESS SOLUTION VECTOR IS ALSO	RDRB142
C		PRINTED.	RDRB143
C	NOPT 29-40	EACH COMPONENT HAS A FIELD WIDTH OF 3.	RDRB144
C		VECTOR OF LENGTH 3 CONTAINING THE OPTIMIZATION	RDRB145
C		CODES (SEE NOTE 5) DEFINED AS --	RDRB146
C		NOPT(1) = NUMBER OF STEPS FOR WHICH INTEGRATION	RDRB147
C		WILL CONTINUE WHEN THE TRUNCATION ERROR	RDRB148
C		EXCEEDS THE SPECIFIED LIMIT WITH THE	RDRB149
C		MINIMUM STEP SIZE.	RDRB150
C		NOPT(2) = NUMBER OF STEPS AFTER WHICH AN ATTEMPT	RDRB151
C		TO OPTIMIZE THE STEP SIZE WILL BE MADE.	RDRB152
C		NOPT(3) = MAXIMUM NUMBER OF STEPS IN THE RUN.	RDRB153
C		EACH COMPONENT HAS A FIELD WIDTH OF 4.	RDRB154
C	IMET 41-43	SWITH FOR INTEGRATING ALGORITHM --	RDRB155
C		IMET = 0, FOURTH ORDER RUNGA-KUTTA-MERSON	RDRB156
C		1, FOURTH ORDER RUNGA-KUTTA-FEHLBERG	RDRB157
C		2, FOURTH ORDER RUNGA-KUTTA-ENGLAND	RDRB158
C		3, CLASSICAL FOURTH ORDER RUNGA-KUTTA	RDRB159
C		4, FOURTH ORDER RALSTON-RUNGA-KUTTA	RDRB160
C		5, FIFTH ORDER KUTTA-NYSTROM	RDRB161
C		6, SIXTH ORDER KUTTA-RUNGA-KUTTA	RDRB162
C		7, SECOND ORDER RUNGA-KUTTA	RDRB163
C		8, THIRD ORDER RUNGA-KUTTA	RDRB164
C		10, A PREDICTOR-CORRECTOR FORMULA	RDRB165
C		(IMET=10 RECOMMENDED FOR CAGELESS	RDRB166
C		BEARINGS ONLY)	RDRB167
C			RDRB168
C	CARD 2		RDRB169
C	-----		RDRB170
C		SEE NOTE 6 FOR DISCUSSION RELEVANT TO THIS CARD.	RDRB171
C			RDRB172

C				RDREB173
C	DINT	11-22	INITIAL DIMENSIONLESS TIME STEP SIZE.	RDREB174
C	DMIN	23-34	MINIMUM DIMENSIONLESS TIME STEP SIZE.	RDREB175
C	DMAX	35-46	MAXIMUM DIMENSIONLESS TIME STEP SIZE.	RDREB176
C	TF	47-58	FINAL DIMENSIONLESS TIME.	RDREB177
C				RDREB178
C				RDREB179
C	*	IF IR.GT.0 AND MODE.EQ.0 GO TO CARD 21.		RDREB180
C	*	IF IR.GT.0 AND MODE.EQ.1 GO TO CARD 13.1.		RDREB181
C				RDREB182
C				RDREB183
C	CARD 3			RDREB184
C	-----			RDREB185
C	KBT	11-13	BEARING TYPE DEFINED AS FOLLOWS --	RDREB186
C			BEARING WITH CAGE = 1	RDREB187
C			CAGELESS BEARING = -1	RDREB188
C	JNT	14-16	SWITCH FOR TRACTION INTEGRAL --	RDREB189
C			SINGLE INTEGRAL FOR EHD	RDREB190
C			CONDITIONS = 0	RDREB191
C			DOUBLE INTEGRAL FOR SOLID	RDREB192
C			LUB CONDITIONS = 1	RDREB193
C	MRR	17-19	SWITCH FOR RE AND RACE MATERIALS --	RDREB194
C			STANDARD DATA = 0	RDREB195
C			DATA SUPPLIED ON CARDS	RDREB196
C			10.1 AND 10.2 = 1	RDREB197
C	MHS	20-22	SWITCH FOR HOUSING AND SHAFT MATERIALS --	RDREB198
C			STANDARD DATA = 0	RDREB199
C			DATA SUPPLIED ON CARDS	RDREB200
C			10.3 AND 10.4 = 1	RDREB201
C	ISPEC	23-70	BEARING SPECIFICATION CODE. ANY ALPHANUMERIC	RDREB202
C			STRING (A MAXIMUM OF 48 CHARACTERS) BY WHICH ALL	RDREB203
C			PRINT AND PLOT OUTPUTS WILL BE IDENTIFIED.	RDREB204
C				RDREB205
C	CARD 4			RDREB206
C	-----			RDREB207
C	ROR	11-22	ROTOR OR SHAFT OUTER DIA (L).	RDREB208
C	OD	23-34	OUTER RACE OUTER DIA (L).	RDREB209
C	SDA	35-46	SHAFT INNER DIA (L).	RDREB210
C	HDA	47-58	HOUSING OUTER DIA (L).	RDREB211
C				RDREB212
C	CARD 5			RDREB213
C	-----			RDREB214
C	SF	11-34	VECTOR OF LENGTH 2 CONTAINING THE DIAMETRAL	RDREB215
C			INTERFERENCE (L) AT THE OUTER RACE/HOUSING AND	RDREB216
C			SHAFT/INNER RACE FITS RESPLY.	RDREB217
C			EACH COMPONENT HAS A FIELD WIDTH OF 12.	RDREB218
C				RDREB219
C	CARD 6			RDREB220
C	-----			RDREB221
C	KTC	11-16	TRACTION CODE DEFINED AS FOLLOWS --	RDREB222
C			SIMULATED TRACTION CURVE = 0	RDREB223
C			SHELL TURBO-33 OIL = 1	RDREB224
C			SP4E POLYPHENOL ETHER = 2	RDREB225
C			MIL-L-7808 OIL = 3	RDREB226
C			ANY ARBITRARY MODEL = 4	RDREB227
C	NR	17-22	NUMBER OF ROLLING ELEMENTS.	RDREB228
C	LU	23-28	SWITCH FOR SELECTION OF UNITS --	RDREB229

C			IN-LB UNITS	= 1	RDREB230
C			SI UNITS	= 2	RDREB231
C	NRW	29-34	NUMBER OF ELEMENTS FOR WHICH OUTPUT WILL BE		RDREB232
C			MONITORED. UPPER LIMIT IS SIX (6).		RDREB233
C	IRW	35-70	VECTOR OF LENGTH NRW. THE COMPONENTS WILL DENOTE		RDREB234
C			THE INDICES OF THE BEARING ELEMENTS.		RDREB235
C			EACH COMPONENT HAS A FIELD WIDTH OF 6.		RDREB236
C	CARD 7				RDREB237
C	-----				RDREB238
C	DF	11-22	BALL DIAMETER (L).		RDREB239
C	DP	23-34	PITCH DIAMETER (L).		RDREB240
C	ALFA	35-46	CONTACT ANGLE (DEG) OR DIAMETRAL PLAY (L).		RDREB241
C			A POSITIVE VALUE DENOTES CONTACT ANGLE AND A		RDREB242
C			NEGATIVE VALUE DENOTES A DIAMETRAL PLAY EQUAL TO		RDREB243
C			THE ABSOLUTE VALUE OF ALFA.		RDREB244
C	RCUR(1)	47-58	OUTER RACE CUR FACTOR.		RDREB245
C	RCUR(2)	59-70	INNER RACE CUR FACTOR.		RDREB246
C	*****				RDREB247
C	* THE SERIES 8 CARDS ARE REQUIRED ONLY IN CASE OF DYNAMIC				RDREB248
C	* SOLUTIONS. MODE.GT.0 ON CARD 1.				RDREB249
C	*****				RDREB250
C	CARD 8.1				RDREB251
C	-----				RDREB252
C	THIS CARD CONTAINS ROLLING ELEMENT INERTIAL PARAMETERS. IF				RDREB253
C	STANDARD VALUES ARE DESIRED THEN SET ALL VALUES EQUAL TO ZERO.				RDREB254
C	XMB	11-22	RE MASS (MA).		RDREB255
C	XIX	23-34	RE POLAR MOMENT OF INERTIA (MA*L**3).		RDREB256
C	XIY	35-46	RE TRANSVERSE MOMENT OF INERTIA (MA*L**3).		RDREB257
C	CARD 8.2				RDREB258
C	-----				RDREB259
C	THIS CARD CONTAINS GAGE INERTIAL PARAMETERS. FOR STANDARD VALUES				RDREB260
C	OR FOR GAGELESS BEARING SET ALL VALUES EQUAL TO ZERO.				RDREB261
C	XMC	11-22	GAGE MASS (MA).		RDREB262
C	XXK	23-34	GAGE POLAR MOMENT OF INERTIA (MA*L**3).		RDREB263
C	XKY	35-46	GAGE TRANSVERSE MOMENT OF INERTIA (MA*L**3).		RDREB264
C	CARD 8.3 AND 8.4				RDREB265
C	-----				RDREB266
C	THE FOLLOWING TWO CARDS (I=1,2) WILL CONTAIN THE EFFECTIVE				RDREB267
C	INERTIAL PARAMETERS FOR THE OUTER (I=1) AND INNER (I=2) RACES				RDREB268
C	RESPLY. IF THE RACE IS CONSTRAINED IN ACCORDANCE WITH THE				RDREB269
C	SPECIFIED MOTION THEN THE RELEVANT PARAMETERS MAY BE SET TO ZERO.				RDREB270
C	ALSO, FOR STANDARD VALUES, SET ALL PARAMETERS EQUAL TO ZERO.				RDREB271
C	XMR(I)	11-22	RACE MASS (MA).		RDREB272
C	XJX(I)	23-34	RACE POLAR MOMENT OF INERTIA (MA*L**3).		RDREB273
C	XJY(I)	35-46	RACE TRANSVERSE MOMENT OF INERTIA (MA*L**3).		RDREB274
C					RDREB275
C					RDREB276
C					RDREB277
C					RDREB278
C					RDREB279
C					RDREB280
C					RDREB281
C					RDREB282
C					RDREB283
C					RDREB284
C					RDREB285
C					RDREB286

C				RDRB287
C	CARD 8.5			RDRB288
C	-----			RDRB289
C	BRDP 11-22	RALL/RACE DAMPING RATIO		RDRB290
C	BCDP 23-34	RALL/CAGE DAMPING RATIO		RDRB291
C	RCDP 35-46	CAGE/RACE DAMPING RATIO		RDRB292
C				RDRB293
C				RDRB294
C	*****			RDRB295
C	* THE SERIES 9 CARDS ARE REQUIRED ONLY WHEN A CAGE IS PRESENT,			* RDRB296
C	* (KBT.GT.0). IF NO CAGE EXISTS GO TO CARD 10.1			* RDRB297
C	*****			RDRB298
C	CARD 9.1			RDRB299
C	-----			RDRB300
C	MCR 11-16	SWITCH FOR CAGE MATERIALS --		RDRB301
C		STANDARD DATA	= 0	RDRB302
C		DATA SUPPLIED ON CARD 10.5	= 1	RDRB303
C	IHRC 17-22	SWITCH FOR RE/CAGE CONTACT --		RDRB304
C		HYDRODYNAMICS NEGLECTED	= 0	RDRB305
C		HYDRODYNAMICS INCLUDED	= 1	RDRB306
C	IHRC 23-28	SWITCH FOR CAGE/RACE CONTACT --		RDRB307
C		HYDRODYNAMICS NEGLECTED	= 0	RDRB308
C		HYDRODYNAMICS INCLUDED BUT		RDRB309
C		NO SQUEEZE FILM DAMPING	= 1	RDRB310
C		HYDRODYNAMICS INCLUDED		RDRB311
C		WITH SQUEEZE FILM DAMPING	= 2	RDRB312
C	IRC 29-34	SWITCH FOR RE/CAGE CONTACT --		RDRB313
C		USE HERTZIAN SPRING	= 0	RDRB314
C		SPRING SUPPLIED IN -PSPRG-	= 1	RDRB315
C	IRC 35-40	SWITCH FOR CAGE/RACE CONTACT --		RDRB316
C		USE HERTZIAN SPRING	= 0	RDRB317
C		SPRING SUPPLIED IN -RSPRG-	= 1	RDRB318
C	IRGS 41-52	VECTOR OF LENGTH 2. COMPONENTS INDICATE TYPE OF		RDRB319
C		GUIDANCE FOR THE TWO LANDS ALONG THE POSITIVE		RDRB320
C		AND NEGATIVE X-AXIS RESPLY --		RDRB321
C		OUTER RACE GUIDANCE	= 1	RDRB322
C		INNER RACE GUIDANCE	= 2	RDRB323
C		EACH COMPONENT HAS A FIELD WIDTH OF 6.		RDRB324
C				RDRB325
C	CARD 9.2			RDRB326
C	-----			RDRB327
C	CDIA 11-34	VECTOR OF LENGTH 2 CONTAINING THE EFFECTIVE		RDRB328
C		OUTER AND INNER DIAMETERS (L) OF CAGE.		RDRB329
C		EACH COMPONENT HAS A FIELD WIDTH OF 12.		RDRB330
C	CWC 35-46	EFFECTIVE CAGE WIDTH (L) FOR MASS COMPUTATION.		RDRB331
C	CCL 47-70	VECTOR OF LENGTH 2 CONTAINING THE EFFECTIVE		RDRB332
C		DIAMETRAL CLEARANCES (L) AT THE CAGE/OUTER RACE		RDRB333
C		AND CAGE/INNER RACE INTERACTIONS RESPLY FOR THE		RDRB334
C		COMPUTATION OF CHURNING EFFECTS.		RDRB335
C		EACH COMPONENT HAS A FIELD WIDTH OF 12.		RDRB336
C				RDRB337
C	CARDS 9.3.1 AND 9.3.2			RDRB338
C	-----			RDRB339
C	*****			RDRB340
C	* CARD 9.3.1 IS ONLY REQUIRED IF IRGS(1).NE.0			* RDRB341
C	*****			RDRB342
C				RDRB343

C				RDRER344
C				RDRER345
C		THESE TWO CARDS (I=1,2) CONTAIN DATA FOR THE TWO GUIDING LANDS		RDRER346
C		ALONG THE POSITIVE (I=1) AND NEGATIVE (I=2) X-AXIS RESPLY.		RDRER347
C	RGL(I)	11-22 GUIDING RACE RADIUS (L).		RDRER348
C	CRL(I)	23-34 GUIDING CAGE RADIUS (L).		RDRER349
C	CWS(I)	35-46 LAND WIDTH (L)		RDRER350
C	CLS(I)	47-58 DIS OF LAND OUTER EDGE FROM CAGE CENTER (L).		RDRER351
C				RDRER352
C	CARD 9.4			RDRER353
C	-----			RDRER354
C	RCL	11-22 RE/CAGE DIAMETRAL CLEARANCE (L).		RDRER355
C	RCLH	23-34 RE/CAGE MAX LUB FILM (L) .LT. RCL FOR STARVED		RDRER356
C		CONTACT. RCLH=RCL FOR FULLY FLOODED CONDITIONS.		RDRER357
C		THIS INPUT IS RELEVANT ONLY FOR BALL BEARINGS.		RDRER358
C	PAN1	35-46 CONE ANGLE (DEG) FOR RE/CAGE GUIDE LAND.		RDRER359
C		= 0. FOR NO RE/CAGE GUIDANCE.		RDRER360
C	PAN2	47-58 CONE HEIGHT (L).		RDRER361
C		.GT. 0. FOR GUIDANCE CONE ON OUTER DIAMETER.		RDRER362
C		.LT. 0. FOR GUIDANCE CONE ON INNER DIAMETER.		RDRER363
C				RDRER364
C	CARD 9.5			RDRER365
C	-----			RDRER366
C	XPOS	11-22 INITIAL AXIAL POSITION (L) OF CAGE MASS CENTER		RDRER367
C		RELATIVE TO THE MEAN AXIAL POSITION OF ROLLING		RDRER368
C		ELEMENTS.		RDRER369
C	RPOS	23-34 INITIAL RADIAL POSITION (L) OF CAGE MASS CENTER		RDRER370
C		RELATIVE TO THE CENTER OF THE GUIDING RACEWAY		RDRER371
C		(BEARING CENTER IN CASE OF RE GUIDANCE)		RDRER372
C	APOS	35-46 INITIAL ROTATION (DEG) OF CAGE ABOUT THE X-AXIS.		RDRER373
C				RDRER374
C	CARD 10.1			RDRER375
C	-----			RDRER376
C	*****			RDRER377
C	* THIS CARD IS REQUIRED ONLY IF MRP=1 ON CARD 3.			RDRER378
C	*****			RDRER379
C				RDRER380
C	ER	11-22 RE ELASTIC MODULUS (F/L**2).		RDRER381
C	POB	23-34 RE POISSON-S RATIO.		RDRER382
C	DEN	35-46 RE MATERIAL DENSITY (MA/L**3).		RDRER383
C				RDRER384
C				RDRER385
C	CARD 10.2			RDRER386
C	-----			RDRER387
C	*****			RDRER388
C	* THIS CARD IS REQUIRED ONLY IF MBP=1 ON CARD 3.			RDRER389
C	*****			RDRER390
C				RDRER391
C	ER	11-22 RACE ELASTIC MODULUS (F/L**2).		RDRER392
C	POR	23-34 RACE POISSON-S RATIO.		RDRER393
C	DENR	35-46 RACE MATERIAL DENSITY (MA/L**3).		RDRER394
C				RDRER395
C				RDRER396
C	CARD 10.3			RDRER397
C	-----			RDRER398
C	*****			RDRER399
C				RDRER400

C	* THIS CARD IS REQUIRED ONLY IF MHS=1 ON CARD 3.			* RDREB401
C	*****			RDREB402
C				RDREB403
C	ES	11-22	SHAFT ELASTIC MODULUS (F/L**2).	RDREB404
C	POS	23-34	SHAFT POISSON-S RATIO.	RDREB405
C	DENS	35-46	SHAFT MATERIAL DENSITY (MA/L**3).	RDREB406
C				RDREB407
C	CARD 10.4			RDREB408
C	-----			RDREB409
C				RDREB410
C	*****			RDREB411
C	* THIS CARD IS REQUIRED ONLY IF MHS=1 ON CARD 3.			* RDREB412
C	*****			RDREB413
C				RDREB414
C	EH	11-22	HOUSING ELASTIC MODULUS (F/L**2).	RDREB415
C	POH	23-34	HOUSING POISSON-S RATIO.	RDREB416
C	DENH	35-46	HOUSING MATERIAL DENSITY (MA/L**3).	RDREB417
C				RDREB418
C	CARD 10.5			RDREB419
C	-----			RDREB420
C				RDREB421
C	*****			RDREB422
C	* THIS CARD IS REQUIRED ONLY IF MCP=1 ON CARD 9.1.			* RDREB423
C	*****			RDREB424
C				RDREB425
C	EC	11-22	CAGE ELASTIC MODULUS (F/L**2).	RDREB426
C	POC	23-34	CAGE POISSON-S RATIO.	RDREB427
C	DENC	35-46	CAGE MATERIAL DENSITY (MA/L**3).	RDREB428
C				RDREB429
C	CARD 11			RDREB430
C	-----			RDREB431
C	JF	11-16	VECTOR OF LENGTH 2. COMPONENTS DENOTE INITIAL PACE CONSTRAINTS ALONG AXIAL AND RADIAL DIRECTIONS (FOR QUASI-STATIC COMPUTATIONS) -- SPECIFIED FORCE = 0 SPECIFIED DISPLACEMENT = 1 EACH COMPONENT HAS A FIELD WIDTH OF 3.	RDREB432
C				RDREB433
C	JN	17-19	NUMBER OF ROLLING ELEMENTS LAGGING THE ZERO DEG POSITION IN THE CASE OF A PARTIAL BEARING.	RDREB434
C	IROT	20-22	SWITCH FOR ROTATING LOAD -- STATIONARY RADIAL LOAD = 0 ROTATING RADIAL LOAD WITH INNER RACE ROTATION = 1	RDREB435
C				RDREB436
C	OF	23-46	VECTOR OF LENGTH 2. COMPONENTS DENOTE EITHER FORCE (F) OR DISPLACEMENT (L) ALONG THE AXIAL AND RADIAL DIRECTIONS, AS PER CONSTRAINTS SPECIFIED BY VECTOR JF. EACH COMPONENT HAS A FIELD WIDTH OF 12.	RDREB437
C				RDREB438
C	GAMA	47-58	INITIAL MISALIGNMENT (DEG)	RDREB439
C	ARC	59-70	ANGLE (DEG) OVER WHICH NO RE EXISTS IN THE CASE OF PARTIAL BEARING. ARC=0. FOR FULL BEARING.	RDREB440
C				RDREB441
C	CARD 12			RDREB442
C	-----			RDREB443
C	RPM	11-34	VECTOR OF LENGTH 2. THE COMPONENTS CONTAIN THE INITIAL ANGULAR VELOCITIES (RPM) OF THE OUTER AND INNER RACES RESPLY.	RDREB444
C				RDREB445
C				RDREB446
C				RDREB447
C				RDREB448
C				RDREB449
C				RDREB450
C				RDREB451
C				RDREB452
C				RDREB453
C				RDREB454
C				RDREB455
C				RDREB456
C				RDREB457



C		EACH COMPONENT HAS A FIELD WIDTH OF 12.	RDRER458
C			RDRER459
C	CARD 13.1		RDRER460
C	-----		RDRER461
C	FCF1 11-58	VECTOR OF LENGTH 4. THE COMPONENTS DENOTE	RDRER462
C		TRACTION PARAMETERS WHEN KTC=0, ON CARD 6, OR	RDRER463
C		WHEN THE ACTUAL CONDITIONS ARE OUT OF LUB MODEL	RDRER464
C		ROUNDS. THESE PARAMETERS ARE ALSO USED FOR THE	RDRER465
C		ROLLER/FLANGE INTERACTIONS IN CASE OF A ROLLER	RDRER466
C		BEARING. THE FOUR COMPONENTS ARE DEFINED AS --	RDRER467
C		(1) TRACTION COEFF AT ZERO SLIP.	RDRER468
C		(2) MAX TRACTION COEFF.	RDRER469
C		(3) TRACTION COEFF AT INFINITE SLIP.	RDRER470
C		(4) SLIP (L/T) AT MAX TRACTION COEFF.	RDRER471
C		THE TRACTION COEFF, MU, IS RELATED TO THE SLIP	RDRER472
C		VELOCITY, V, BY THE RELATION OF THE FORM --	RDRER473
C		$MU = (A+B*V)*EXP(C*V)+D$	RDRER474
C		WHERE THE COEFFICIENTS A, B, C AND D ARE DETER-	RDRER475
C		MINED BY THE ABOVE FOUR CONDITIONS. WHEN THE	RDRER476
C		FOURTH COMPONENT OF FCF1 IS SET EQUAL TO ZERO,	RDRER477
C		IT IS USED AS A SWITCH AND THE FIRST THREE	RDRER478
C		COMPONENTS MUST THEN CONTAIN THE VALUES OF A, B	RDRER479
C		AND C DIRECTLY. IT SHOULD BE NOTED THAT B AND C	RDRER480
C		HAVE DIMENSIONS (T/L). IF THE FOURTH COMPONENT	RDRER481
C		IS NEGATIVE THEN THE VALUES FOR A, B AND C ARE	RDRER482
C		STILL CONTAINED IN THE FIRST THREE COMPONENTS.	RDRER483
C		HOWEVER, THE MAXIMUM VALUE OF THE TRACTION	RDRER484
C		COEFFICIENT IS NOT LIMITED TO ABS(FCF1(4)).	RDRER485
C		EACH COMPONENT HAS A FIELD WIDTH OF 12.	RDRER486
C			RDRER487
C	CARD 13.2		RDRER488
C	-----		RDRER489
C		*****	RDRER490
C		THIS CARD IS REQUIRED ONLY IF KTC.NE.0 ON CARD 6.	RDRER491
C		*****	RDRER492
C			RDRER493
C			RDRER494
C	IMOD 11-16	FILM THICKNESS COMPUTATION CODE --	RDRER495
C		GRUBIN-S FORMULA = 0	RDRER496
C		DOWSON-HIGGINSON FORMULA = 1	RDRER497
C		HAMROCK-DOWSON FORMULA = 2	RDRER498
C	HC 17-28	MINIMUM FILM FOR TRACTION MODEL BREAKDOWN (L).	RDRER499
C	STR 29-40	STARVATION PARAMETER - DISTANCE OF THE FILM	RDRER500
C		BOUNDARY FROM THE EDGE OF THE CONTACT ZONE	RDRER501
C		DIVIDED BY THE CONTACT HALF WIDTH (SEMI-MINOR	RDRER502
C		AXIS IN CASE OF ELLIPTIC CONTACT).	RDRER503
C	TEM 41-64	VECTOR OF LENGTH 2 CONTAINING OUTER AND INNER	RDRER504
C		RACE TEMPERATURES (TM).	RDRER505
C		EACH COMPONENT HAS A FIELD WIDTH OF 12.	RDRER506
C			RDRER507
C	CARD 13.3		RDRER508
C	-----		RDRER509
C		*****	RDRER510
C		THIS CARD IS REQUIRED ONLY IF KTC=4 ON CARD 6.	RDRER511
C		*****	RDRER512
C			RDRER513
C			RDRER514

C	XMU	11-22	VISCOCITY PARAMETER (F*T/L**2).	RDRER515
C	GAMMA	23-34	PR-VIS PARAMETER (L**2/F).	RDRER516
C	BETA	35-46	TEMP-VIS PARAMETER (1/TM).	RDRER517
C	VR	47-58	CHARACTERISTIC VELOCITY (L/T) IN THE ROLLING	RDRER518
C			SPEED EFFECT EXPRESSION.	RDRER519
C	VN	59-70	EXPONENT IN THE ROLLING SPEED EFFECT EXPRESSION.	RDRER520
C				RDRER521
C	CARD 13.4			RDRER522
C	-----			RDRER523
C				RDRER524
C	*****			RDRER525
C	* THIS CARD IS REQUIRED ONLY IF KTC=1 OR 4 ON CARD 6.			RDRER526
C	*****			RDRER527
C				RDRER528
C	T0	11-22	INLET TEMPERATURE (TM).	RDRER529
C	XMU0	23-34	INLET VISCOCITY (F*T/L**2).	RDRER530
C	GAM	35-46	PR-VIS COEFFICIENT (L**2/F).	RDRER531
C	RET	47-58	TEMP-VIS COEFFICIENT (TM).	RDRER532
C	FK	59-70	THERMAL CONDUCTIVITY (F/T/TM).	RDRER533
C				RDRER534
C	CARD 14			RDRER535
C	-----			RDRER536
C	ICHR	11-16	SWITCH FOR CHURNING EFFECTS --	RDRER537
C			CHURNING NEGLECTED = 0	RDRER538
C			CHURNING CONSIDERED = 1	RDRER539
C			EFFECTIVE VISCOCITY IS	RDRER540
C			DERIVED FROM LUB MODEL	RDRER541
C			(KTC.GT.0 ON CARD 6) = 2	RDRER542
C	CRO	17-28	EFFECTIVE LUB DENSITY (MA/L**3).	RDRER543
C	VISC	29-40	EFFECTIVE VISCOCITY (F*T/L**2). IF ICHR=2 ON	RDRER544
C			THIS CARD THEN EFF VIS = VISC*(LUB MODEL VIS).	RDRER545
C	CARD 15.1			RDRER546
C	-----			RDRER547
C				RDRER548
C	*****			RDRER549
C	* THIS CARD IS REQUIRED ONLY IF A CAGE IS PRESENT.			RDRER550
C	* KRT.GT.0 ON CARD 3.			RDRER551
C	*****			RDRER552
C				RDRER553
C	FCF2	11-58	VECTOR OF LENGTH 4 CONTAINING THE TRACTION PARA-	RDRER554
C			METERS FOR RE/CAGE INTERACTION. THE PARAMETERS	RDRER555
C			HAVE SAME DEFINITIONS AS FOR FCF1 ON CARD 13.1.	RDRER556
C			EACH COMPONENT HAS A FIELD WIDTH OF 12.	RDRER557
C	HCBP	59-70	CRITICAL FILM (L) FOR RE/CAGE CONTACT.	RDRER558
C				RDRER559
C	CARD 15.2			RDRER560
C	-----			RDRER561
C				RDRER562
C	*****			RDRER563
C	* THIS CARD IS REQUIRED ONLY IF A CAGE IS GUIDED ON THE RACE.			RDRER564
C	* KRT.GT.0 ON CARD 3 AND IRGS(1)+IRGS(2).GT.0 ON CARD 9.1.			RDRER565
C	*****			RDRER566
C				RDRER567
C	FCF3	11-58	VECTOR OF LENGTH 4 CONTAINING THE TRACTION PARA-	RDRER568
C			METERS OF RACE/CAGE INTERACTION. THE PARAMETERS	RDRER569
C			HAVE SAME DEFINITIONS AS FOR FCF1 ON CARD 13.1.	RDRER570
C			EACH COMPONENT HAS A FIELD WIDTH OF 12.	RDRER571

C	HCCR	59-70	CRITICAL FILM (L) FOR RACE/CAGE CONTACT.	RDRER572
C				RDRER573
C	CARD 16			RDRER574
C	-----			RDRER575
C				RDRER576
C	*****			RDRER577
C	*	THIS CARD IS REQUIRED ONLY IF A CAGE IS PRESENT.		* RDRER578
C	*	KBT.GT.0 ON CARD 3.		* RDRER579
C	*****			RDRER580
C	CFOR	11-46	VECTOR OF LENGTH 3 CONTAINING THE X, Y AND Z	RDRER581
C			COMPONENTS (INERTIAL FRAME) OF ANY EXTERNAL	RDRER582
C			FORCE (F) VECTOR ACTING ON THE CAGE, SUCH AS	RDRER583
C			LUBRICANT JET FORCE.	RDRER584
C			EACH COMPONENT HAS A FIELD WIDTH OF 12.	RDRER585
C	RTC	47-58	RADIAL COORDINATE (L) RELATIVE TO THE BEARING	RDRER586
C			CENTER AT WHICH THE ABOVE FORCE IS APPLIED.	RDRER587
C	THC	59-70	ORBITAL COORDINATE (OEG) DEFINING THE POSITION	RDRER588
C			VECTOR LOCATING THE POINT OF APPLICATION OF	RDRER589
C			CFOR IN THE INERTIAL FRAME.	RDRER590
C				RDRER591
C	CARD 17			RDRER592
C	-----			RDRER593
C				RDRER594
C				RDRER595
C	*****			RDRER596
C	*	THIS CARD IS REQUIRED ONLY IF KTC=0 ON CARD 6, KBT.GT.0 ON		* RDRER597
C	*	CARD 3 AND IHBC+IHRC.GT.0 ON CARD 9.1.		* RDRER598
C	*****			RDRER599
C	VISP	11-22	FFF LUB VIS (F*T/L**2) FOR RE/CAGE INTERACTION.	RDRER600
C			A ZERO MAY BE SPECIFIED IF IHBC=0 ON CARD 9.1.	RDRER601
C	VISR	23-34	FFF LUB VIS (F*T/L**2) FOR RACE/CAGE INTERACTION.	RDRER602
C			A ZERO MAY BE SPECIFIED IF IHRC=0 ON CARD 9.1.	RDRER603
C				RDRER604
C				RDRER605
C	CARD 18			RDRER606
C	-----			RDRER607
C				RDRER608
C	*****			RDRER609
C	*	THIS CARD IS REQUIRED ONLY IF MODE.GE.0 ON CARD 1.		* RDRER610
C	*****			RDRER611
C	THE FOLLOWING CARD SPECIFIES RACE CONSTRAINTS FOR DYNAMIC			RDRER612
C	SOLUTIONS. IRF AND IRM ARE TWO DIMENSIONAL ARRAYS (2,3). THE			RDRER613
C	FIRST INDEX DENOTES THE RACE (OUTER=1, INNER=2) AND THE SECOND			RDRER614
C	INDEX DENOTES THE THREE COMPONENTS OF THE INERTIAL TRIAD --			RDRER615
C				RDRER616
C	IRF	11-28	LINEAR CONSTRAINT VECTOR OF LENGTH 6. THE	RDRER617
C			COMPONENTS ARE DEFINED AS --	RDRER618
C			SPECIFIED FORCE = 0	RDRER619
C			SPECIFIED DISPLACEMENT = 1	RDRER620
C			EACH COMPONENT HAS A FIELD WIDTH OF 3.	RDRER621
C	IRM	29-46	ANGULAR CONSTRAINT VECTOR OF LENGTH 6. THE	RDRER622
C			COMPONENTS ARE DEFINED AS --	RDRER623
C			SPECIFIED MOMENT = 0	RDRER624
C			SPECIFIED ANG DISPLACEMENT = 1	RDRER625
C			EACH COMPONENT HAS A FIELD WIDTH OF 3.	RDRER626
C				RDRER627
C				RDRER628

C	CARD 19		RDRER629
C	-----		RDRER630
C			RDRER631
C	*****		RDRER632
C	* THIS CARD IS REQUIRED ONLY IF MODE=0 ON CARD 1.	*	RDRER633
C	*****		RDRER634
C			RDRER635
C	6 11-46 VECTOR OF LENGTH 3 CONTAINING THE COMPONENTS OF		RDRER636
C	THE ACCELERATION (L/T**2) DUE TO GRAVITY VECTOR		RDRER637
C	IN THE INERTIAL FRAME. EACH COMPONENT HAS A		RDRER638
C	FIELD WIDTH OF 12.		RDRER639
C			RDRER640
C	*****		RDRER641
C	* THE FOLLOWING SERIES 20 CARDS ARE REQUIRED ONLY IF MODE=2 ON	*	RDRER642
C	* CARD 1.	*	RDRER643
C	*****		RDRER644
C			RDRER645
C	CARD 20.1		RDRER646
C	-----		RDRER647
C	TI 11-25 INITIAL DIMENSIONLESS TIME.		RDRER648
C			RDRER649
C	CARDS 20.2 TO CARD 20.N		RDRER650
C	-----		RDRER651
C	X 11-70 THE DIMENSIONLESS SOLUTION VECTOR OF LENGTH		RDRER652
C	(3U+12*NB+6*KBT/ABS(KRT)) WHICH WILL BE USED AS		RDRER653
C	INITIAL CONDITIONS. EACH CARD WILL HAVE FOUR		RDRER654
C	COMPONENTS, EACH ONE HAVING A FIELD WIDTH OF 15.		RDRER655
C			RDRER656
C	CARDS 21 TO .....		RDRER657
C	-----		RDRER658
C	ANY INPUT DATA REQUIRED BY THE USER ACCESSIBLE ROUTINES -ALOAD-,		RDRER659
C	-PSPRG- AND -RSPRG- SHOULD BE SUPPLIED IN ORDER. (SEE DISCUSSION		RDRER660
C	OF SPECIAL ROUTINES BELOW).		RDRER661
C			RDRER662
C	OUTPUT DATA		RDRER663
C	*****		RDRER664
C			RDRER665
C	OUTPUT SOLUTIONS MAY BE EITHER PRINTED, PLOTTED OR BOTH. AS DIS-		RDRER666
C	CUSSSED UNDER THE INPUT DESCRIPTIONS SEVERAL DIFFERENT OPTIONS FOR		RDRER667
C	MONITORING THE OUTPUT ARE AVAILABLE. ALL THE OUTPUT IS VERY WELL		RDRER668
C	DOCUMENTED IN ORDER TO MAKE IT SELF-EXPLANATORY. ALL DIMENSIONAL		RDRER669
C	VARIABLES ARE PRINTED WITH PROPER UNITS.		RDRER670
C			RDRER671
C			RDRER672
C			RDRER673
C			RDRER674
C	FILE SYSTEM		RDRER675
C	*****		RDRER676
C			RDRER677
C	THE PROGRAM HAS FULL RESTART CAPABILITIES AND IT CAN MONITOR THE		RDRER678
C	MOTION OF A TOTAL OF SIX REARING ELEMENTS INCLUDING THE CAGE AND		RDRER679
C	THE RACEWAYS. THE ELEMENT SELECTION IS DESCRIBED UNDER THE INPUT		RDRER680
C	DESCRIPTION AND SOME DETAILS OF THE FILING SYSTEM ARE DISCUSSED		RDRER681
C	BELOW.		RDRER682
C			RDRER683
C			RDRER684
C	FILE ESOL		RDRER685

C	-----	RDRB686
C	THIS IS THE MASTER DATA FILE WHICH CONTAINS ALL THE BEARING	RDRB687
C	INFORMATION AND SOLUTION VECTORS AT SELECTED TIME STEPS. THIS	RDRB688
C	FILE MUST BE SAVED IF THE EXECUTION HAS TO BE RESTARTED LATER.	RDRB689
C		RDRB690
C	FILE FSOL	RDRB691
C	-----	RDRB692
C	AT THE END OF A SUCCESSFUL RUN THE LAST SOLUTION VECTOR IS	RDRB693
C	WRITTEN IN THIS FILE IN A FORMAT SUCH THAT THE DATA COULD BE	RDRB694
C	PUNCHED ON CARDS AND DIRECTLY USED UNDER THE ARBITRARY INITIAL	RDRB695
C	CONDITIONS OPTION. THIS FILE IS COMPLETELY REWRITTEN AT THE	RDRB696
C	END OF EACH EXECUTION OF THE PROGRAM.	RDRB697
C		RDRB698
C	FILES GSOL1 TO GSOL6	RDRB699
C	-----	RDRB700
C	THESE SIX FILES STORE ALL SOLUTIONS FOR THE SIX PRESELECTED BEAR-	RDRB701
C	ING ELEMENTS. IF THE NUMBER OF ELEMENTS SELECTED IS LESS THAN SIX	RDRB702
C	THEN THE FIRST FILE NUMBERS ARE FILLED. IN OTHER WORDS IF THERE	RDRB703
C	ARE ONLY THREE ELEMENTS MONITORED THEN THE SOLUTIONS ARE CONTAIN-	RDRB704
C	ED IN FILES GSOL1 TO GSOL3 AND THE FILES GSOL4 TO GSOL6 REMAIN	RDRB705
C	EMPTY. WHEN A COMPLETE CASE CONSISTS OF SEVERAL EXECUTIONS OF	RDRB706
C	THE PROGRAM, THEN IT WILL BE NECESSARY TO ATTACH ALL THE FILES	RDRB707
C	USED WITH THE PROPER WRITE PERMISSION SO THAT SOLUTIONS FOR THE	RDRB708
C	ENTIRE TIME RANGE MAY BE STORED FOR PLOTTING PURPOSES.	RDRB709
C		RDRB710
C	FILE HSOL	RDRB711
C	-----	RDRB712
C	THE OVER ALL BEARING PARAMETERS, WHICH CONSISTS OF LOAD*SLIP,	RDRB713
C	TRACTION*SLIP, AND TORQUE VARIATIONS, ARE STORED IN THIS FILE AS	RDRB714
C	A FUNCTION OF TIME.	RDRB715
C		RDRB716
C	ALL DATA FILES CONTAIN APPROPRIATE IDENTIFICATION CODES, WHICH ARE	RDRB717
C	CHECKED WHENEVER THE FILES ARE ATTACHED. THE FILES PRODUCED WITH	RDRB718
C	TWO DIFFERENT RUNS, THEREFORE, MAY NOT BE INTERCHANGED.	RDRB719
C		RDRB720
C		RDRB721
C	SPECIAL ROUTINES	RDRB722
C	=====	RDRB723
C		RDRB724
C	THE FOLLOWING SPECIAL ROUTINES ARE AVAILABLE TO THE USER IN ORDER	RDRB725
C	TO CLOSELY SIMULATE THE APPLICATION UNDER QUESTION --	RDRB726
C		RDRB727
C	1. APLoad - APPLIED LOAD	RDRB728
C	2. PSPRG - ARBITRARY SPRING AT RALL/CAGE CONTACT	RDRB729
C	3. RSPRG - ARBITRARY SPRING AT RACE/CAGE CONTACT	RDRB730
C		RDRB731
C	SEE DOCUMENTATION SUPPLIED WITH THE ABOVE ROUTINES FOR NOTES ON	RDRB732
C	PROGRAMMING THE FEATURES OF A GIVEN APPLICATION IN THE ABOVE	RDRB733
C	SUBROUTINES.	RDRB734
C		RDRB735
C		RDRB736
C	EXTERNALS CALLED	RDRB737
C	=====	RDRB738
C		RDRB739
C	THE FOLLOWING LIST OF SUBROUTINES INCLUDES THE ROUTINES CALLED	RDRB740
C	DIRECTLY BY -RDRP- AND ALSO THOSE CALLED BY THE ROUTINES	RDRB741
C	INITIALLY CALLED BY -RDRP- ---	RDRB742

C				RDREB743
C	1.	ARM	- PREDICTOR-CORRECTOR ALGORITHM	RDREB744
C	2.	ACCN	- ANGULAR ACCELERATION TRANSFORMATION	RDREB745
C	3.	ARTAN	- MODIFIED ARCTAN	RDREB746
C	4.	ACCON	- RALL/CAGE INTERACTION	RDREB747
C	5.	BGEOM	- BEARING GEOMETRY	RDREB748
C	6.	BLOAD	- RALL/RACE LOAD	RDREB749
C	7.	BTRAC	- RALL/PACE TRACTION	RDREB750
C	8.	CELIL	- ELLIPTIC INTEGRALS	RDREB751
C	9.	CHURN	- CHURNING MOMENTS	RDREB752
C	10.	CRCON	- CAGE/RACE INTERACTION	RDREB753
C	11.	CURF	- CURVATURE FUNCTION FOR ELASTIC CONTACT	RDREB754
C	12.	DERIV	- COMPUTATION OF DERIVATIVES	RDREB755
C	13.	ELCON	- ELASTICITY SOLUTION	RDREB756
C	14.	FCEFF	- TRACTION COEFFICIENT	RDREB757
C	15.	FCT	- CURVATURE FUNCTION FOR ELASTIC CONTACT	RDREB758
C	16.	FCTT	- CAGE/RACE CONTACT COORDINATE FUNCTION	RDREB759
C	17.	FLB	- LONG BEARING FUNCTION	RDREB760
C	18.	FLIFE	- FATIGUE LIFE COMPUTATION	RDREB761
C	19.	FPHI	- RACE AXIMUTH	RDREB762
C	20.	FRIC	- FRICTION FORCE FUNCTION	RDREB763
C	21.	FSB	- SHORT BEARING FUNCTION	RDREB764
C	22.	FTRS	- TRACTION PARAMETER FUNCTION	RDREB765
C	23.	FUNC	- INTEGRAND FOR TRACTION INTEGRAL	RDREB766
C	25.	HYDRO	- HYDRODYNAMICS FOR SHORT AND LONG BEARING MODELS	RDREB767
C	26.	IANG	- INITIAL ANGULAR VELOCITIES	RDREB768
C	27.	PCOEFF	- POLYNOMIAL COEFFICIENTS FOR PREDICTOR-CORRECTOR	RDREB769
C	28.	PHITS	- THERMAL AND SIDE LEAKAGE FACTORS	RDREB770
C	29.	PLOAD	- PALMGREN FORMULA	RDREB771
C	30.	POUT	- PRINT OUTPUT	RDREB772
C	31.	PRVIT	- PRESSURE-VISCOCITY-TEMPERATURE RELATION	RDREB773
C	32.	QG10	- TENTH ORDER GAUSSIAN QUADRATURE INTEGRATION	RDREB774
C	33.	QSTAT	- QUASI-STATIC EQUILIBRIUM	RDREB775
C	34.	RKM4	- EXPLICIT INTEGRATING ALGORITHMS	RDREB776
C	35.	ROLLF	- ROLLING FUNCTION	RDREB777
C	36.	RTMI	- ROOT EVALUATION FOR A GIVEN FUNCTION	RDREB778
C	37.	SLIP	- SLIP VELOCITY BETWEEN TWO INTERACTING BODIES	RDREB779
C	38.	STEOM	- STATIC EQUILIBRIUM	RDREB780
C	39.	TRAC	- TRACTION ON INCREMENTAL AREA	RDREB781
C	40.	TRCF	- TRACTION DATA FOR MINERAL OILS	RDREB782
C	41.	TRFM	- TRANSFORMATION MATRIX	RDREB783
C	42.	TRMOD	- FHD TRACTION MODELS	RDREB784
C	43.	TPSLP	- COEFFICIENTS FOR SIMPLIFIED TRACTION RELATION	RDREB785
C	44.	VELC	- ANGULAR VELOCITY TRANSFORMATION	RDREB786
C	45.	VPDT	- VECTOR PRODUCT	RDREB787
C	46.	ZINT	- LINEAR INTERPOLATION	RDREB788
C	47.	ALOAD	- APPLIED LOAD	RDREB789
C	48.	PSPRG	- ARBITRARY SPRING AT RALL/CAGE CONTACT	RDREB790
C	49.	RSPRG	- ARBITRARY SPRING AT RACE/CAGE CONTACT	RDREB791
C				RDREB792
C				RDREB793
C				RDREB794
C				RDREB795
C				RDREB796
C				RDREB797
C				RDREB798
C				RDREB799
C				RDREB800
C				RDREB801
C				
C	NOTES			
C	*****			
C	(1)	A MAXIMUM OF 40 ROLLING ELEMENTS ARE ALLOWED. IF THE ACTUAL		
C		NUMBER EXCEEDS 40, THEN ALL DIMENSION DECLARATIONS, INCLUDING		
C		THOSE IN THE COMMON BLOCKS WILL HAVE TO BE CHANGED		
C		ACCORDINGLY.		

C	(2)	THE PROGRAM WITH ALL THE ROUTINES USES A CENTRAL MEMORY OF	RDREB802
C		ABOUT 158000B WORDS.	RDREB803
C			RDREB804
C	(3)	THIS PROGRAM HAS BEEN DEVELOPED ON THE CDC SYSTEM WHICH	RDREB805
C		EMPLOYS 60 BIT WORDS. ON OTHER SYSTEMS WHERE SHORTER WORDS	RDREB806
C		ARE USED IT MAY BE NECESSARY TO USE DOUBLE PRECISION.	RDREB807
C			RDREB808
C	(4)	FOR THE PURPOSE OF ROOT FINDING AND TEST AGAINST ZEROS THE	RDREB809
C		PROGRAM USES TOLERANCES WHICH RESIDE IN THE ARRAY TOLR IN	RDREB810
C		THE COMMON BLUCK TCOMA. THE ARRAY HAS THREE COMPONENTS.	RDREB811
C		THE FIRST AND SECOND COMPONENTS ARE TOLERANCES FOR ABSOLUTE	RDREB812
C		AND RELATIVE ZEROS RESPLY. THE THIRD COMPONENT IS A	RDREB813
C		TOLERANCE ON ACCELERATION COMPONENTS. IF ANY EXT FORCE	RDREB814
C		HAS AN ABSOLUTE VALUE LESS THAN THIS TOLERANCE THEN IT IS	RDREB815
C		SET EQUAL TO ZERO. PROPER VALUES TO THE ARRAY TOLR ARE	RDREB816
C		ASSIGNED IN THE BEGINNING OF THE MAIN PROGRAM -DREB-.	RDREB817
C			RDREB818
C	(5)	TIME STEP SIZE OPTIMIZATION IS PROVIDED BY NOPT VECTOR AND	RDREB819
C		THE VALUE OF TOL IN -RDREB-. TOL SHOULD BE 1 TO 2 ORDEKS	RDREB820
C		OF MAGNITUDE GREATER THAN THE TOLERANCE ON RELATIVE ZEROS	RDREB821
C		DISCUSSED ABOVE. IF THE TRUNCATION AT ANY STEP EXCEEDS TOL	RDREB822
C		THEN THE STEP SIZE IS SUCCESSIVELY HALVED UNTIL EITHER THE	RDREB823
C		TOLERANCE CRITERION IS MET OR THE MIN STEP SIZE, SPECIFIED	RDREB824
C		ON CARD 2, IS REACHED. IF THE TOLERANCE CRITERION IS NOT	RDREB825
C		MET FOR NOPT(1) CONSECUTIVE STEPS THEN THE EXECUTION IS TER-	RDREB826
C		MINATED. A TYPICAL VALUE FOR NOPT(1) MAY BE ABOUT 3 TO 6.	RDREB827
C		IF THE TOLERANCE CRITERION IS MET FOR NOPT(2) SUCCESSIVE	RDREB828
C		STEPS THEN AN ATTEMPT IS MADE TO SUCCESSIVELY DOUBLE THE	RDREB829
C		STEP SIZE UNTIL EITHER THE MAX STEP SIZE OR AN UNACCEPTABLE	RDREB830
C		TRUNCATION ERROR IS REACHED. THE OPTIMUM STEP IS THEN	RDREB831
C		SELECTED FOR THE NEXT NOPT(2) STEPS. A TYPICAL VALUE FOR	RDREB832
C		NOPT(2) MAY BE 10. IF NO OPTIMIZATION IS REQUIRED THEN	RDREB833
C		NOPT(2) MAY BE SET TO A VALUE GREATER THAN THE MAX NUMBER	RDREB834
C		OF STEPS IN THE RUN, WHICH IS SPECIFIED AS NOPT(3). THE	RDREB835
C		MAXIMUM NUMBER OF STEPS SHOULD BE SELECTED ON THE BASIS OF	RDREB836
C		THE EXPECTED COMPUTING TIME PER STEP AND THE PERMISSIBLE	RDREB837
C		TIME LIMIT ON THE JOB. ADEQUATE ALLOWANCE MUST BE MADE IN	RDREB838
C		ORDER TO PREVENT -TIME LIMIT- ERROR, WHICH ON SOME SYSTEMS	RDREB839
C		MAY RESULT IN IMPROPER CLOSURE OF DATA FILES AND HENCE A	RDREB840
C		SUBSTANTIAL PORTION OF THE OUTPUT MAY BE LOST.	RDREB841
C			RDREB842
C	(6)	FOR MOST BEARINGS A TIME STEP SIZE OF ABOUT 10 MICROSECS	RDREB843
C		WILL BE ADEQUATE FOR CONVERGENCE TO WITHIN REASONABLE	RDREB844
C		TOLERANCE LIMITS. A TRIAL RUN WILL PRINT THE RELEVANT TIME	RDREB845
C		SCALE WHICH CAN BE USED TO ESTIMATE THE DIMENSIONLESS STEP	RDREB846
C		SIZE. THE MIN AND MAX STEP SIZES, SPECIFIED AS DMIN AND	RDREB847
C		DMAX RESPLY ON CARD 2, MAY BE ESTIMATED BY THE TRANSIENT	RDREB848
C		DETAILS REQUIRED IN THE SIMULATIONS. THE INITIAL STEP	RDREB849
C		SIZE, DINT, MUST BE BETWEEN DMIN AND DMAX. IF DINT=DMIN=	RDREB850
C		DMAX THEN NO STEP OPTIMIZATION WILL BE PERFORMED AND UNDER	RDREB851
C		SUCH A CONDITION NOPT(2) ON CARD 1 SHOULD BE SET EQUAL TO	RDREB852
C		A VALUE GREATER THAN THE MAX NUMBER OF STEPS IN THE RUN.	RDREB853
C			RDREB854
C			RDREB855
C			RDREB856
C			RDREB857
C			RDREB858
C			RDREB859
C			RDREB860

PRANFED K. GUPTA  
VERSION RAPIDRER.0

JULY 1981





C	-----			RDRBP59
C	ITP	11-12	SWITCH FOR PLOTTING TITLE PAGE --	RDRBP60
C			ITP = 0 PLOT TITLE PAGE.	RDRBP61
C			= 1 SUPPRESS TITLE PAGE PLOTTING.	RDRBP62
C	JTP	13-16	NUMBER OF POINTS TO BE SKIPPED IN THE PLOT	RDRBP63
C			JTP=0 WILL PLOT ALL POINTS. THE TOTAL NUMBER OF	RDRBP64
C			POINTS TO BE PLOTTED MUST BE .LE. 3000	RDRBP65
C	JRI	17-23	RECORD NUMBER FROM WHICH PLOT SHOULD START.	RDRBP66
C	JRF	24-30	RECORD NUMBER AT WHICH PLOT SHOULD END.	RDRBP67
C	IPLT	31-70	A VECTOR WHOSE LENGTH IS EQUAL TO THE NUMBER OF	RDRBP68
C			PLOTS FOR THE BEARING ELEMENT UNDER CONSIDERAT-	RDRBP69
C			ION. THERE COULD BE A MAXIMUM OF TEN PLOTS.	RDRBP70
C			THE VALUE ASSIGNED TO EACH COMPONENT HAS THE FOL-	RDRBP71
C			LOWING SIGNIFICANCE --	RDRBP72
C			IPLT(I) = 0 ITH PLOT IS SUPPRESSED.	RDRBP73
C			= 1 AUTOMATIC SCALING IS USED ON THE ITH	RDRBP74
C			PLOT.	RDRBP75
C			= 2 SCALE INFORMATION IS SUPPLIED IN THE	RDRBP76
C			FOLLOWING CARDS.	RDRBP77
C			EACH COMPONENT HAS A FIELD WIDTH OF 4.	RDRBP78
C				RDRBP79
C			IF NONE OF THE COMPONENTS OF IPLT ARE SET EQUAL TO 2 THEN NO AD-	RDRBP80
C			DITIONAL DATA CARDS ARE NECESSARY. IF THE VALUE 2 IS ASSIGNED TO	RDRBP81
C			ANY COMPONENT THEN CARDS 2 TO 5 MUST BE SUPPLIED FOR EACH COMPON-	RDRBP82
C			ENT OF IPLT (=2) IN ORDER.	RDRBP83
C				RDRBP84
C	CARD 2			RDRBP85
C	-----			RDRBP86
C	ISCX(I)	11-15	TIME AXIS SCALE CODE WITH FOLLOWING SIGNIFI-	RDRBP87
C			CANCE --	RDRBP88
C			ISCX(I) = 0 AUTOMATIC SCALE FOR TIME AXIS.	RDRBP89
C			= 1 SCALE TIME AXIS ACCORDING TO SPEC-	RDRBP90
C			IFIED PARAMETERS.	RDRBP91
C	XIX(I)	16-25	MINIMUM VALUE OF TIME.	RDRBP92
C	XFX(I)	26-35	MAXIMUM VALUE OF TIME.	RDRBP93
C	NXX(I)	36-40	SCALE FACTOR (IN TERMS OF 10*NXX) TO BE USED FOR	RDRBP94
C			THE TIME AXIS.	RDRBP95
C				RDRBP96
C	CARD 3		(SEE NOTE (5) FOR CAGE MOTION PLOTS)	RDRBP97
C	-----			RDRBP98
C	ISCY(1,I)	11-15	SCALE CODE FOR THE Y AXIS NO. 1 WITH THE FOLLOW-	RDRBP99
C			ING SIGNIFICANCE --	RDRBP100
C			ISCY(1,I)=0 AUTOMATIC SCALE FOR Y AXIS NO. 1.	RDRBP101
C			= 1 SCALE Y-AXIS NO.1 AS SPECIFIED AND	RDRBP102
C			SKIP AXIS IF DATA OUT OF SCALE.	RDRBP103
C			= 2 SCALE Y-AXIS NO.1 AS SPECIFIED AND	RDRBP104
C			PLOT EVEN IF DATA OUT OF SCALE.	RDRBP105
C			= 3 SCALE Y-AXIS NO.1 AS SPECIFIED AND	RDRBP106
C			TRUNCATE DATA IF OUT OF SCALE.	RDRBP107
C	YIY(1,I)	16-25	MINIMUM VALUE OF THE VARIABLE TO BE PLOTTED ON Y	RDRBP108
C			AXIS NO. 1.	RDRBP109
C	YFY(1,I)	26-35	MAXIMUM VALUE OF THE VARIABLE TO BE PLOTTED ON Y	RDRBP110
C			AXIS NO. 1.	RDRBP111
C	NYI(1,I)	36-40	SCALE FACTOR (IN TERMS OF 10*NXX) TO BE USED FOR	RDRBP112
C			THE X AXIS.	RDRBP113
C				RDRBP114
C				RDRBP115
C	CARDS 4 AND 5			



C	1. AXC	- COMPUTE SCALE FACTORS FOR GIVEN AXIS.	RDRER173
C	2. FNUMBR	- PLOT REAL NUMBER IN CONVENTIONAL E FORMAT.	RDRER174
C	3. MINMAX	- FIND MINIMUM AND MAXIMUM VALUES FOR A GIVEN AXIS.	RDRER175
C	4. MTI	- PLOT MTI INSIGNIA.	RDRER176
C	5. SFAC	- PLOT SCALE FACTOR ON A GIVEN AXIS.	RDRER177
C	6. SIGF	- EXTRACT SIGNIFICANT FIGURES OF A REAL NUMBER.	RDRER178
C	7. TITLE	- SET-UP ALL PLOT TITLES.	RDRER179
C			RDRER180
C	NOTES		RDRER181
C	=====		RDRER182
C			RDRER183
C	(1)	A MAXIMUM OF 3000 POINTS MAY BE PLOTTED IN A GIVEN CURVE. IF THE NUMBER OF POINTS .GT. 3000 THEN EITHER THE DIMENSION STATEMENTS IN THE UNLABELLED COMMON (APPEARING IN THE MAIN PROGRAM AND THE SUBROUTINE -MINMAX-) MUST BE CHANGED OR THE START, FINISH AND NUMBER OF POINTS TO BE SKIPPED SHOULD BE ADJUSTED (SEE CARD 1) SO THAT NO MORE THAN 3000 POINTS ARE PLOTTED.	RDRER184
C			RDRER185
C			RDRER186
C			RDRER187
C			RDRER188
C			RDRER189
C			RDRER190
C			RDRER191
C	(2)	APPROPRIATE VALUES FOR -MACH-, -TAB- AND -SMAR- MUST BE SET IN THE DATA STATEMENT FOR PROPER PROGRAM OPERATION --	RDRER192
C		MACH = 1, TEN CHARACTERS PER WORD FOR THE CDC SYSTEM.	RDRER193
C		MACH = 2, FOUR CHARACTERS PER WORD FOR THE IBM SYSTEM.	RDRER195
C		TAB = *WIDTH (INCH) OF PAPER BETWEEN TEAR LINES IF ANY. TAB MUST BE .GE.8.5. ALL PLOTS ARE DESIGNED TO FIT ON A 8.5 INCH WIDE PAPER.	RDRER196
C		SMAR = *WIDTH OF MARGIN USED BY THE SYSTEM FOR USER IDENTIFICATION. FOR NO SYSTEM MARGIN, SMAR=0.	RDRER197
C			RDRER198
C			RDRER199
C			RDRER200
C			RDRER201
C	(3)	THE FIRST FOUR COMPONENTS OF ARRAY -IFOR-, DEFINED IN A DATA STATEMENT, ARE USED ONLY WITH MACH=1 FOR THE CDC SYSTEM. IF THE 10H FIELD IN THE DATA STATEMENT IS UNACCEPTABLE ON THE IBM SYSTEM WITH MACH=2 THEN THE VALUES FOR THE FIRST FOUR COMPONENTS MAY BE TRUNCATED BUT UNDER NO CIRCUMSTANCE THE DIMENSIONS OF -IFOR- MAY BE ALTERED.	RDRER202
C			RDRER203
C			RDRER204
C			RDRER205
C			RDRER206
C			RDRER207
C			RDRER208
C	(4)	THE FORM OF THE CALCOMP INITIALIZATION ROUTINE -PLOTS- MUST BE CHECKED FOR THE GIVEN INSTALLATION AND THE STATEMENT 72 IN -RDRERP- MUST BE ADJUSTED ACCORDINGLY.	RDRER209
C			RDRER210
C			RDRER211
C			RDRER212
C	(5)	PLOT NO. 9 FOR THE CAGE MOTION IS A CAGE MASS CENTER ORBIT PLOT AND IT CONTAINS ONLY TWO AXES CORRESPONDING TO THE Y AND Z POSITION OF THE CAGE MASS CENTER. IF ANY SCALING INFORMATION IS SUPPLIED FOR THIS PLOT THEN THE DATA FOR Y POSITION SHOULD BE SUPPLIED ON CARD 2 AND THE DATA FOR Z POSITION SHOULD BE SUPPLIED ON CARD 3, WHICH IS NORMALLY USED FOR Y AXIS NO. 1. ALSO IN THIS CASE ISCY(1,1) MAY BE EQUAL TO ONLY A 0 OR 1. THE OTHER TWO OPTIONS ARE NOT AVAILABLE FOR THIS PLOT.	RDRER213
C			RDRER214
C			RDRER215
C			RDRER216
C			RDRER217
C			RDRER218
C			RDRER219
C			RDRER220
C			RDRER221
C			RDRER222
C	(6)	-RDRERP- REQUIRES A CENTRAL MEMORY OF ABOUT 1640008 WORDS ON A CDC SYSTEM.	RDRER223
C			RDRER224
C			RDRER225
C			RDRER226
C	PRADDEEP K. GUPTA		RDRER227
C	VERSION RAPIDRERP1	SEPTEMBER 1981	RDRER228
C			RDRER229
C			RDRER230
C			RDRER231

APPENDIX B

TYPICAL COMPUTER OUTPUT FOR THE  
100 mm AND 150 mm DMA BEARINGS

# RAPID SIMULATION OF THE BEARINGS

-A REAL TIME PERFORMANCE SIMULATION-  
(VERSION RAPIDREB.0)

PRADIP K. GUPTA  
MECHANICAL TECHNOLOGY INCORPORATED  
968 ALRANY-SHAKER ROAD  
LATHAM, NEW YORK  
U. S. A.

BEARING TYPE	--	BALL	SPEC CODE	--	100MM-DMA-BRG	IRG-CAGE	60RPM	178N**
--------------	----	------	-----------	----	---------------	----------	-------	--------

BEARING GEOMETRY

	(M) =	OUTER RACE SHRINK FIT	(M) =
BORE	= 1.0000E-01	INNER RACE SHRINK FIT	= 1.0000E-05
OUTSIDE DIAMETER	= 1.5000E-01	HOUSING OUTER DIA	= 2.0000E-01
SHAFT INNER DIA	= 8.0000E-02	NUMBER OF BALLS	= 19
BALL DIAMETER	= 1.5875E-02	OUTER RACE CUR FACTOR	= 5.2000E-01
PITCH DIAMETER	= 1.2500E-01	INNER RACE CUR FACTOR	= 5.2000E-01
PITCH ANGLE	= 2.6000E+01	DIA METRAL PLAY	= 1.28532E-04
CONTACT ANGLE	= 5.5673E-04	CAGE OUTER DIA CLS	= 3.5000E-03
END PLAY		CAGE INNER DIA CLS	= 4.0000E-04
CAGE OUTER DIA	= 1.3500E-01	DIA WF/CAGE CLEARANCE	= 3.0000E-04
CAGE INNER DIA	= 1.1500E-01		
EFF CAGE WIDTH	= 2.6000E-02	GUIDING RADIUS	CAGE HALF WIDTH (M)
		GUIDING RADIUS (M)	
GUIDANCE TYPE	GUIDING RADIUS (M)		
I	2	5.7500E-02	5.0000E-03
II	2	5.7500E-02	5.0000E-03
GUIDING LAND I			1.3000E-02
GUIDING LAND II			1.3000E-02

# LUBRICATION DETAILS -----

## 1. ROLLING ELEMENT/CAGE AND RACE/CAGE PARAMETERS ---

	INTERACTION CODE	LUBRICATION (N*S/M**2)	MAX FILM (M)
ROLLING ELEMENT/CAGE INTERACTION	0	0.	1.00000E-04
RACE/CAGE INTERACTION	0	0.	

	CRIT FILM THICKNESS (M)	COEFFICIENT A	COEFFICIENT C	1/ (M/S)	COEFFICIENT B	COEFFICIENT D	1/ (M/S)
RE/CAGE DRY CONTACT TRACTION PARAMETERS --	2.50000E-07	1.00000E-02	0.	0.	0.	-1.00000E-02	0.

## CAGE/RACE DRY CONTACT TRACTION PARAMETERS --

	CRIT FILM THICKNESS (M)	COEFFICIENT A	COEFFICIENT C	1/ (M/S)	COEFFICIENT B	COEFFICIENT D	1/ (M/S)
	2.50000E-07	1.00000E-02	0.	0.	0.	-1.00000E-02	0.

## 2. ROLLING ELEMENT/RACE PARAMETERS (TRACTION CODE = 0) ---

	COEFFICIENT A	COEFFICIENT C	1/ (M/S)	COEFFICIENT B	COEFFICIENT D	1/ (M/S)
	0.	0.	0.	4.10000E-02	-1.00000E-02	0.

# APPLIED LOADS AND SPEEDS

## 1. QUASI-STATIC SIMULATION ---

AXIAL LOAD (N) = 1.78000E+02 OUTER RACE ANG VEL (RPM) = 0.  
 RADIAL DISPLACEMENT (M) = 0. INNER RACE ANG VEL (RPM) = 6.00000E+01  
 RELATIVE MISALIGNMENT (DEG) = 0.

## 2. DYNAMIC SIMULATION ---

\*\*\*\*\* LOADS (N) \*\*\*\*\*  
 I II III  
 \*\*\*\*\* MASS CEN ACC (M/S\*\*2) \*\*\*\*\*  
 I II III

OUTER RACE 0. 0. 0.  
 INNER RACE 0. 0. 0.

\*\*\*\*\* MOMENTS (N\*M) \*\*\*\*\*  
 I II III  
 \*\*\*\*\* ANG ACCELERATION (RPM/S) \*\*\*\*\*  
 I II III

OUTER RACE 0. 0. 0.  
 INNER RACE 0. 0. 0.

\*\*\*\*\* ANGULAR VELOCITIES (RPM) \*\*\*\*\*  
 I II III

OUTER RACE 0. 0.  
 INNER RACE 6.00000E+01 0. 0.

COMPONENTS OF ACCELERATION DUE TO GRAVITY VECTOR (M/S\*\*2) = 0. 0. 9.81000E+00  
 EXTERNALLY APPLIED FORCE VECTOR ACTING ON CAGE (N) = 0. 0.  
 CORRESPONDING POSITION VECTOR IN INERTIAL FRAME (M) = 1.30000E-02 0. 0.

# MATERIAL PROPERTIES AND INERTIAL PARAMETERS

	ROLLING ELEMENT	CAGE	RACEWAYS	SHAFT	HOUSING
ELASTIC MODULUS (N/M**2)	1.99948E+11	3.44738E+09	1.99948E+11	1.99948E+11	1.99948E+11
POISSON-S RATIO	2.50000E-01	4.50000E-01	2.50000E-01	2.50000E-01	2.50000E-01
MASS DENSITY (KG/M**3)	7.75037E+03	1.19854E+03	7.75037E+03	7.75037E+03	7.75037E+03

	ROLLING ELEMENT	CAGE	OUTER RACE	INNER RACE
MASS (KGM)	1.62354E-02	7.55796E-02	9.13017E-01	7.15787E-01
MOM OF INER -X (KGM*CM**2)	4.09157E-07	2.97122E-04	4.68519E-03	2.12084E-03
MOM OF INER -Y (KGM*CM**2)	4.09157E-07	1.52819E-04	2.42097E-03	1.12055E-03
MOM OF INER -Z (KGM*CM**2)	4.09157E-07	1.52819E-04	2.42097E-03	1.12055E-03

BALL/RACE DAMPING RATIO = 0.  
 RALL/CAGE DAMPING RATIO = 0.  
 RACE/CAGE DAMPING RATIO = 0.

## SCALE FACTORS, INTEGRATION DETAILS AND OUTPUT CONTROLS

LENGTH SCALE (M)	= 7.93750E-03	MIN STEP SIZE	= 1.00000E-03	INITIAL STEP SIZE	= 2.00000E-01
LOAD SCALE (N)	= 1.78000E+02	MAX STEP SIZE	= 1.00000E+01	TRUNCATION LIMIT	= 1.00000E-04
TIME SCALE (S)	= 8.50870E-04	FINAL TIME	= 2.00000E+03	STEP OPT CODES	= 6 50 1
DATA MONITOR CODE	= 500	PRINT CODES	= 5200 5	AUTO PLOT CODES	= 1 20
INT METHOD CODE	= 0	SOLUTION MODE	= 4		

OUTPUT FROM USER ACCESSIBLE ROUTINES ----  
 \*\*\*\*\*



STEP NO 1 TAU = 0. TIME = 0. S 100MM-DMA-BMG IRG-CAGE 60RPM 178N\*\*

# ROLLING ELEMENT PARAMETERS

RE \*\*\*\*\* CONTACT ANGLES \*\*\*\*\* CONTACT LOADS \*\*\* CONTACT DEFLS \*\*\* CONTACT STRESSES \*  
 NO (DEG) (N) (M) (N/MM<sup>2</sup>)  
 OUTER RACE OUTER RACE INNER RACE INNER RACE OUTER RACE INNER RACE OUTER RACE INNER RACE  
 1 2.467E+01 0. 2.245E+01 2.244E+01 7.387E-07 7.550E-07 3.752E+08 4.168E+08  
 7 2.467E+01 0. 2.245E+01 2.244E+01 7.387E-07 7.550E-07 3.752E+08 4.168E+08  
 13 2.467E+01 0. 2.245E+01 2.244E+01 7.387E-07 7.550E-07 3.752E+08 4.168E+08  
 19 2.467E+01 0. 2.245E+01 2.244E+01 7.387E-07 7.550E-07 3.752E+08 4.168E+08

RE \*\*\*\*\* CONTACT HALF WIDTHS \*\*\*\*\* LOAD\*SLIP INTEGRALS \* TRAC\*SLIP INTEGRALS \* \* SPIN/ROLL RATIOS \*\*  
 NO (M) (N\*H/S) (N\*H/S)  
 OUTER RACE INNER RACE OUTER RACE INNER RACE OUTER RACE INNER RACE OUTER RACE INNER RACE  
 1 4.663E-04 4.749E-04 6.125E-05 5.414E-05 1.031E-02 1.391E-03 2.829E-07 7.081E-09 -1.200E-01 0.  
 7 4.663E-04 4.749E-04 6.125E-05 5.414E-05 1.031E-02 1.391E-03 2.829E-07 7.081E-09 -1.200E-01 0.  
 13 4.663E-04 4.749E-04 6.125E-05 5.414E-05 1.031E-02 1.391E-03 2.829E-07 7.081E-09 -1.200E-01 0.  
 19 4.663E-04 4.749E-04 6.125E-05 5.414E-05 1.031E-02 1.391E-03 2.829E-07 7.081E-09 -1.200E-01 0.

RE \*\* ORB POS \*\*\*\* MASS CENTER VELOCITIES \*\*\* ANGULAR VELOCITIES \*\*\*\*\* RE/CAGE CON FORCES \*\*\*\*\*  
 NO (DEG) (M/S) (RPM) (M/S) (RPM) (N) (N) (N)  
 AXIAL RADIAL ORBITAL X COMP Y COMP Z COMP NORMAL TRACTION CON ANGLE  
 1 0. 0. 2.654E+01 -2.060E+02 0. 1.100E+02 0. 0. 0.  
 7 1.137E+02 0. 2.654E+01 -2.060E+02 0. 1.100E+02 0. 0. 1.800E+02  
 13 2.274E+02 0. 2.654E+01 -2.060E+02 0. 1.100E+02 0. 0. 4.233F-13  
 19 3.411E+02 0. 2.654E+01 -2.060E+02 0. 1.100E+02 0. 0. 3.600F+02

RE \*\* RE/CAGE \*\* RE/CAGE SLIP VELOCITIES \*\*\*\*\* RE/RACE SLIP VELOCITIES \*\*\*\*\* RE/RACE TRACTION COEFFICIENTS \*\*\*\*\*  
 NO MIN CLS (M) (M/S) OUTER RACE OUTER RACE INNER RACE INNER RACE OUTER RACE INNER RACE OUTER RACE INNER RACE  
 1 1.500E-04 0. 0. 1.036E-15 0. 4.637E-05 0. 4.246E-17 0. 1.901E-06  
 7 1.080E-05 0. 0. 1.036E-15 0. 4.637E-05 0. 4.246E-17 0. 1.901E-06  
 13 3.817E-05 0. 0. 1.036E-15 0. 4.637E-05 0. 4.246E-17 0. 1.901E-06  
 19 1.006E-04 0. 0. 1.036E-15 0. 4.637E-05 0. 4.246E-17 0. 1.901E-06

STEP NO 1 TAU = 0. TIME = 0. S 100MM-DMA-BRG IRG-CAGE 60RPM 17BN\*\*

# RACE AND CAGE PARAMETERS

\*\*\* MASS CENTER POSITIONS \*\*\* MASS CENTER VELOCITIES \*\*\* ANGULAR POSITIONS \*\*\*

	AXIAL (M)	RADIAL (M)	ORBITAL (M)	AXIAL (M/S)	RADIAL (M/S)	ORBITAL (M/S)	X COMP (DEG)	Y COMP (DEG)	Z COMP (DEG)
CAGE	-6.364E-06	1.520E-04	0.	0.	0.	0.	0.	0.	0.
OUTER RACE	0.	0.	0.	0.	0.	0.	0.	0.	0.
INNER RACE	-1.268E-05	0.	0.	0.	0.	0.	0.	0.	0.

\*\*\* ANGULAR VELOCITIES \*\*\* NET ACC FORCES \*\*\* NET ACC MOMENTS \*\*\*

	X COMP (RPM)	Y COMP (RPM)	Z COMP (RPM)	X COMP (N)	Y COMP (N)	Z COMP (N)	X COMP (N*MM)	Y COMP (N*MM)	Z COMP (N*MM)
CAGE	2.654E+01	0.	0.	0.	-7.414E-02	-7.457E+00	-6.018E-04	0.	2.165E-03
OUTER RACE	0.	0.	0.	1.780E+02	5.810E-12	-4.348E-12	7.254E-05	-9.788E-14	-8.910E-14
INNER RACE	6.000E+01	0.	0.	-1.780E+02	-5.850E-12	3.715E-12	-2.952E-05	9.537E-14	5.396E-14

\*\*\* RACE/CAGE FORCES \*\*\* RACE/CAGE MIN CLS SLIP VEL EFFECTIVE

	NORMAL (N)	TRACTION (N)	CON ANGLE (DEG)	ATT ANGLE (DEG)	MIN CLS (M)	SLIP VEL (M/S)	EFFECTIVE DIA PLAY (M)
LAND NO 1	0.	0.	0.	0.	4.443F-05	0.	3.929E-04
LAND NO 2	0.	0.	0.	0.	4.443F-05	0.	3.929E-04

## APPLIED PARAMETERS

\*\*\* FORCES \*\*\* MOMENTS \*\*\*

	X COMP (N)	Y COMP (N)	Z COMP (N)	X COMP (N*MM)	Y COMP (N*MM)	Z COMP (N*MM)
OUTER RACE	-1.780E+02	-5.810E-12	4.348E-12	-7.254E-05	9.788E-14	8.910E-14
INNER RACE	1.780E+02	5.850E-12	-3.715E-12	2.952E-05	-9.537E-14	-5.396E-14

\*\*\* MASS CENTER ACCELERATIONS \*\*\* ANGULAR ACCELERATIONS \*\*\*

	X COMP (M/S**2)	Y COMP (M/S**2)	Z COMP (M/S**2)	X COMP (RPM/S)	Y COMP (RPM/S)	Z COMP (RPM/S)
OUTER RACE	0.	0.	0.	0.	0.	0.
INNER RACE	0.	0.	0.	0.	0.	0.

NET BRG LOSS (N\*MM/S) = 1.763E-02  
 CURRENT LIFE (HOURS) = 2.926E+13  
 INTERNAL CLEARANCE (M) = 1.132E-04  
 O.R. HOOP (N/M\*\*2) = -1.158E+07  
 CAGE HOOP (N/M\*\*2) = 4.059E+01  
 NET LOAD\*SLIP (N\*MM/S) = 1.985E+00  
 OUTER RACE FIT (M) = 1.000E-05  
 INNER RACE FIT (M) = 1.000E-05  
 I.R. HOOP (N/M\*\*2) = 1.434E+07

[illegible]

# RAPID SIMULATION OF THE DYNAMICS OF ROLLING ELEMENT BEARINGS

--A REAL TIME PERFORMANCE SIMULATION-  
(VERSION RAPIDRE8.0)

**PRANEEP K. GUPTA**  
**MECHANICAL TECHNOLOGY INCORPORATED**  
**968 ALBANY-SHAKER ROAD**  
**LATHAM, NEW YORK**  
**U. S. A.**

150MM-0MA-BRG 86-CAGE 62.5RPM 534N

**BEARING GEOMETRY**

BORE	(M)	=	1.50000E-01	OUTER RACE SHRINK FIT	(M)	=	1.00000E-05
OUTSIDE DIAMETER	(M)	=	2.25000E-01	INNER RACE SHRINK FIT	(M)	=	1.00000E-05
SHAFT INNER DIA	(M)	=	1.37000E-01	HOUSING OFER DIA	(M)	=	2.44000E-01
BALL DIAMETER	(M)	=	2.22250E-02	NUMBER OF BALLS			16
PITCH DIAMETER	(M)	=	1.87500E-01	OUTER RACE CUR FACTOR			5.20000E-01
CONTACT ANGLE	(DEG)	=	1.80000E+01	INNER RACE CUR FACTOR			5.30000E-01
END PLAY	(M)	=	6.86790E-04	DIAMETRAL PLAY	(M)	=	1.08777E-04
CAGE OUTER DIA	(M)	=	1.97104E-01	CAGE OUTER DIA CLS	(M)	=	3.98780E-03
CAGE INNER DIA	(M)	=	1.77165E-01	CAGE INNER DIA CLS	(M)	=	4.28600E-04
EFF CAGE WIDTH	(M)	=	3.35280E-02	DIA RF/CAGE CLEARANCE	(M)	=	4.06400E-04
RF/CAGE CONE ANG	(DEG)	=	3.75000E+01	RE/CAGE CONE HEIGHT	(M)	=	-3.18353E-03

# LUBRICATION DETAILS -----

## 1. ROLLING ELEMENT/CAGE AND RACE/CAGE PARAMETERS ---

	INTERACTION CODE	LUBRICITY (N*5/M**2)	MAX FILM (M)
ROLLING ELEMENT/CAGE INTERACTION	0	0.	1.00000E-04
RACE/CAGE INTERACTION	0	0.	

RE/CAGE DRY CONTACT TRACTION PARAMETERS --

CRIT FILM THICKNESS (M)	= 2.50000E-07
COEFFICIENT A	= 1.00000E-02
COEFFICIENT C	1/ (M/S) = 0.
COEFFICIENT B	1/ (M/S) = 0.
COEFFICIENT D	= -1.00000E-02

## 2. ROLLING ELEMENT/RACE PARAMETERS (TRACTION CODE = 0) ---

COEFFICIENT A	= 0.
COEFFICIENT C	1/ (M/S) = 0.
COEFFICIENT B	1/ (M/S) = 4.10000E-02
COEFFICIENT D	= -1.00000E-02

# APPLIED LOADS AND SPEEDS

## 1. QUASI-STATIC SIMULATION ---

AXIAL LOAD (N) = 5.34000E+02 OUTER RACE ANG VEL (RPM) = 0.  
 RADIAL DISPLACEMENT (M) = 0. INNER RACE ANG VEL (RPM) = 6.25000E+01  
 RELATIVE MISALIGNMENT (DEG) = 0.

## 2. DYNAMIC SIMULATION ---

\*\*\*\*\* LOADS (N) \*\*\*\*\* MASS CEN ACC (M/S\*\*2) \*\*\*\*\*  
 I II III I II III

OUTER RACE 0. 0. 0.  
 INNER RACE 0. 0. 0.

\*\*\*\*\* MOMENTS (N\*M) \*\*\*\*\* ANG ACCELERATION (RPM/S) \*\*\*\*\*  
 I II III I II III

OUTER RACE 0. 0. 0.  
 INNER RACE 0. 0. 0.

\*\*\*\*\* ANGULAR VELOCITIES (RPM)\*\*\*\*\*  
 I II III

OUTER RACE 0. 0. 0.  
 INNER RACE 6.25000E+01 0. 0.

COMPONENTS OF ACCELERATION DUE TO GRAVITY VECTOR (M/S\*\*2) = 0. 0. 9.81000E+00

EXTERNALLY APPLIED FORCE VECTOR ACTING ON CAGE (N) = 0. 0. 0.  
 CORRESPONDING POSITION VECTOR IN INERTIAL FRAME (M) = 1.67640E-02 0. 0.

# MATERIAL PROPERTIES AND INERTIAL PARAMETERS

	ROLLING ELEMENT	CAGE	RACEWAYS	SHAFT	HOUSING
ELASTIC MODULUS (N/M**2)	1.99948E+11	3.44730E+09	1.99948E+11	1.99948E+11	1.99948E+11
POISSON'S RATIO	2.50000E-01	4.50000E-01	2.50000E-01	2.50000E-01	2.50000E-01
MASS DENSITY (KG/M**3)	7.75037E+03	1.19954E+03	7.75037E+03	7.75037E+03	7.75037E+03

	ROLLING ELEMENT	CAGE	OUTER RACE	INNER RACE
MASS (KG)	4.45499E-02	1.81437E-01	3.02448E+00	2.33032E+00
MOM OF INER -X (KG*M**2)	2.20054E-06	1.64186E-03	3.40526E-02	1.56168E-02
MOM OF INER -Y (KG*M**2)	2.20054E-06	8.38715E-04	1.75243E-02	8.19210E-03
MOM OF INER -Z (KG*M**2)	2.20054E-06	8.38715E-04	1.75243E-02	8.19210E-03

BALL/RACE DAMPING RATIO = 0.  
 BALL/CAGE DAMPING RATIO = 0.  
 RACE/CAGE DAMPING RATIO = 0.

## SCALE FACTORS, INTEGRATION DETAILS AND OUTPUT CONTROLS

LENGTH SCALE (M)	= 1.11125E-02	MIN STEP SIZE	= 1.00000E-03	INITIAL STEP SIZE	= 2.00000E-01
LOAD SCALE (N)	= 5.34000E+02	MAX STEP SIZE	= 1.00000E+01	TRUNCATION LIMIT	= 1.00000E-04
TIME SCALE (S)	= 9.62850E-04	FINAL TIME	= 2.00000E+03	STEP OPT CODES	= 6 10 1
DATA MONITOR CODE	= 500	PRINT CODES	= 5200 5	AUTO PLOT CODES	= 1 17
INT METHOD CODE	= 0	SOLUTION MODE	= 4		

OUTPUT FROM USER ACCESSIBLE ROUTINES ---  
 \*\*\*\*\*

```

STEP NO 1          TAU = 0.          TIME = 0.          150MM-DMA-BHG  BG-CAGE  62.5RPM  534N***

```

## ROLLING ELEMENT PARAMETERS

NO	OUTER RACE	OUTER RACE	INNER RACE	INNER RACE	CONTACT ANGLES (DEG)	*****	CONTACT LOADS (N)	*****	CONTACT DEFLECTIONS (M)	*****	CONTACT STRESSES (N/M <sup>2</sup> )	
							OUTER RACE	INNER RACE	OUTER RACE	INNER RACE	OUTER RACE	INNER RACE
1	1.779E+01	0.	1.779E+01	0.			1.093E+02	1.092E+02	1.897E-06	2.124E-06	5.087E+08	6.123E+08
7	1.779E+01	0.	1.779E+01	0.			1.093E+02	1.092E+02	1.897E-06	2.124E-06	5.087E+08	6.123E+08
13	1.779E+01	0.	1.779E+01	0.			1.093E+02	1.092E+02	1.897E-06	2.124E-06	5.087E+08	6.123E+08

RE NO	***** CONTACT	HALF WIDTHS (M)	***** LOAD*SLIP INTEGRALS (N*MM/S)	***** TRAC*SLIP INTEGRALS (N*MM/S)	* * SPIN/ROLL RATIOS * *			
	OUTER RACE	INNER RACE	OUTER RACE	INNER RACE	OUTER RACE			
	INNER RACE	OUTER RACE	INNER RACE	OUTER RACE	INNER RACE			
1	8.842E-04	7.673E-04	1.160E-04	1.110E-04	1.668E-07	2.354E-06	2.942E-16	6.516E-02
7	8.842E-04	7.673E-04	1.160E-04	1.110E-04	1.668E-07	2.354E-06	2.942E-16	6.516E-02
3	8.842E-04	7.673E-04	1.160E-04	1.110E-04	1.668E-07	2.354E-06	2.942E-16	6.516E-02

RE NO	** ORB POS (DEG)	*** MASS CENTER VELOCITIES *** (M/S)	RADIAL	ORBITAL (RPM)	**** ANGULAR (RPM)	X COMP	Y COMP	Z COMP	NORMAL (N)	RE/CAGE CON FORCES (N)	***** RE/CAGE CON FORCES ***** (NEG)
1	0.	0.	0.	2.772E+01	-2.505E+02	0.	7.146E+01	0.	0.	0.	0.
7	1.350E+02	0.	0.	2.772E+01	-2.505E+02	0.	7.146E+01	0.	0.	0.	1.800F+02
13	2.700E+02	0.	0.	2.772E+01	-2.505E+02	0.	7.146E+01	0.	2.705E-01	2.705E-03	3.600E+02

RE NO	** RE/CAGE MIN CLS (M)	** RE/CAGE SLIP VELS (M/S)	***** RE/RACE OUTER RACE I	***** RE/RACE INNER RACE II	***** RE/RACE TWINFR RACE II	***** RE/RACE OUTER RACE I	***** RE/RACE INNER RACE II	***** RE/RACE TRACTION COEFFICIENTS *****
1	2.032E-04	0.	0.	-1.020E-04	0.	0.	-6.181E-06	0.
7	5.952E-05	0.	0.	-1.020E-04	0.	0.	-6.181E-06	0.
13	2.467E-18	3.348E-01	0.	-1.020E-04	0.	0.	-6.181E-06	0.

NO	NOR LOAD (N)	FRIC LOAD (N)	MIN FILM (N)	SLIP VEL (M/S)	CON ANGLE (DEG)
1	0.	0.	1.750E-04	0.	0.
7	0.	0.	1.504E-04	0.	1.800E+02
3	0.	0.	4.787E-05	0.	3.823E-12

STEP NO 1 TAU = 0. S 150MM-DMA-BRG BG-CAGE 62.5RPM 534N\*\*\*

# RACE AND CAGE PARAMETERS

\*\*\* MASS CENTER POSITIONS \*\*\* MASS CFNTR VELOCITIES \*\*\* ANGULAR POSITIONS \*\*\*

	AXIAL (M)	RADIAL (M)	ORBITAL (M)	AXIAL (M/S)	RADIAL (M/S)	ORBITAL (M/S)	X COMP (DEG)	Y COMP (DEG)	Z COMP (DEG)
CAGE	-1.002E-06	2.032E-04	0.	0.	0.	0.	0.	0.	0.
OUTER RACE	0.	0.	0.	0.	0.	0.	0.	0.	0.
INNER RACE	-2.661E-06	0.	0.	0.	0.	0.	0.	0.	0.

\*\*\* ANGULAR VELOCITIES \*\*\* NET ACC FORCES \*\*\* NET ACC MOMENTS \*\*\*

	X COMP (RPM)	Y COMP (RPM)	Z COMP (RPM)	X COMP (N)	Y COMP (N)	Z COMP (N)	X COMP (N*M)	Y COMP (N*M)	Z COMP (N*M)
CAGE	2.772E+01	0.	0.	0.	-5.241E-03	1.239E+00	-5.930E-05	0.	1.260E-04
OUTER RACE	0.	0.	0.	5.340E+02	3.107E-11	-2.561E-11	5.024E-04	-6.641E-13	-5.692E-13
INNER RACE	6.250E+01	0.	0.	-5.340E+02	-2.869E-11	2.324E-11	-9.485E-04	6.325E-13	7.379E-13

\*\*\* RACE/CAGE FORCES \*\*\* RACE/CAGE EFFECTIVE

	NORMAL (N)	TRACTION (N)	CON ANGLE (DEG)	ATT ANGLE (DEG)	MIN CLS (M)	RACE/CAGE SLIP VEL (M/S)	DIA PLAY (M)
LAND NO 1	0.	0.	0.	0.	0.	0.	0.
LAND NO 2	0.	0.	0.	0.	0.	0.	0.

## APPLIED PARAMETERS

\*\*\* FORCES \*\*\* MOMENTS \*\*\*

	X COMP (N)	Y COMP (N)	Z COMP (N)	X COMP (N*M)	Y COMP (N*M)	Z COMP (N*M)
OUTER RACE	-5.340E+02	-3.107E-11	2.561E-11	-5.024E-04	6.641E-13	5.692E-13
INNER RACE	5.340E+02	2.869E-11	-2.324E-11	9.485E-04	-6.325E-13	-7.379E-13

\*\*\* MASS CENTER ACCELERATIONS \*\*\* ANGULAR ACCELERATIONS \*\*\*

	X COMP (M/S**2)	Y COMP (M/S**2)	Z COMP (M/S**2)	X COMP (RPM/S)	Y COMP (RPM/S)	Z COMP (RPM/S)
OUTER RACE	0.	0.	0.	0.	0.	0.
INNER RACE	0.	0.	0.	0.	0.	0.

NET BRG LOSS (N\*M/S) = 1.426E+00  
 CURRENT LIFE (HOURS) = 6.850E+11  
 INTERNAL CLEARANCE (M) = 9.861E-05  
 O.R. HOOP (N/M\*\*2) = -5.098E+06  
 CAGE HOOP (N/M\*\*2) = 9.549E+01  
 NET LOAD/SLIP (M) = 1.000E-05  
 OUTER RACE FIT (M) = 1.000E-05  
 INNER RACE FIT (M) = 1.000E-05  
 I.R. HOOP (N/M\*\*2) = 6.457E+06



APPENDIX C

TYPICAL COMPUTER OUTPUT FOR THE  
100 mm ENGINE BEARING

[illegible]

RAPID SIMULATION OF THE  
 DYNAMICS OF ROLLING ELEMENT BEARINGS

---A REAL TIME PERFORMANCE SIMULATION-  
(VERSION RAPIDRER.0)

**PRADEEP K. GUPTA**  
**MECHANICAL TECHNOLOGY INCORPORATED**  
**968 ALRANY-SHAKER ROAD**  
**LATHAM, NEW YORK**  
**U. S. A.**

BEARING TYPE -- BALL SPEC CODE -- 100MM ENGINE BRG MOD CAGE 18/4.5KN 20KRPM

## BEARING GEOMETRY

BORE	(M) = 1.00000E-01	OUTER RACE SHRINK FIT	(M) = 1.00000E-05
OUTSIDE DIAMETER	(M) = 1.80000E-01	INNER RACE SHRINK FIT	(M) = 5.00000E-05
SHAFT INNER DIA	(M) = 2.00000E-02	HOUSING OUTER DIA	(M) = 2.05000E-02
BALL DIAMETER	(M) = 1.90500E-02	NUMBER OF BALLS	18
PITCH C METER	(M) = 1.40000E-01	OUTER RACE CUR FACTOR	(M) = 5.20000E-01
CONTACT ANGLE	(DEG) = 2.50000E+01	INNER RACE CUR FACTOR	(M) = 5.40000E-01
END PLAY	(M) = 9.66105E-04	DIAMETRAL PLAY	(M) = 2.14180E-04
CAGE OUTER DIA	(M) = 1.48800E-01	CAGE OUTER DIA CLS	(M) = 7.00000E-03
CAGE INNER DIA	(M) = 1.29700E-01	CAGE INNER DIA CLS	(M) = 3.00000E-03
EFF CAGE WIDTH	(M) = 2.73000E-02	DIA RF/CAGE CLEARANCE	(M) = 8.26000E-04

GUIDANCE	GUIDANCE TYPE	GUIDING RADIUS (M)	GUIDING CAGE RADIUS (M)	EFF LAND WIDTH (M)	CAGE HALF WIDTH (M)
GUIDING LAND 1	2	6.42350E-02	6.48500E-02	4.00000E-03	1.36500E-02
GUIDING LAND 11	2	6.42350E-02	6.48500E-02	4.00000E-03	1.36500E-02

# LUBRICATION DETAILS -----

## 1. ROLLING ELEMENT/CAGE AND RACE/CAGE PARAMETERS ---

	INTERACTION CODE	LUB VISCOSITY (N*S/M**2)	MAX FILM (M)
ROLLING ELEMENT/CAGE INTERACTION	1	7.12466E-03	4.00000E-04
RACE/CAGE INTERACTION	1	7.12466E-03	

RE/CAGE DRY CONTACT TRACTION PARAMETERS --	
CRIT FILM THICKNESS (M)	= 5.00000E-07
TRAC COEFF AT ZERO SLIP	= 0.
TRAC COEFF AT INFINITE SLIP	= 1.60000E-02

CAGE/RACE DRY CONTACT TRACTION PARAMETERS --	
CRIT FILM THICKNESS (M)	= 5.00000E-07
TRAC COEFF AT ZERO SLIP	= 0.
TRAC COEFF AT INFINITE SLIP	= 1.60000E-02

MAXIMUM TRAC COEFF (M/S) = 2.00000E-02	
SLIP AT MAX TRAC	
MAXIMUM TRAC COEFF (M/S)	= 1.00000E+00
SLIP AT MAX TRAC	

## 2. ROLLING ELEMENT/RACE PARAMETERS (TRACTION CODE = 3) ---

FILM THICKNESS CODE	= 2	CRIT FILM THICKNESS (M)	= 1.00000E-07
INLET TEMP (DEG-K)	= 3.30000E+02	PR-VIS COEFF (M**2/N)	= 1.01447E-08
INLET VIS (N*S/M**2)	= 7.12466E-03	TEMP-VIS COEFF (DEG-K)	= 2.85205E+03
THERMAL COND (N/S/DEG-C)	= 9.65788E-02	STARVATION PARAMETER	= 1.00000E+01
VISCOSITY* (N*S/M**2)	= 7.87989E-02	ROLLING SPEED EFFECT	
PR-VIS COEFF* (M**2/N)	= 5.22136E-09	PARAMETERS - VR	(M/S) = 2.28600E+01
TEMP-VIS COEFF* (1/DEG-K)	= 5.46451E-02	VN	= -7.03200E-01
OUTER RACE TEMP (DEG-K)	= 3.30000E+02	INNER RACE TEMP (DEG-K)	= 3.30000E+02

## 3. TRACTION PARAMETERS OUT OF LUR MODEL ROUNDS ---

TRAC COEFF AT ZERO SLIP	= 0.	MAXIMUM TRAC COEFF (M/S)	= 2.00000E-02
TRAC COEFF AT INFINITE SLIP	= 1.60000E-02	SLIP AT MAX TRAC	= 1.00000E+00

## 4. LUBRICANT DRAG AND CHURNING PARAMETERS ---

EFF LUB VIS (N*S/M**2)	= 7.12466E-03	FFF LUR DEN (KGM/M**3)	= 1.00000E+01
------------------------	---------------	------------------------	---------------

# APPLIED LOADS AND SPEEDS

## 1. QUASI-STATIC SIMULATION ---

AXIAL LOAD (N) = 1.80000E+04 OUTER RACE ANG VEL (RPM) = 0.  
 RADIAL LOAD (N) = 4.50000E+03 INNER RACE ANG VEL (RPM) = 2.00000E+04  
 RELATIVE MISALIGNMENT (DEG) = 0.

## 2. DYNAMIC SIMULATION ---

\*\*\*\*\* LOADS (N) \*\*\*\*\*  
 I II III  
 \*\*\*\*\* MASS CEN ACC (M/S\*\*2) \*\*\*\*\*  
 I II III

0. 0. 0.  
 0. 0. 0.

OUTER RACE  
 INNER RACE

\*\*\*\*\* MOMENTS (N\*M) \*\*\*\*\*  
 I II III  
 \*\*\*\*\* ANG ACCELERATION (RPM/S) \*\*\*\*\*  
 I II III

0. 0. 0.  
 0. 0. 0.

OUTER RACE  
 INNER RACE

\*\*\*\*\* ANGULAR VELOCITIES (RPM)\*\*\*\*\*  
 I II III

OUTER RACE 0. 0.  
 INNER RACE 2.00000E+04 0. 0.

9.81000E+00

COMPONENTS OF ACCELERATION DUE TO GRAVITY VECTOR (M/S\*\*2) = 0.

0.

EXTERNALLY APPLIED FORCE VECTOR ACTING ON CAGE (N) = 0.  
 CORRESPONDING POSITION VECTOR IN INERTIAL FRAME (M) = 1.36500E-02 0.

0.

# MATERIAL PROPERTIES AND INERTIAL PARAMETERS

ROLLING ELEMENT		CAGE	RACEWAYS	SHAFT	HOUSING
ELASTIC MODULUS	(N/M**2)	2.00000E+11	1.99948E+11	1.99948E+11	1.99948E+11
POISSON-S RATIO		2.50000E-01	2.50000E-01	2.50000E-01	2.50000E-01
MASS DENSITY	(KGM/M**3)	7.75037E+03	7.75037E+03	7.75037E+03	7.75037E+03

ROLLING ELEMENT		CAGE	OUTER RACE	INNER RACE
MASS	(KGM)	4.70585E-01	2.32900E+00	1.62894E+00
MOM OF INER -X	(KGM**2)	2.29196E-03	1.59413E-02	5.50250E-03
MOM OF INER -Y	(KGM**2)	1.17521E-03	8.25241E-03	2.94830E-03
MOM OF INER -Z	(KGM**2)	1.17521E-03	8.25241E-03	2.94830E-03

BALL/RACE DAMPING RATIO = 0.  
 BALL/CAGE DAMPING RATIO = 0.  
 RACE/CAGE DAMPING RATIO = 0.

## SCALE FACTORS, INTEGRATION DETAILS AND OUTPUT CONTROLS

LENGTH SCALE	(M) = 9.52500E-03	MIN STEP SIZE	= 2.00000E-02	INITIAL STEP SIZE	= 1.00000E-01
LOAD SCALE	(N) = 1.80000E+04	MAX STEP SIZE	= 1.00000E+01	TRUNCATION LIMIT	= 1.00000E-04
TIME SCALE	(S) = 1.21843E-04	FINAL TIME	= 4.00000E+02	STEP OPT CODES	= 6 50 2
DATA MONITOR CODE	= 200	PRINT CODES	= 5 50 5	AUTO PLOT CODES	= 1 19 21
INT METHOD CODE	= 0	SOLUTION MODE	= 1		

OUTPUT FROM USER ACCESSIBLE ROUTINES ---

STEP NO 1 TAU = 0. TIME = 0. S 100MM ENGINE BRG MOD CAGE 18/4.5KN 20KRPM  
 =====

ROLLING ELEMENT PARAMETERS  
 -----

RE \*\*\*\*\* CONTACT ANGLES \*\*\*\*\* CONTACT LOADS \*\*\* \*\* CONTACT DEFLS \*\*\* \*\* CONTACT STRESSES \*  
 NO (DEG) (N) (N) (N/M\*\*2)

OUTER RACE OUTER RACE INNER RACE INNER RACE OUTER RACE INNER RACE OUTER RACE INNER RACE  
 1 1.590E+01 0. 2.527E+01 0. 4.420E+03 2.852E+03 2.350E+05 2.098E+05 1.921E+09 2.147E+09  
 7 1.434E+01 0. 2.640E+01 -4.467E-03 3.599E+03 2.005E+03 2.049E+05 1.658E+05 1.793E+09 1.908E+09  
 13 1.434E+01 0. 2.640E+01 4.467E-03 3.599E+03 2.005E+03 2.049E+05 1.658E+05 1.793E+09 1.908E+09

RE \*\*\*\*\* CONTACT HALF WIDTHS \*\*\*\*\* LOAD\*SLIP INTEGRALS \* TRAC\*SLIP INTEGRALS \* \* SPIN/ROLL RATIOS \*\*  
 NO (M) (N\*M/S) (N\*M/S)

OUTER RACE INNER RACE OUTER RACE INNER RACE OUTER RACE INNER RACE OUTER RACE INNER RACE  
 1 2.880E-03 1.934E-03 3.815E-04 3.281E-04 2.099E+03 4.124F+03 3.039E+01 7.434E+01 -3.606E-15 2.311E-01  
 7 2.689E-03 1.719E-03 3.564E-04 2.919E-04 1.496E+03 3.055F+03 1.692E+01 5.088E+01 6.642E-16 2.754E-01  
 13 2.689E-03 1.719E-03 3.564E-04 2.919E-04 1.496E+03 3.055E+03 1.692E+01 5.088E+01 1.727E-15 2.754E-01

RE \*\* ORB POS \*\*\* MASS CENTER VELOCITIES \*\*\* \*\* ANGULAR VELOCITIES \*\*\*\*\* \*\* RE/CAGE CON FORCES \*\*\*\*\*  
 NO (DEG) (M/S) (RPM) (RPM) (N) (N) (DEG)

1 0. 0. 8.804E+03 -7.143E+04 0. 1.794E+04 2.149E-02 2.617E-02 2.700E+02  
 7 1.200E+02 0. 8.859E+03 -7.232E+04 0. 1.622E+04 1.276E+00 2.217E-01 1.791E+02  
 13 2.400E+02 0. 8.859E+03 -7.232E+04 0. 1.622E+04 1.276E+00 2.217E-01 8.611E-01

RE \*\* RE/CAGE \*\* RE/CAGE SLIP VELOCITIES \*\*\*\*\* \*\* RE/RACE TRACTION COEFFICIENTS \*\*\*\*\*  
 NO MIN CLS SLIP VELS (M/S) (M/S) (M/S)

1 4.050E-04 1.790E+01 0. -3.523E-01 0. 0. -2.000E-02 0. 0.  
 7 1.471E-04 7.392E+01 0. -3.087E-01 -1.407E-03 -5.555F-13 0. -2.000E-02 -1.405E-13  
 13 1.471E-04 7.392E+01 -3.439E-14 -3.087E-01 1.407E-03 0. -2.228E-15 -2.000E-02 0.

RE \*\*\*\* RE/RACE ISO FILM THERMAL\*SIDE LFAKAGE DRAG FORCE CHURN MOM NET DRAG\*  
 NO (M) (N) (N\*M)

OUTER RACE INNER RACE OUTER RACE INNER RACE  
 1 1.043E-06 9.395E-07 3.798E-01 2.731E+00 2.880F-03 1.986E+02  
 7 1.063E-06 9.597E-07 3.818E-01 2.766E+00 2.907E-03 2.023E+02  
 13 1.063E-06 9.597E-07 3.818E-01 2.766E+00 2.907E-03 2.023E+02

STEP NO 1 TAU = 0. TIME = 0. 100MM ENGINE BRG MOD CAGE 18/4.5KN 20KRPM

# RACE AND CAGE PARAMETERS

\*\*\*\* MASS CENTER POSITIONS \*\*\*\* MASS CENTER VELOCITIES \*\*\*\* ANGULAR POSITIONS \*\*\*\*

	(M)	(M)	(M)	(M/S)	(M/S)	(RPM)	(DEG)
	AXIAL	RADIAL	ORBITAL	AXIAL	RADIAL	ORBITAL	X COMP Y COMP Z COMP
CAGE	-5.760E-05	3.070E-04	0.	0.	0.	0.	0. 0. 0.
OUTER RACE	0.	0.	0.	0.	0.	0.	0. 0. 0.
INNER RACE	-3.747E-05	7.039E-06	0.	0.	0.	0.	0. 0. 0.

\*\*\*\* ANGULAR VELOCITIES \*\*\*\* NET ACC FORCES \*\*\*\* NET ACC MOMENTS \*\*\*\*

	(RPM)	(N)	(N)	(N)	(N)	(N)
	X COMP	Y COMP	Z COMP	X COMP	Y COMP	Z COMP
CAGE	8.841E+03	0.	0.	3.288E-03	-2.478E+00	-9.451E+00
OUTER RACE	0.	0.	0.	1.800E-04	-1.932E+01	4.364E+03
INNER RACE	2.000E+04	0.	0.	-1.800E-04	-3.820E+00	-4.498E+03

\*\*\*\* RACE/CAGE FORCES \*\*\*\* RACE/CAGE RACE/CAGE EFFECTIVE

	(N)	(N)	(N)	(DEG)	MIN CLS	SLIP VEL	DIA PLAY
	NORMAL	TRACTION	CON ANGLE	ATT ANGLE	(M)	(M/S)	(M)
LAND NO 1	8.395E-02	1.753E+00	1.800E+02	-5.230E+01	2.781E-04	7.459E+01	1.156E-03
LAND NO 2	8.395E-02	1.753E+00	1.800E+02	-5.230E+01	2.781E-04	7.459E+01	1.156E-03

CAGE CHURN MOH (N\*M) = 7.962E-02 CAGE NET CHURN LOSS (N\*M/S) = 6.153E+02

# APPLIED PARAMETERS

\*\*\*\* FORCES \*\*\*\* MOMENTS \*\*\*\*

	(N)	(N)	(N)	(N)	(N)	(N)
	X COMP	Y COMP	Z COMP	X COMP	Y COMP	Z COMP
OUTER RACE	-1.800E+04	1.932E+01	-4.364E+03	1.462E+01	-1.312E+02	2.829E-02
INNER RACE	1.800E+04	3.820E+00	4.498E+03	-3.108E-01	1.332E+02	1.170E-01

\*\*\*\* MASS CENTER ACCELERATIONS \*\*\*\* ANGULAR ACCELERATIONS \*\*\*\*

	(M/S**2)	(M/S**2)	(M/S**2)	(RPM/S)	(RPM/S)	(RPM/S)
	X COMP	Y COMP	Z COMP	X COMP	Y COMP	Z COMP
OUTER RACE	0.	0.	0.	0.	0.	0.
INNER RACE	0.	0.	0.	0.	0.	0.

NET BRG LOSS (N\*M/S) = 6.182E+03  
 CURRENT LIFE (HOURS) = 1.536E+03  
 INTERNAL CLEARANCE (M) = 1.062E-04  
 O.R. HOOP (N/M\*\*2) = -1.427E+07  
 CAGE HOOP (N/M\*\*2) = 3.511E+07  
 NET LOAD\*SLIP (N\*M/S) = 9.324E+04  
 OUTER RACE FIT (M) = 1.000E-05  
 INNER RACE FIT (M) = 9.767E-07  
 I.R. HOOP (N/M\*\*2) = 1.183E+08

**DATE**  
**ILME**